CHARACTERIZATION OF HUMAN PYRUVATE DEHYDROGENASE KINASE ISOFORM 2 (PDHK2)

by

LIANGYAN HU

B.S., Chengdu University of Science and Technology, 1994
M.S., Shanghai Institute of Biochemistry, 1997

AN ABSTRACT OF A DISSERTATION

submitted in partial fulfillment of the requirements for the degree

DOCTOR OF PHILOSOPHY

Department of Biochemistry
College of Arts and Sciences

KANSAS STATE UNIVERSITY
Manhattan, Kansas

2008

Abstract

Specific mutants were developed to evaluate the roles of several residues in α8 helix of the regulatory (R) domain of human pyruvate dehydrogenase kinase 2 (PDHK2) in the linkage between the Regulatory (R) and catalytic (Cat) domain (Q144A), dichloroacetate (DCA)/pyruvate inhibition (R154C, R158A, I157F) and stimulation by reductive acetylation (L160A, R154C/L160A). All mutants, with the exception of L160A, were active, and were bound to and had their activities enhanced by dihydrolipoyl acetyltransferase (E2). The cross arms between subunits are anchored by W383. Based on the studies on the W383F mutant, W383 provided majority of the intrinsic Trp fluorescence; and ligand(s) binding quenched primarily (pyruvate) or exclusively (ADP or ATP) the fluorescence of W383.

The Q144 mutation in the R domain caused 14-fold weaker K^+ binding with ATP in the Cat domain but did not alter the weaker K^+ binding with ADP unless Pi was included. Similarly, with 100 mM K^+, the Q144A mutant had weaker ATP binding but the affinity for ADP was not changed even in the presence of Pi, which enhanced the binding of ADP to kinase by 2-fold.

R154 and R158 were shown to be important residues in the inhibition by pyruvate, DCA and Cl^-. The R154C, R154C/L160A and R158A mutations reduced the inhibition by DCA or pyruvate using E1 or E1•E2 as the substrates. Pyruvate plus ADP did not significantly hinder the binding of GST-L2 to these mutants in AUC studies. Cl^- appears to bind to kinase at the same site as DCA/pyruvate based on lack of Cl^- effects with above mutants and evidence that Cl^- weakened the inhibition by DCA or pyruvate of native PDHK2.

Q144 and L160 may play important roles in the signal transmission from the lipoyl group-binding site to the active site. Q144A and R154C/L160A mutants were less stimulated by reductive acetylation than other mutants and native PDHK2. Nov3r binds to where lipoyl goup binds PDHK2. Using E1 alone as substrate, Nov3r binding caused a 20% increase of kinase activity at low levels. Nov3r binding also reduced the inhibition of DCA/pyruvate with elevated K^+ plus Pi.

CHARACTERIZATION OF HUMAN PYRUVATE DEHYDROGENASE KINASE ISOFORM 2 (PDHK2)

by

LIANGYAN HU

B.S., Chengdu University of Science and Technology, 1994
M.S., Shanghai Institute of Biochemistry, 1997

A DISSERTATION

submitted in partial fulfillment of the requirements for the degree

DOCTOR OF PHILOSOPHY

Department of Biochemistry
College of Arts and Sciences

KANSAS STATE UNIVERSITY
Manhattan, Kansas

2008

Approved by:

Major Professor
Thomas E. Roche

Abstract

Specific mutants were developed to evaluate the roles of several residues in α8 helix of the regulatory (R) domain of human pyruvate dehydrogenase kinase 2 (PDHK2) in the linkage between the Regulatory (R) and catalytic (Cat) domain (Q144A), dichloroacetate (DCA)/pyruvate inhibition (R154C, R158A, I157F) and stimulation by reductive acetylation (L160A, R154C/L160A). All mutants, with the exception of L160A, were active, and were bound to and had their activities enhanced by dihydrolipoyl acetyltransferase (E2). The cross arms between subunits are anchored by W383. Based on the studies on the W383F mutant, W383 provided majority of the intrinsic Trp fluorescence; and ligand(s) binding quenched primarily (pyruvate) or exclusively (ADP or ATP) the fluorescence of W383.

The Q144 mutation in the R domain caused 14-fold weaker K^+ binding with ATP in the Cat domain but did not alter the weaker K^+ binding with ADP unless Pi was included. Similarly, with 100 mM K^+, the Q144A mutant had weaker ATP binding but the affinity for ADP was not changed even in the presence of Pi, which enhanced the binding of ADP to kinase by 2-fold.

R154 and R158 were shown to be important residues in the inhibition by pyruvate, DCA and Cl^-. The R154C, R154C/L160A and R158A mutations reduced the inhibition by DCA or pyruvate using E1 or E1•E2 as the substrates. Pyruvate plus ADP did not significantly hinder the binding of GST-L2 to these mutants in AUC studies. Cl^- appears to bind to kinase at the same site as DCA/pyruvate based on lack of Cl^- effects with above mutants and evidence that Cl^- weakened the inhibition by DCA or pyruvate of native PDHK2.

Q144 and L160 may play important roles in the signal transmission from the lipoyl group-binding site to the active site. Q144A and R154C/L160A mutants were less stimulated by reductive acetylation than other mutants and native PDHK2. Nov3r binds to where lipoyl goup binds PDHK2. Using E1 alone as substrate, Nov3r binding caused a 20% increase of kinase activity at low levels. Nov3r binding also reduced the inhibition of DCA/pyruvate with elevated K^+ plus Pi.

Table of Contents

List of Figures

Chapter 1

Chapter 2

List of Tables

Chapter 1:

Chapter 2:

List of Abbrevations

PDHK2, pyruvate dehydrogenase, isoform 2

DCA, dichloroacetate

E2, dihydrolipoyl acetyltransferase

PDC, pyruvate dehydrogenase complex

E1, pyruvate dehydrogenase

E3, dihydrolipoyl dehydrogenase

E3BP, E3 binding protein

PDHK, pyruvate dehydrogenase

PDHP, pyruvate dehydrogenase phosphatase

L1, amino-terminal lipoyl domain of E2

L2, inner lipoyl domain of E2

L3, lipoyl domain of E3BP

B, E1 binding domain

B', E3 binding domain

I, carboxyl terminal domain of E2

I, carboxyl terminal domain of E3BP

ΔBE2, E2 without B domain

GST, glutathione-S-transferase

IPTG, isopropyl-β-D-thiogalactopyranoside

Hepes, N-[2-hydroxyethyl] piperazine-N'-[2-ethanesulfonic acid]

Tris, hydroxymethylaminoethane

Acknowledgements

I wish to thank Dr. Thomas E. Roche for his expert mentorship and help in leading me into the field of life science and giving me his excellent academic guidance and perennial support. I also like to thank Dr. Roche for his great patience in teaching me to write this thesis. The help provided by him will be very beneficial in my life in many respects. I also want to thank my committee members: Dr. Anna Zolkiewska, Dr. Michael Kanost and Dr. Rollie Clem for their gracious help and service on my committee. I also owe a lot of thanks to the entire faculty, supporting staff and colleagues in the Biochemistry Department for their guidance and kindness.

At the same time, I also want to thank all previous and current members of Dr. Roche's lab, especially Dr. Yasuaki, Hiromasa, who finished these works involving CD spectra, AUC, fluorescence spectra and fluorescence quenching. Without their help, this work could not be complete. Your friendships will never be forgotten.

Dedication

This degree is dedicated to my mother Guorong He, who brought up me in a difficult time, and the rest of my loving family and relatives for their support and encouragement. This degree is also dedicated to my loving wife, Shufei Zhuang, who encouraged me to pursue my goals and took care of our son.

Characterization of human pyruvate dehydrogenase kinase isoform 2 (PDHK2)

Chapter 1

General Introduction

PDC reaction and its components

The mitochondrial pyruvate dehydrogenase complex (PDC) catalyzes the irreversible oxidative decarboxylation of pyruvate to acetyl-CoA (Fig. 1-1). It results in the irreversible loss of glucose carbon and controls the metabolic fate of pyruvate acid and carbohydrate fuels in general as animals lack the means of converting acetyl-CoA to glucose (1, 2, 3). The PDC reaction connects glycolysis to oxidative metabolism to provide the oxidative fuel for the generation of ATP. The PDC reaction also provides acetyl-CoA for fatty acids synthesis in fat synthesizing tissues when carbohydrate intake is excessive.

Mammalian PDC is a huge complex with several components: pyruvate dehydrogenase (E1), dihidrolipoyl transactylase (E2), E3 binding domain (E3BP) and dihydrolipoyl dehydrogenase (E3) (see Table 1-1) (1). E1 catalyzes the irreversible first step of PDC reaction (4, 5) and also the second step (Fig. 1-1). It decarboxylates pyruvate and forms hydroxyethylidene-TPP intermediate (step 1), followed by reductive acetylation of lipoamide group of the E2 to form acetyl-dihydrolipoamide-E2 (step 2). E2 then catalyzes the transfer of acetyl group to CoA to form acetyl-CoA and dihydrolipoamide-E2 (step 3). E3 oxidizes dihydrolipoamide group back to lipoamide using a tightly bound FAD group on E3 (step 4). Finally, reduced E3 is re-oxidized with the transferring of protons and electron to NAD^+ to form

NADH (step 5). The PDC reaction exemplifies how intermediate channeling in a multi-enzyme system can achieve high efficiency of catalysis. The lipoyl-lysyl arm and flexible linker regions of E2 and E3BP give mobility for intermediate carrier to access directly the active sites of E1 and E3, therefore greatly enhancing the efficiency of reactions.

E1 is a hetero-tetramer with two α subunits and two β subunits (4, 5). E1 has two active sites, each is located between one α subunit and one β subunit. In each active site, there is a non-covalently bound thiamine pyrophosphate (TPP) cofactor and a Mg^{2+} ion. The active sites of E1 are chemically equivalent but catalysis proceeds asynchronously at the two active sites. Kinetic, crystallographic, and spectroscopic evidence supports an alternating-site mechanism for E1 (4-7). Crystal structure of *B. stearothermophilus* E1 reveals a solvated tunnel containing four Asp and six Glu residues, which connects the two active sites. This acidic tunnel can serve as a proton wire to shuttle a proton from one active site to another. This proton-wire mechanism is also proposed to explain "half of the sites" phenomena in E1 reaction (4). A flip-flop mechanism has also been suggested in which the two active sites affect each other and perform alternate phases of the catalytic reaction at given moment (5-7). The major difference between these two alternative mechanisms is that communication of active centers is linked either to proton transfer with no major structural changes in the proton-wire mechanism or to structural changes that switch on or off the alternative active site in the flip-flop mechanism.

The core of mammalian PDC is an integrated structure formed by association of the multi-domain E2 and E3-binding protein (E3BP). E2 subunits have four globular domains: inner domain (I) in the C-terminal end, E1 binding domain, and two lipoyl domains (L1 and L2) in the N-terminus (Fig. 1-2) (8). E3BP has single lipoyl domain (L3) at its N-terminus, a C-terminal inner domain (I') and E3 binding domain (B') between them (9). These globular domains of E2

and E3 are connected by flexible linkers or hinge regions that make it easy for rapid and flexible movement. Yeast E2 forms a pentagonal dodecahedron 60mer using I domains and I' domains of E3BP associate with this inner core (10). Based on small-angle X-ray scattering, cryoelectron microscopy and analytical sedimentation analyses, a model for the inner core of human E2-E3BP (also called E2BP) was proposed to be composed of 48 E2 I domains and 12 E3BP I' domains while keeping the dodecahedron shape and symmetry (11). The lipoyl groups of lipoyl domains varied between oxidized, reduced or acetylated forms during PDC reactions. The lipoyl domains also bind to PDHK and PDHP isoforms (Fig. 1-2) and play important roles in their regulation (8-10).

PDC activity regulation

PDC activity is firmly controlled so tissues can adjust to different energy sources (1-3, 12). When there is abundant carbohydrate, PDC is activated for tissues to use glucose as the energy source (2). While under starvation conditions, PDC activity is down regulated to lower the use of glucose in most tissues to conserve glucose for use by neural tissues, which use glucose as the major energy sources. PDC activity is also down regulated in animals that are fed a high fat diet (3).

E1 catalyzes an irreversible and rate-limiting step in pyruvate reaction (4, 5). It is the major target in the regulation of PDC activity. The primary means of control of PDC activity is by the co-valent modification of E1 (13-16). Pyruvate dehydrogenase kinase (PDHK) phosphorylates α subunit of the E1 tetramer to inactivate it. Pyruvate dehydrogenase phosphatase (PDHP) dephosphorylates inactive E1 to recover PDC activity (Fig. 1-3).

There are 4 isoforms of human PDHK and two isoforms of human PDHP (Table 1-1) (17-21). PDHK1 is expressed in heart, pancreatic islets and skeleton muscle (17-21). PDHK2 is

widely distributed in heart, liver, kidney and most other organs (17-21). Distribution of PDHK3 is relatively limited. It is expressed in testis, kidney and brain (17-21). There is low endogenous PDHK4 in heart, skeletal muscle, liver, kidney and pancreatic islet that is increased when carbohydrate stores are reduced (18). PDHP1 is expressed in most tissues. It needs Mg^{2+} and is stimulated by Ca^{2+} (20, 22, 23). PDHP2 is expressed in liver, kidney, brain and heart. It is not activated by Ca^{2+} (20).

There are three serine residues in each α subunit of E1 that can be phosphorylated by PDHKs: Serine 264 (site 1), Serine 271 (site 2) and Serine 203 (site 3) (24). Phosphorylation of only one site in an E1 tetramer (total six potential phosphorylation sites) causes inactivation of E1 demonstrating half-of-the-sites-inactivation (6, 25). Using mutants E1 with only a single site available to be phosphorylated, site-specificity and phosphorylation rates were measured for individual PDHK isoform (14, 16, 26, 27). Site 1 and 2 can be phosphorylated by all PDHK isoforms, while site 3 can only be used efficiently by PDHK1. All PDHK isoforms, apart from PDHK3, have higher rates of phosphorylation of site 1 than site 2. For site 1, the relative rates of phosphorylation are in the order PDHK2>PDHK4>PDHK1 >PDHK3. For site 2, the relative rates of phosphorylation are in the order PDHK3> PDHK4> PDHK2>PDHK1. The rate of phosphorylation on site 3 by PDHK1 is close to its rate on site 2 but far slower than on site 1. Using native E1 as substrate, Kasten S.A. found that both PDHK3 and PDHK2 had higher activity (7 fold and 20 fold) on site 1 than on site 2. There was also significantly more phosphorylation at site 2 by PDHK3 than PDHK2 in the presence of E2, although phosphorylation at site 2 was relatively slow for both kinases in the absence of E2 (Kasten, S.A. PhD thesis). All sites were shown to be phosphorylated to a different extent with more phosphorylation of site 1 and less phosphorylation of site 2 and 3 *in vivo* (28). Both PDHP1 and

PDHP2 can remove the phosphates from all three sites with the order of dephosphorylation rates site 2 > site 3 ≈ site 1 using mutant E1 as substrate (20).

E2 influence on PDHK activity

E2 plays important roles in the functional regulation of PDHK activity (8, 29). Using micromolar levels of E1, PDHK2 activity is enhanced several fold in the presence of E2. The enhancement of PDHK2 activity by E2 was greatly increased when nM levels of E1 were used (~5000 fold) (Hiromasa, Y. *et. al.*, unpublished data from our lab). To accomplish this, PDHK must be bound by lipoyl domains of E2. PDHK activity is enhanced because an E2-bound kinase greatly gains in access to E2-bound E1. When ΔBE2 (E2 constructs with E1 binding domain deleted) is used, there is only a 22% increase in PDHK2 activity (30). Different PDHK isoforms have different binding preferences for different lipoyl domain and activity enhancement (Fig. 1-2) (31-39). PDHK1 can bind to both L1 and L2 domain in E2. Bovine kidney PDHK2 prefers to bind to L2 domain of E2. Human PDHK2 also preferred to bind to L2 with increased activity (32, 34). Purified PDHK3 is not stable and tends to self-associate. L1 has minimal influence on PDHK3 activity. GST-L1 causes 2-fold activity increase. Both L2 and GST-L2 enhance PDHK3 activity 7-8 -fold comparing with 17-fold activation by E2 (32). Hiromasa, Y., *et. al.* found that PDHK3 could be a stable dimer at 4 °C by using freshly prepared PDHK3 and removing aggregate by gel-filtration (unpublished data from our lab). This form of PDHK3 was very active but underwent a lesser activity enhancement by GST-L2 or E2. These findings suggests that PDHK3 that undergoes significant activity enhancement by L2 contains abundant aggregates that are prevented or reversed by binding to L2 to contribute to the large enhancement of activity. In agreement with this, L2•PDHK3 is a stable dimer (Peng, T. PhD thesis). Human PDHK4 has the highest activity with E1 alone among all PDHK isoforms (Dong, J. PhD thesis).

PDHK regulation

There are two kinds of regulation of PDHK activity: short-term control and long-term control (2). In short-term control, small molecular effectors including the substrate and products of PDC reaction directly influence the activity of PDHK (Fig. 1-3). In long-term control, the mRNA and protein levels of PDHK are regulated.

Among all PDHK isoforms, PDHK2 is the most responsive isoform to the known effectors (19, 21, 30, 32, 40). Pyruvate, substrate of PDC reaction, directly binds and inhibits PDHK2 activity. Catalysis by TPP-loaded E1 involving either partial reactions or the first two steps of PDC reaction deplete pyruvate and produce intermediates that affect PDHK activities (below). DCA (dichloridacetate), an analog of pyruvate (41), is widely used to study inhibition at this site in PDHK because DCA cannot be used as substrate by E1 (42, 43). In comparison to PDHK2, the activity of PDHK3 is relatively insensitive to pyruvate inhibition (21, 32). Human PDHK4 is sensitive to DCA inhibition (Dong, J., PhD thesis). Elevated ADP and Pi levels, indicators of a lowered energy state, inhibit the activities of PDHK isoforms (32). ADP dissociation appears to be the rate-limiting step of PDHK2 reaction in the presence of E2. ADP plus DCA or pyruvate (using E1 free of TPP) show coupled binding and synergistically inhibit PDHK2 (40).

NADH and acetyl-CoA, products of the PDC reaction and also fatty acid oxidation, stimulate PDHK activity. When fatty acid oxidation produces abundant NADH and acetyl-CoA, this stimulation of PDHK activity down-regulates PDC activity (2). NADH nearly doubles PDHK2 activity through reducing lipoyl groups of E2. AUC data demonstrate that lipoyl domains with reduced prosthetic groups bind tighter to PDHK2 (34). NADH plus acetyl-CoA support more than 3.5-fold stimulation of PDHK2 by reductive acetylation of lipoyl groups.

Reductive acetylation speeds up the dissociation of ADP to increase PDHK2 activity (30). NADH and acetyl-CoA also stimulate PDHK1 but increase PDHK3 activity only in the presence of ADP (32). Our work on PDHK4 show that there is no NADH and acetyl-CoA stimulation on modified human PDHK4, in which Gly-Glu-Glu residues are added to its C-terminus. NADH and acetyl-CoA stimulation is found using unmodified PDHK4 (Dong, J., PhD thesis). These data suggest that the C-terminal region plays an important role in the stimulation of PDHK activity by reductive acetylation.

In the long-term control, mRNA and protein levels of PDHK isoforms vary in response to nutritional states and endocrine manipulations. The combination of up-regulation of PDHK and short-term stimulation of PDHK activity decrease the activity of PDC in order to conserve glucose for the brain and other central neural system. Expression of PDHK2 is increased in liver (44, 45) and kidney (45, 46) during starvation. PDHK4 mRNA is increased 2 to 4- fold in the kidney, liver, white adipose tissue, and brain of starved rats (45, 47). PDHK4 is the major isoform over-expressed in muscle tissues (3, 48-52). Up-regulation of PDHK4 is also observed in rats fed a high fat (low carbohydrate) diet (3, 16, 53), and due to diabetes (48, 54, 55) or carnitine deficient rats (56). Transcription of PDHK4 is rapidly activated before those genes involved in fatty acids metabolism when mice are treated with fibrates, which are used clinically to reduce triglyceride levels (57). Apart from the increased expression of PDHK4, PDHP2 levels are also lowered in heart and kidney of starved rats (58). Re-feeding of starved rats decreases the PDHK4 mRNA level and protein amount of PDHK4 portion in heart (46). Insulin treatment of diabetic rats reduces PDHK4 mRNA and protein to non-diabetic levels. Insulin has no effect on PDHK1 but causes small decreases in heart PDHK2 levels in diabetic rats (46).

PDHK4 gene control

PDHK4 is the major target of long-term control of PDHK (see above). Histone deacetylase inhibitors retinoic acid and trichostain A increase the transcription of human PDHK4 (59, 60). Peroxisome proliferator-activated receptors (PPARα, δ, β/δ), lipid-activated transcriptional factors involved in lipid storage and catabolism, are suggested to be involved in PDHK4 gene regulation. Glucocorticoids dexamethasone and WY 14,643 (an agonist of PPARα) promote expression of PDHK4 (61, 62). PPARα mRNA level is 7-17 fold enriched in heart and liver of starved mice. The capacity of starvation to induce increases of heart and liver PDHK4 is less in PPARα knockout mice than in wild type mice. However, there is no difference in the starvation-induced increase of expression of skeletal muscle PDHK4 (63). A highly selective PPARδ agonist also increased expression of PDHK4 (63, 64). siRNA for PPARβ/δ gene significantly reduced transcription of PDHK4 (90%), PDHK2 (33%) and PDHK3 (21%) (65). The level of peroxisome proliferators-activated receptor gamma co-activator (PGC-1α), a transcriptional co-activator of PPARγ, is elevated in diabetic rat liver, leading to increasing mitochondrial biogenesis and speeding up fatty acid oxidation. PGC-1α elevates PDHK4 transcription by 14-fold (possibly through PPARα but not PPARγ) (66). Hepatic nuclear factor-4 (HNF4), a nuclear glucocorticoid receptor (GR) that interacts with PGC-1α, also stimulates both rat and mouse PDHK4 gene transcription (66). A model (Fig. 1-4) is proposed to explain the glucocorticoid-induced stimulation and insulin inhibition of transcription of PDHK4 (67). There are two glucocorticoid response elements (GRE) and three insulin response sequences (IRS) in the human PDHK4 promoter. When treated with glucocorticoid, activated GR is translocated into the nucleus to recruit P300/CBP complex (histone acetyltransferases). The whole complex then binds to GRE in PDHK4 promoter through dimerized GR. At the same time, P300/CBP complex also binds to FOXO (Forkhead Box factors) that in turn binds to IRS (Fig. 1-4A). The

whole complex stimulates the transcription of PDHK4. Insulin prevents the binding of FOXO to IRS, breaking the complex to decrease the transcription of PDHK4 (Fig. 1-4B).

PDHK structure

PDHK isoforms add phosphate to serine residues in E1. However, PDHK isoforms lack the characteristic structural motifs of general eukaryotic serine/threonine kinases (18, 68-70). Instead they are more like bacterial histidine kinases (70-75). PDHK monomer can be divided into two domains: N-terminal regulatory domain (R domain) and C-terminal catalytic (Cat) domain (75). In human PDHK2 (76), the R domain includes residues 1 to 171. It contains 8 α helices connected by flexible loops. There is a flexible loop from Ser171 to Pro177 that connects the R domain to the Cat domain. The Cat domain (178-360) of PDHK2 is an αβ mixed secondary structure (74, 76). There are five β-strands, which form a single β-sheet.

PDHK2 is a dimer in solution (33, 34). The crystal structures of human (76) and rat (74) PDHK2 show that the major contacts supporting dimerization are formed between the β-sheet regions of Cat domain of two monomers (Fig. 1-5). Interactions between helix α11 and the loop connecting β5 and β6 from the other subunit also contribute to dimer formation. The C-terminal tail beyond the Cat domain can also contribute to the formation of dimer in human PDHK2. Each C-terminal tail (from residues Val 360 to Cys 384) first extends along the R domain of the same subunit and then forms a cross arm extending across to the other subunit (Fig. 1-5) (76). Trp383 from one tail is inserted between Arg 362 on same C-terminal tail and Arg 149 (on helix 8) of the other subunit. Residue Cys 384 from one tail is sandwiched between Pro 22 (on loop between helix 1 and helix 2) and Val 365 (on C-terminal tail) of the other subunit. These interactions act to anchor the cross arm. In the crystal structure of rat PDHK2•ADP (74) and human PDHK2•ADP•DCA (76), the cross arms were not resolved.

At the ends of the PDHK2 dimer, there is a large solvent exposed cleft between the R and Cat domains within each subunit that contains the active site of PDHK2 (74, 76). At the bottom of the cleft, helices α7 and the C-terminus of α8 of the R domain form one side of a groove and the N-terminus of helix α10 and helix α12 from Cat domain form the other side of the groove.

The ATP or ADP binding sites are formed by segments from the Cat domain β-sheet, α helices and loops (Fig. 1-6). A conserved G1 box (Asp-282-X-Gly284-X-Gly286) on the loop connecting β6 and α11 binds to the adenine part of ADP or ATP. Another conserved motif, G2 box (Gly317-X-Gly319-X-Gly321), located in the C-terminal end of the loop connecting helices α11 and α12, forms parts of the catalytic site through binding of α and β phosphate of ADP or ATP. A third conserved N-box (Glu243-X-X-Lys246-Asn247) on helix α10 binds to the Mg^{2+} ion using Asn247, Glu243 and two water molecules. Human PDHK2 was crystallized under conditions that included minimal K^+ (76). Crystal structures of related branch-chain α-ketoacid dehydrogenase (BCKD) kinase (72) and PDHK3 (77-79) show that a K^+ ion is involved in nucleotide binding. Knoechel *et. al.* proposed that a K^+ ion is also located in the catalytic site of PDHK2 (see below) (76).

The overall crystal structure obtained for PDHK3 is similar to PDHK2 (77). The crystal structure of PDHK3/L2 also resolved how lipoyl domain bound to kinase. The lipoyl domain binding includes both hydrophobic interactions in the lipoyl prosthetic group binding pocket and electrostatic interactions in the other parts of the R domain and also helix α13 of the C-terminal tail. The hydrophobic pocket for lipoyl group binding is formed mainly by helices α1/α2, the loop connecting them and also the C-terminus of helix α8. Residues 389 to 393 of the C-terminal tail from the other subunit are also part of this pocket. Substitutions of residues in this pocket (Leu19A, Phe27A and Phe40A) weaken the binding affinity for L2 and the activity of kinase

were less enhanced by L2 (79). The electrostatic interactions are formed by positive residues of the helices α1/α13 with acidic residues in the lipoyl domain. These positive residues (Arg13, Lys366 and Arg370) are conserved or replaced by other positive charged residues in all PDHK isoforms. They form electrostatic interactions with the acidic residues on L2 (Glu162, Asp164, Glu179, Glu182 and Glu183). Mutation of Glu162 and Glu179 on L2 weakened the binding of L2 to PDHK3 and decreased the capability of L2 to activate PDHK3 (79) as previously reported (8).

The resolution of the C-terminal tail of PDHK3 (77) is informative because the C-terminal tail beyond Cys384 of PDHK2 is not resolved for rat (74) and human PDHK2 (76). Residues 378 to 383 of the C-terminal tail of one subunit form several hydrogen bonds with conserved residues of the other subunit in the PDHK3 dimer. There are two important hydrogen bonds formed by Asn383 with Asp399 in the same subunit and Ser382 from one subunit with Leu361 on the other subunit. Both hydrogen bonds are eliminated in other PDHK isoforms with substitution of Ser382 by cysteine and Asp399 by valine or isoleucine, as the side chain of cysteine is a poor hydrogen donor and valine or isoleucine are unable to form hydrogen bonds.

Residues 384 to 389 make contacts with L2 residues around lipoyl-Lys173 in PDHK3. Arg389 of PDHk3 can form 2 hydrogen bonds with Asp172 on L2 instead of a possible single hydrogen bond as lysine replaces Arg389 in other PDHK isoforms. Three interactions involving the C-terminal tail with structural adjacent groups help to stabilize the C-terminal region from 389 to 393 that are part of the lipoyl group binding pocket: 1) Hydrogen bond between Arg389 and Gln23, 2) Hydrogen bond between Ser392 and Asp30, and 3) Electrostatic interaction between Asp390 and Lys393. In other PDHK isoforms, some or all of these residues are substituted by residues that cannot maintain these interactions. Therefore their binding to lipoyl

domains would be weakened as it is found that PDHK3 has the highest binding affinity to L2 (8, 32, 33). The importance of the C-terminal tail in the tighter binding of PDHK3 to L2 was demonstrated with a series of deletions in this region (79). Deletion of PDHK3 from Glu387 to the C-terminus resulted in significantly weaker binding between PDHK3 and L2. Further deletion (from 384 to 366) almost abolished the binding of PDHK3 to L2. Although the C-terminal tail of PDHK2 was not resolved (74, 76), it is important for the activation of PDHK2 by E2. Deletion of the C-terminal tail from 386 to the C-terminus abolished the activation of PDHK2 by E2 (37).

Research focus

Previous studies on PDHK indicated that elevated K^+ and Pi significantly altered the capacity of effectors to influence the kinase activity (32). Elevated K^+ lowers the K_m for ATP with an equivalent decrease in k_{cat} and causes stronger inhibition by ADP and DCA (40, 80). Steady-state kinetic studies indicated that pyruvate/DCA bind efficiently to the PDHK2•ADP intermediate while also bind to the PDHK2•ATP (40). Fluorescence quenching studies found that ADP bound tighter in the presence of pyruvate or DCA while pyruvate/DCA binding were also much tighter in the presence of ATP or ADP (43). The combination of pyruvate plus ADP greatly weakens the binding of the lipoyl domain to PDHK2 (43). NADH and acetyl-CoA stimulation by reductive acetylation of L2 requires elevated K^+ and Cl^- ions and is enhanced by Pi (30, 32). But the molecular mechanism supporting the communication between the catalytic site, the DCA/pyruvate binding site and the lipoyl domain-binding site was not understood. As previous studies on PDHK2 generally used E1•E2 as substrate, it is not clear how those interactions influence the PDHK2 activity. Using E1 alone as substrate would eliminate the E2 interference. It is also not clear how K^+ or Cl^- influences the activity of PDHK2. At the same time, although a DCA binding site is indicated in the crystal structure of human PDHK2•ADP•DCA, it has not been established whether this site represents a physiologically functional DCA-binding pocket or which residues are most important for binding.

The specific aims of this thesis include:

1) To study the DCA/pyruvate binding pocket of PDHK2 using site-specific mutagenesis.
2) To evaluate inhibition of PDHK2 activity using E1 alone as substrate.
3) To study how K^+ and Cl^- ions influence PDHK2 activity.

4) Using Nov3r to better understand the communication between the lipoyl group binding site and the DCA binding site and the catalytic site.

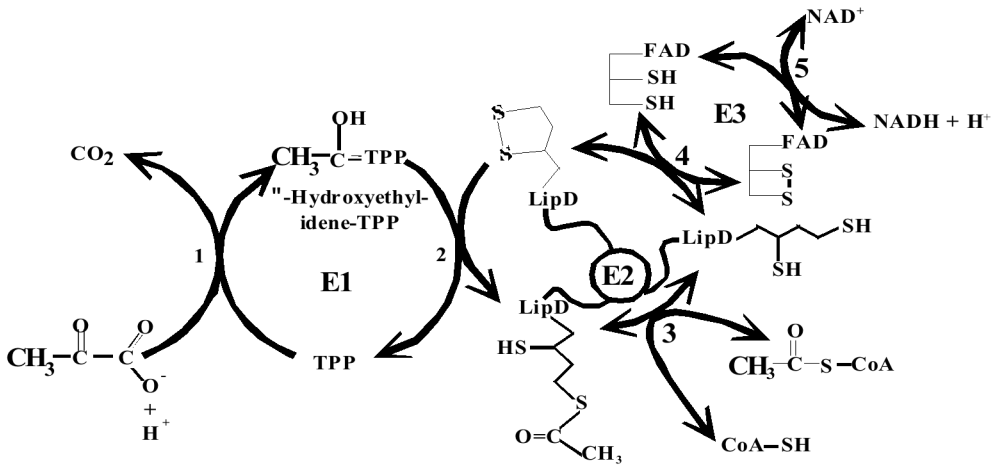

$$\text{Pyruvate} + \text{CoA} + \text{NAD}^+ \longrightarrow \text{acetyl-CoA} + \text{CO}_2 + \text{NADH}$$

Figure 1-1. Overall reaction of the pyruvate dehydrogenase complex (PDC). E1 catalyzes decarboxylation of pyruvate (step 1) and reductive acetylation of lipoyl groups on E2 lipoyl domains (lip D) (step 2). E2 catalyzes transferring of acetyl group to CoA (step 3). E3 oxidizes reduced dihydrolipoamide groups back to oxidized form (step 4). Re-oxidation of E3 (step 5) is catalyzed by E3 with reduction of NAD^+.

Table 1-1. Components of mammalian PDC. The molecular weights, component oligomeric states and stoichiometries in the nature complex are given with the best estimates to date. * E2 can form 60mer by itself but mammalian E2BP core is a 60mer with 48 E2 and 12 E3BP.

Protein		Molecular weight	Component oligomeric state	Stoichiometry of complex
PDC reaction enzymes				
E1			tetramer α2β2	20-30
E1α		40,183		
E1β		30,863		
E2BP				48E2 + 12 E3BP
E2		59,551	60mer *	
E3BP	48,040			
E3		50,216	dimer	12 maximal
Regulatory enzymes				
PDHK1		48,391	dimer	
PDHK2		45,066	dimer	
PDHK3		45,883	dimer	
PDHK4		46,230	dimer	
PDHP1			αβ	
PDHP1c	α	52,625		
PDHP1r	β	95,656		
PDHP2		52,396	unknown	

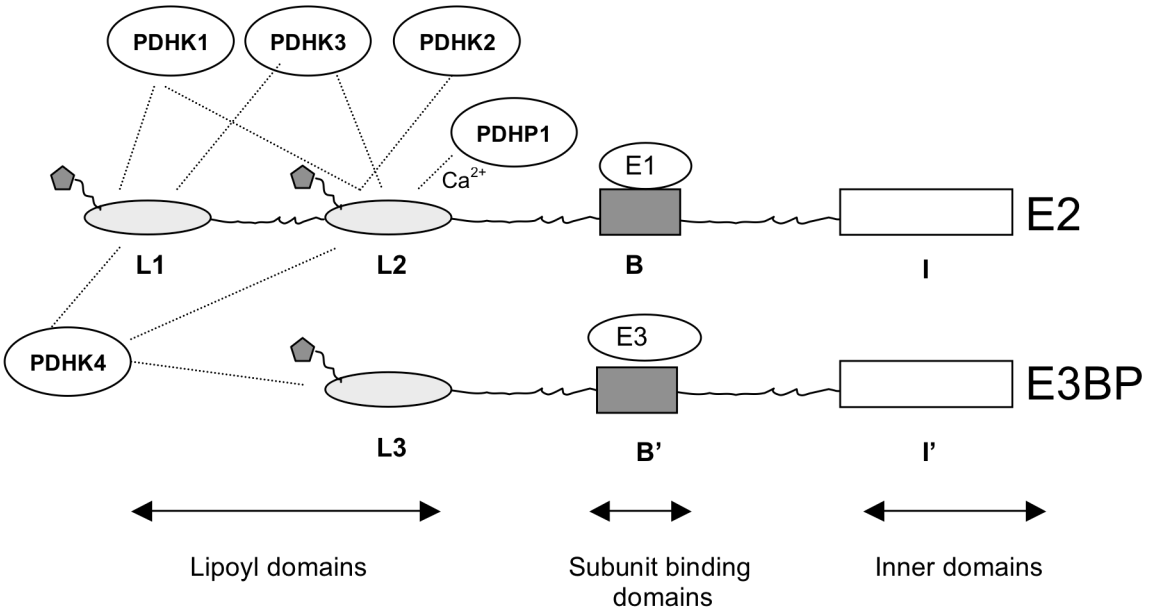

Figure 1-2. E2 and E3BP domains and their binding interactions. E2 subunit domains: L1, n-terminal lipoyl domain; L2, inner lipoyl domain; B, E1 binding domain; I, oligomer-forming, acetyl-transferase catalyzing domain. E3BP domains: L3, N-terminal lipoyl domain; B', E3 binding domain; I', inner domain which associates with the inner domain of E2. Dotted connections indicate binding interactions to kinase isoforms (PDHK1, PDHK2, PDHK3, PDHK4) and PDHP1.

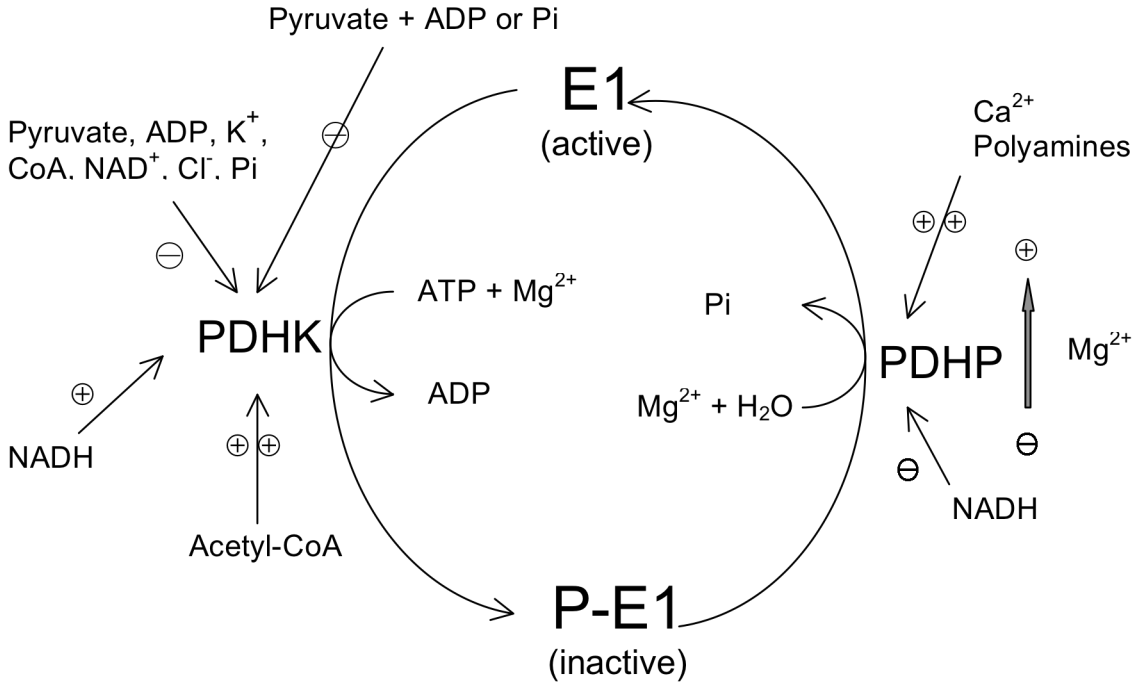

Figure 1-3. Regulation of PDC reaction by reversible phosphorylation. Sign ⊕ indicates enhancing of the activity of regulatory enzymes. Sign ⊖ indicates that activities of regulatory enzymes are inhibited. Double signs imply larger effects.

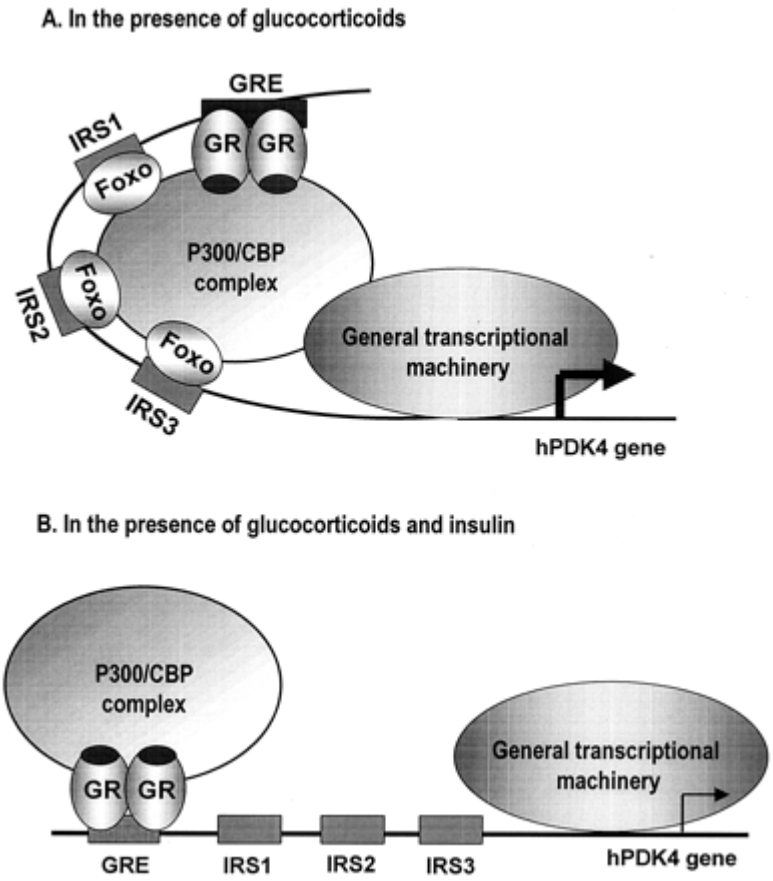

Figure 1-4. A model for hPDHK4 gene regulation. GRE is the glucocorticoids response element on the hPDHK4 promoter. There are three insulin response sequences (IRS) on the hPDHK4 promoter. A: In the presence of glucocorticoids, GRE recruits the glucocorticoids bound and dimerized glucocorticoids receptors (GR), which in turn bind to the P300/CBP complex (histone acetyltransferases). Forkhead Box factors (FOXO) also bind to IRS and P300/CBP complex. The whole complex interacts with transcriptional machinery to increase transcription of hPDHK4 gene. B: In the presence of both glucocorticoids and insulin, binding of FOXO to IRS is disrupted. Thus transcription of hPDHK4 is decreased to normal levels. Kwon, H., *et al.* *Diabetes*. (2004) 53, 899-910. (67)

Figure 1-5. Structure of Apo-PDHK2 dimer. The helix α8 (in orange color) spans the regulatory (R) domain. The Cross arms (360-385) are shown in yellow color. Tryptophan residues are shown in red color. W383 is inserted between R149 and R362 (green).

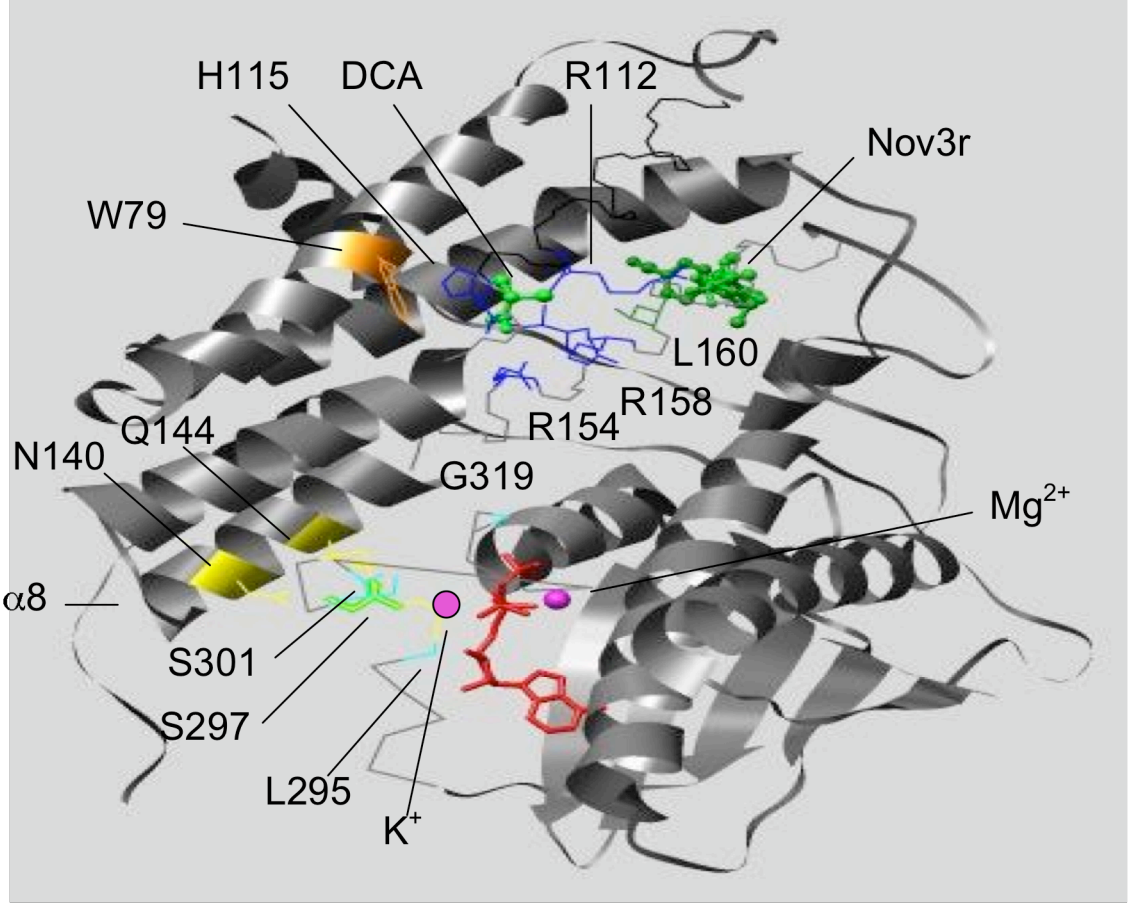

Figure 1-6. Structure of PDHK2•ATP•DCA•Nov3r. ATP (red) binds to the catalytic (Cat) domain. Residues involved in K^+ binding are shown in cyan. Yellow color indicates residues interacting between the R domain and the Cat domain (N140, Q144 from α8 of the R domain and S297, Y298, F296 from the Cat domain). DCA and Nov3R are shown in green. Residues involved in DCA site are shown in blue (R112, H115, R154, I157, R158). L160 (light sea green) is at the bottom of the Nov3r (also lipoyl group) binding site. W79 is shown in orange. The ions involved in the ATP/ADP binding are shown in purple.

Chapter 2: Characterization of human PDHK2

Abstract

Using kinetic assays, analytical ultracentrifugation (AUC) studies and fluorescence quenching of intrinsic tryptophan by bound ligand, the role of several residues that are located in the α8 helix of the R domain of PDHK2 in K^+ binding, DCA/pyruvate inhibition and stimulation by reductive acetylation were evaluated using site-specific mutations. One of these mutants, L160A, was inactive. Other mutants, including double mutant R154C/L160A, were active and maintained the capacity to bind to L2 based on the AUC studies and activity enhancement by E2. Elevated K^+ and Cl^- reduced the specific activities of native and wild type PDHK2 with a smaller decrease for R158A, R154C/L160A and Q144A with or without E2. Mutation of the cross arm anchoring W383 caused almost two-thirds decrease of Trp fluorescence. ADP or ATP binding at the active site quenched the fluorescence of native kinase but not the fluorescence of W383F. Pyruvate also quenched the fluorescence of not only native kinase but also W383F, to a much less extent. Therefore, W383 provides the majority of intrinsic Trp fluorescence and its fluorescence is sensitive to ligand binding.

The Q144A mutants had very different response to K^+ binding at the active site. The specific activity of Q144A increased 2-fold with 10 mM K^+ and then decreased at higher levels of K^+ using E1 as substrate. Based on the fluorescence quenching by ATP/ADP binding, the Q144A mutation caused weaker K^+ binding with ATP but did not alter the weaker K^+ binding with ADP unless Pi was included. With 100 mM K^+, the Q144A mutation weakened ATP but not ADP binding along with a 2-fold effect of Pi in enhancing ADP binding.

Pyruvate or DCA weakly inhibited the specific activities of the R154C, R158A and R154C/L160A mutants. In AUC studies, pyruvate plus ADP caused no significant dissociation

of GST-L2 from these mutants. The importance of both R154 and R158 was also confirmed by the lack of pyruvate-enhanced fluorescence quenching of the above mutants by ADP. Cl^- inhibited the activities of R154C/L160A and R158A relatively weaker than the native kinase activity. Cl^- also reduced the DCA or pyruvate inhibition with or without E2. All of these data could be fitted into a model where Cl^- binds to same site as DCA/pyruvate and competes with them.

Q144 (through K^+ binding) and L160 (by interaction with acetyl-lipoyl group) may play important roles in the signal transmission from the lipoyl group-binding site to the active site because Q144A and R154C/L160A (but not R154C) were less stimulated by reductive acetylation than the other mutants and native PDHK2. Nov3r binding at the lipoyl group binding site reduced but did not eliminate the inhibition of DCA/pyruvate at nearby DCA/pyruvate site with elevated K^+ plus Pi. Nov3r appeared to not significantly affect the inhibition by Cl^- at the same site.

Introduction

PDHK2 is the most widely distributed of the four PDHK isoforms. Numerous studies have been done on the influence of PDHK2 activity by effectors such as pyruvate, DCA, ADP, K^+, Cl^-, Pi, NADH and acetyl-CoA (19, 21, 30, 32, 40). It has been found that PDHK2 is the most responsive isoform to these known effectors.

In a MOPS-K^+ buffer containing physiological concentration of K^+ and Cl^-, the specific activity of PDHK2 is less than 10 $nmol \cdot min^{-1} \cdot mg^{-1}$. The activity of PDHK2 increases ~ 10-fold in the presence of E2 under the same conditions (32). Constructs of L1, L2 and L1-L2 have weak binding to the PDHK2 while dimeric construct GST-L2 binds more tightly to PDHK2 (34). Lipoyl domain binding alone increases PDHK2 activity less than 30%. The activity of PDHK2

increases only 20% when ΔBE2, in which E1 binding domain is deleted, is used (30). At the same time, constructs of L2-E1BD (L2 with the E1 binding domain) and L1-L2-E1BD increase the activity of PDHK2 almost up to the same level as in the presence of E2 (36). These data suggest that co-localization of PDHK2 and E1 is the major reason for PDHK2 activity increasing in the presence of E2. The large activity increase in the presence of E2 is the result of lipoyl domain-bound PDHK2 gaining access to E2-bound E1.

Pyruvate, the substrate of the PDC reaction, is an inhibitor of PDHK2. Because pyruvate can serve as a substrate in E1-catalyzed reductive acetylation of lipoyl groups (TPP dependent) that stimulate kinase activity, the pyruvate analog, DCA, is normally used in regulatory studies (32). In a buffer containing K^+, Cl^- and Pi, PDHK2 is poorly inhibited by DCA in the absence of E2 while DCA strongly inhibits PDHK2 in the presence of E2. Using E1 free of TPP to prevent pyruvate being used in the E1 reaction, pyruvate is a stronger inhibitor of PDHK2 than DCA in the presence of E2 (32).

Using 100 μM ATP, 200 μM ADP inhibits the activity of PDHK2 by 50% in the absence of E2 and this is not significantly changed in the presence of E2 (32). ADP binds tighter to PDHK2 in the presence of pyruvate/DCA while there is no significant change in ATP binding. On the other hand, pyruvate/DCA binding is greatly enhanced by ATP or ADP (43). Steady-state kinetic studies indicated that pyruvate/DCA binds efficiently to the PDHK2•ADP intermediate and also bind to PDHK2•ATP (40). AUC data uncover that pyruvate alone modestly weakens the binding of PDHK2 to lipoyl domain while ADP plus pyruvate greatly weakens the binding between lipoyl domain and PDHK2 (43). Thus, pyruvate/DCA inhibition is in part a result of the dissociation of lipoyl domain from PDHK2, which decreases the access of PDHK2 to substrate E2-bound E1.

Through reaction with increasing NADH:NAD^+ and acetyl-CoA:CoA ratios, oxidized lipoyl groups are converted to reduced and acetylated forms which stimulate PDHK2 activity. Stimulation of PDHK2 activity by reductive acetylation can only be observed in buffers containing elevated K^+, Cl^- and / or Pi (32, 40). Reduction of lipoyl domain alone gives ~ 1.6-fold increase in PDHK2 activity; acetylation of E2 increases PDHK2 activity up to 3.5-fold from the initial activity without effectors (32). $E2_{ox}$ in which most lipoyl groups are in the oxidized state greatly decreases the capacity of E2 to stimulate PDHK2 activity (40). It is found that GST-$L2_{red}$ with reduced lipoyl groups binds PDHK2 more than 7-fold tighter than GST-L2 with oxidized lipoyl groups (34). While the extent of binding of PDHK2 to $E2_{ox}$ is not significantly decreased from that with untreated E2, reduction of lipoyl group of $E2_{ox}$ with NADH:NAD^+ or DTT increased the binding of PDHK2 to E2 60mer (40).

An ordered mechanism in which ATP binds first and the dissociation of ADP as rate limiting step is proposed for PDHK2 in the presence of E2 with no stimulatory effectors (30, 40). Reductive acetylation of lipoyl group increases V_{max} and the K_m for ATP of PDHK2 while K_m for ATP decreases in the presence of $E2_{ox}$ (40).

The PDHK inhibitor Nov3r does not prevent the binding of ATP at the active site of PDHK. Nov3r class compounds do not inhibit the phosphorylation of peptide substrate (83). Nov3r inhibits E2-enhanced PDHK2 activity and but only slightly inhibits the phosphorylation of free E1. Nov3r appears to be an analog of acetyl-dihydrolipoyl-lysine (86). Crystal structures revealed that Nov3r and the lipoyl prosthetic group of L2 bind to PDHK2 at the same site. The mechanism for Nov3r inhibition is to prevent the binding of lipoyl domain to PDHK2 by preventing the binding of L2's lipoyl group.

Previous studies indicate that elevated K^+ and Pi significantly altered the capacity of effectors to influence PDHK2 activity (32). Elevated K^+ lowers the K_m for ATP with an equivalent decrease in k_{cat} and causes stronger inhibition by ADP and DCA (40, 80).

The crystal structure of Apo-PDHK2 dimer reveals a cross arm structure that is formed by the C-terminal tail (residues 365-384) from both subunits that is anchored by Trp383 and Cys384 (Fig. 1-6) (76). A similar cross arm has also been found in the PDHK3•L2 structure. The cross arm interacts with L2 (77). This cross arm is not resolved in the crystal structure of rat PDHK2•ADP (74) and human PDHK2•ADP•DCA, suggesting that cross arm might change with the binding of ADP and DCA. An AUC study found that pyruvate plus ADP resulted in formation of PDHK2 tetramer (43). There are three tryptophan residues in PDHK2. Apart from Trp383, Trp371 is also located in the cross arm and is exposed to the solvent. Trp fluorescence (especially of Trp383) can be a good indicator of cross arm change with ligand binding because Trp fluorescence is sensitive to changes in the surrounding electrostatic environment (81, 82).

The catalytic site, DCA binding site, lipoyl domain and lysine-lipoyl group (also Nov3r) binding site, and K^+ binding site are identified or suggested from the crystal structures of human PDHK2 (76) and PDHK3 (77) (Fig. 1-6). The ATP/ADP binding site (catalytic site) is located in the Cat domain with several conserved residues and sequence segments (termed boxes) that bind to adenine, phosphate groups and also Mg^{2+} (see above). Based on the crystal structure of PDHK3 and related BCDK, a K^+ ion is proposed to bind at the active site (76). The backbone carbonyl groups of Leu 295, Ser297, Gly319 and hydroxyl group of Ser301 were modeled to chelate K^+ ion along with α-phosphate of ATP or ADP. Gln144 from the N-terminus of α8 forms hydrogen bonds with Phe296 and Tyr298 in the Cat domain. There is also a hydrogen bond between Asn140 from α8 and Ser297 in the Cat domain. These interactions may connect

helix α8 of the R domain to bound K^+ and therefore to the ATP/ADP binding site in the Cat domain.

Based on the crystal structure of human PDHK2, the binding site for Nov3r is located at the end of the R domain at a position far from the ATP binding site (Fig. 1-6) (76). It is the same site that binds lipoyl prosthetic group based on the crystal structure of PDHK3•L2 (77). The lipoyl group binding site of PDHK2 is a hydrophobic cylindrical pocket formed by residues Leu23, Phe28, Phe31, Phe44, Leu45, Leu160, Ile167, Phe168 on helices α2/α3/α8 and other residues which are conserved in other PDHK isoforms. Based on the crystal structure of PDHK2•ATP•Nov3r (76), Leu160 is positioned next to where the CH3 group of acetyl-dihydrolipoylamide is predicted to interact in this site. This residue may play important role in the stimulation of PDHK2 activity by reductive acetylation.

The DCA/pyruvate site is located in the center of the R domain with the entry facing the extended groove of the active site cavity formed between the R and the Cat domains with conserved arginine residues Arg154 and Arg158 (Fig. 1-6) (76). The other residues forming the binding pocket are Leu53, Tyr80, Ilelll, His 115, Ser153, Ile157, and Ile161 in PDHK2. The carboxyl group of bound DCA appears to form an electrostatic interaction with Arg154 and may also interact with R158 and His115. Arg158 appears to block the entry to the DCA site in the structure with DCA bound. These residues involved in the DCA binding are highly conserved in the PDHK family with the exception of PDHK3, in which Ile157 is replaced by Phe. This replacement may be the reason for weak DCA/pyruvate inhibition of PDHK3.

From above introduction, helix α8 connects the catalytic site, the DCA site and the lipoyl group binding site (Nov3r site). It may play important role in the communicating effects between

these sites. To understand the communication, site-specific mutagenesis was used to test the importance of specific residues on helix α8.

Materials and Methods

Materials

Recombinant human E1, E2 and E3 were prepared as previous reported (32). Using KOD Hot Start DNA polymerase (Novagen), mutagenesis was conducted on human PDHK2 using a two-step PCR procedure. The primers used for mutation were listed in Table 2-1. T7 and T3 primers were sequencing primers that flank the cDNA of human PDHK2 in the vector PET28a (Novagen). The forward and reverse primers for specific mutants had a complementary sequence. In the first-step PCR, T7 and T3 were coupled separately with reverse and forward primers for specific targeted residues to get the cDNA segments encoding the N-terminal part and C-terminal part of mutant PDHK2. The cDNA fragments from first PCR were purified for using in the second PCR. In the second step, products of the first-step PCR denatured, annealed using the complementary bases and then extended using each other as template to get a full-length cDNA for individual mutant. The whole full-length mutated cDNA was then amplified by PCR using T7 and T3 as primers also in the second PCR (Fig. 2-1). The amplification cycle was set as following for PCR of both steps:

Initial denature: 95 °C, 10 min.

Elongation cycles: 95 °C, 25 s; 50 °C, 25 s; 70 °C, 40 s. Total 25 cycles

Final extension: 70 °C, 10 min.

The final products were purified and cut by restriction enzymes *XbaI* and *HindIII* (New England Biolabs) and inserted into expression PET28a plasmids (Novagen) treated with the same restriction enzymes. The introduction of each mutation was confirmed by sequencing.

Table 2-1. Primers used for site-specific mutagenesis. T7 and T3 are vector sequences flanking hPDHK2 cDNA in previous PDHK2 vector (32). Mutant-introducing bases are in bold.

T7: TAATACGACTCACTATAGGG

T3: GCTAGTTATTGCTCAGCGG

Q144A:

Forward: CCAGAACATC**GCG**TACTTCC

Reverse: GGAAGTA**CGC**GATGTTCTGG

I157F:

Forward: GCATCTCC**TTC**CGCATG

Reverse: CATGCG**GAA**GGAGATGC

R154C:

Forward: CTACCTCAGC**TGC**ATCTCCATC

Reverse: GATGGAGAT**GCA**GCTGAGGTAG

L160A:

Forward: GCATCTCCATCCGCATG**GCC**ATCAACCAGCACACC

Reverse: GGTGTGCTGGTTGAT**GGC**CATGCGGATGGAGATGC

R158A:

Forward: GCCGCATCTCCATC**GCC**ATGCTCATCAACCAGC

Reverse: GCTGGTTGATGAGCAT**GGC**GATGGAGATGCGGC

W383F:

Forward: GGCCGGCGAC**TTC**TGTGTGCCCAG

Reverse: CTGGGCACACA**GAA**GTCGCCGGCC

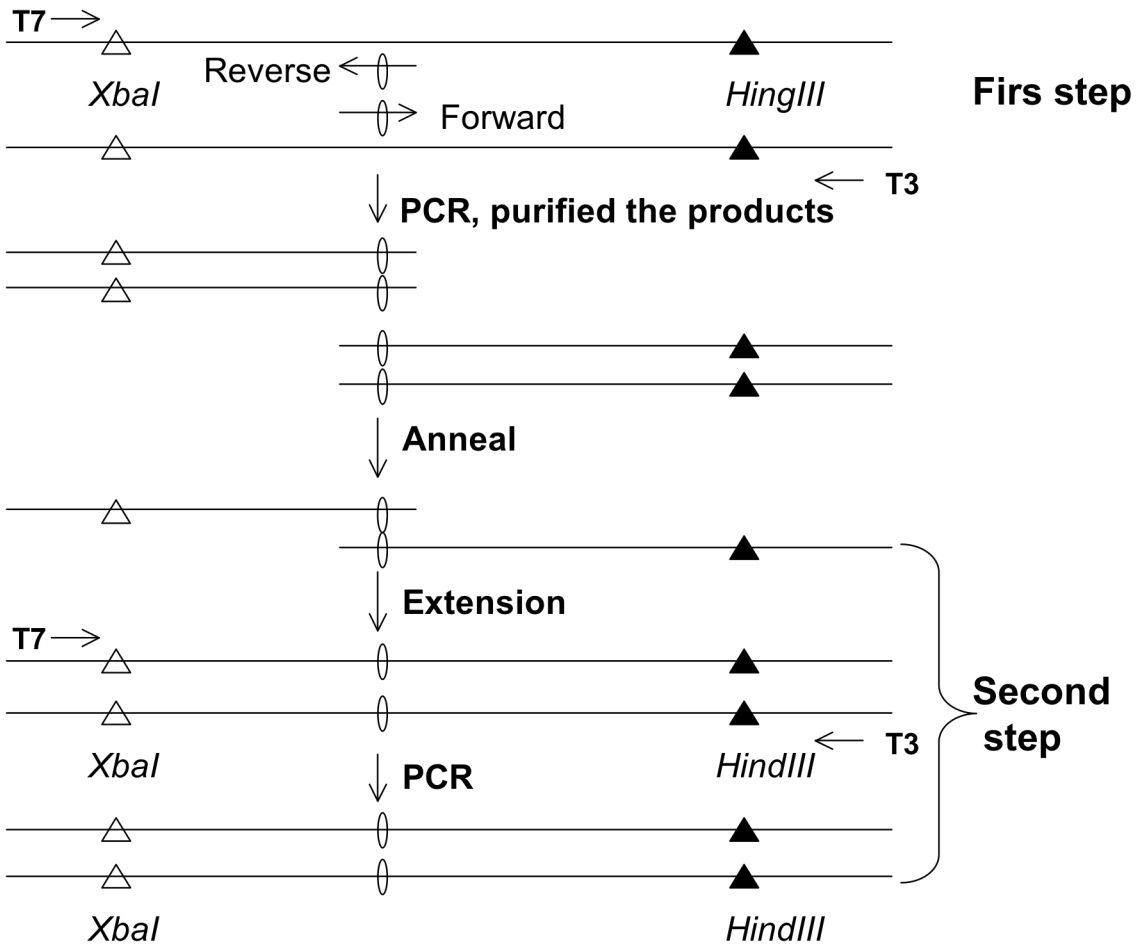

Figure 2-1. Procedures for site-specific mutagenesis. In the first step, Primers T7 and T3 were coupled with reverse or forward primers of specific mutant separately to produce fragments of PDHK2 DNA with specific mutation. The products were purified and used in the second step. In the second step, the DNA fragments were denatured, annealed using the complementary sequence and then extended to get the whole mutated DNA. Finally, the mutated DNA was amplified using T7 and T3 as primers. The final PCR products were purified and cut with restriction enzymes *XbaI* and *HindIII* to be inserted into PET28a plasmids. The open circles represent the bases mutated. The restriction sites for *XbaI* and *HindIII* are marked respectively with open or closed triangles.

All expressed PDHK2 mutants had a His-tag and a PreScission protease site at their N-terminus. [γ-^{32}P]ATP was from Dupont NEN. Pyruvate, DCA, NADH, NAD, Coenzyme A, and acetyl-CoA were from Sigma Chemical Co.

Expression and purification of PDHK2 mutant proteins

To express and purify the PDHK2 mutant proteins, a general procedure developed for wild type PDHK2 (43) were used. Plasmid of specific PDHK2 mutant was co-transformed along with a plasmid encoding GroEL and GroES (Dupont) into competent *E. coli* BL21(DE3). Selection for the presence of both plasmids was done on LB plates containing 50 μg/ml kanamycin and 50 μg/ml chloramphenicol. PDHK plasmid-containing bacteria were grown at 37 °C to mid-log phase (A_{600} 0.6) in LB media containing 50 μg/ml kanamycin and 50 μg/ml chloramphenicol. 0.5 mM isopropyl--D-thiogalactopyranoside (IPTG) was added to induce the expression at room temperature (22-24 °C) for 16 h. Bacteria were harvested by centrifugation at 4,000 × *g* for 20 min at 4 °C. The bacterial pellets were resuspended to 10% (w/v) in HN buffer (20 mM Hepes-Na buffer, pH 8.0, 0.5 M NaCl, 1% (v/v) ethylene glycol). Ice water-cooled suspensions were sonicated by six repetitions of 50% pulsing at 250 watts for 30 s followed by at least 1 min of cooling. Supernatants were cleared by centrifugation at 10,000 × *g* for 20 min at 4 °C. Pluronic-F68 and imidazole were added to the supernatant to a level of 0.1% (w/v) and 5 mM separately. The supernatant was loaded into column filled with 1-2 ml of equilibrated TALON resin (CLONTECH) that was balanced with HN buffer at 4 °C. The gel resin was washed with HN buffer containing 0.1% Pluronic F68 and 5 mM imidazole until the absorbance of flow through was lower than 0.2 at 280 nm. The resin was then washed with HN buffer containing 0.1% Pluronic F68 and 15 mM imidazole until the absorbance of flow through was lower than 0.2 at 280 nm. HG buffer (20 mM Hepes-Na, pH 8.0, 0.5 M NaCl, 1% (v/v) ethylene

glycol, 10% (v/v) glycerol, 0.1% (m/v) Pluronic F-68) containing 100 mM imidazole was used to elute PDHK2 protein. 1 mM dithiothreitol, 1 mM EDTA, and 100 units of PreScission protease (Amersham Pharmacia Biotech) were added into PDHK2 protein fractions pool for a 1- or 3-h incubation on ice. Following PreScission protease digestion, protease was removed by passing the mixture through a column with 0.25 ml of GSH-Sepharose (Amersham Pharmacia Biotech) equilibrated with HG buffer. PDHK2 preparations were desalted on a Sephadex G-25 column equilibrated with Hepes-Na buffer (20 mM, pH 8.0, 0.5 mM EDTA, 0.1% (m/v) pluronic F-68, 10% (v/v) glycerol, 1% (v/v) ethylene glycol and 100 mM NaCl). The purified PDHK2 mutants' protein were more than 90% pure based on the SDS-PAGE analysis. PDHK2 preparations were stored unfrozen at 20 °C. Final PDHK2 recovery was typically 5-10 mg per liter of bacterial growth media for PDK2. For L160A, I157F and W383F mutants, the recovery was around 1-3 mg per liter of bacterial growth media.

PDHK2 activity assays

PDHK2 activity assays were measured in duplicate as the initial rate of incorporation of ^{32}P-phosphate from [γ-^{32}P]ATP into E1 at 30°C. In 25 μl assay system, 10 μg E1 was used for each assay. For measuring E2-activated PDHK2 activity, 10 μg E2 was included, resulting in all E1 being bound to E2 (~ 24 E1 tetramer/E2 60mer). The kinase concentration was ~ 0.1 μg/assay or ~ 0.02 μg/assay depending on E1 or E1•E2 was used as substrate. The ATP concentration used was 100 μM unless stated otherwise. The standard buffer system used was 50 mM Hepes-Tris, pH 7.6, 0.1% Pluronics F68, 2 mM DTT, 2 mM $MgCl_2$, 0.5 mM EDTA (Low salt buffer). K^+ (balanced with Hepes), Cl^- (balanced with Tris) and Pi (balanced with Tris) were additionally added to specific levels in some experiments. In most assays, ~ 8 mM potassium phosphate was introduced with E1 that was stored in 50 mM potassium phosphate buffer, pH 7.5, containing 1.0

mM DTT and 0.5 mM EDTA. E1 precipitated in other buffers tested. In studies that evaluated the influence of specific ions on PDHK activity, concentrated E1 (more than 8.0 mg/ml in 10 mM potassium phosphate buffer) was used. Using this concentrated E1, the initial potassium phosphate concentration was reduced to ~ 0.5 mM.

When E1•E2 was used as substrate, E1, E2 and kinase were mixed and pre-incubated on ice for 1-2 hr prior to assay. When E1 alone was used as substrate, kinase was added into E1 first before the assays. In general, diluted PDHK2 (less than 0.01 g/l) was stable within 0.5 hr. Reaction mixtures (kinase, substrate and buffer) were incubated 1 min at 30°C. ATP was added to initiate the kinase reaction for 1 or 2 min. Reactions were terminated by spotting to dry Whatmann 3MM filter paper (Millipore Co.) discs pre-soaked with 10% trichloroacetic acid (TCA) solution. The discs were washed five times with 10% TCA to remove unbounded radioactive ATP. TCA was removed by washing the discs with ethanol and ethyl ether. The disks were dried and counted using Beckman LS 6500 multi-purpose scintillation counter.

Regulatory assays

In the assays evaluating DCA or pyruvate inhibition, DCA or pyruvate was added 1 min before ATP. Nov3r (in DMSO) was also added 1 min before ATP (final concentration of DMSO was 2%). Stimulation assays were performed using a buffer containing 50 mM Hepes-Tris, pH 7.6, 0.1% Pluronics F68, 2 mM $MgCl_2$, 0.5 mM EDTA, 90 mM K^+, 60 mM Cl^- and 20 mM Pi. NADH and NAD^+ were added at a 3:1 ratio (0.6 mM/0.2 mM) 60 s and 50 μM acetyl-CoA, when included, was added 20 s before ATP in the presence of NADH and NAD^+. When NADH/NAD^+ and acetyl-CoA were used, 2 μM E3 was included to catalyze the reversible reduction of lipoyl groups on E2.

Circular dichroism (CD)

Circular dichroism spectra were collected for all mutants and wild type PDHK2 using a quartz cell with a 1 mm light path in 20 mM potassium phosphate (pH 7.5) including 0.5 mM EDTA at 20°C. Using a Jasco J720 spectrometer at least 16 scans were averaged with each accumulated at 50 nm/min. Spectra were collected from 190 nm to 260 nm at a kinase concentration of 0.2 mg/ml. Protein concentrations were based on the Pierce BCA (bicinchoninic acid) Protein Assays. The instrument was calibrated using D-10-camphorsulfonic acid as a standard.

Fluorescence quenching

Steady-state fluorescence spectra were recorded with a Cary Eclipse fluorescence spectrophotometer (Varian, Inc.) at 25°C in 50 mM potassium phosphate buffer, pH7.5, containing 0.5 mM EDTA and 2.0 mM $MgCl_2$. Fluorescence spectra of wild type and mutant PDHK2 were recorded from 320 nm to 420 nm (with 5 or 2.5 nm slit) with exitation at 290 nm (with 10 nm or 5 nm slit). Standard quartz (1X1 cm) cuvette and 2.0 ml initial volume were used. The concentration of kinase was continuously corrected for the dilution due to addition of concentrated ligand during the titration of PDHK2 by ligands. Although spectra from 320nm to 420 nm were recorded, the corrected fluorescence change at 350 nm was used to assess fluorescence quenching with the change of the varied ligand. Kinase concentration was ~ 0.5 μM. The calculation of half quenching ($L_{0.5}$) was done as previous described (43).

Sedimentation velocity analysis

Sedimentation velocity experiments were conducted as previously described using an Optima XL-I ultracentrifuge (11, 23, 34). The buffer used was 50 mM potassium phosphate buffer, pH 7.5, containing 0.5 mM EDTA and 2.0 mM $MgCl_2$. 3.7 μM PDHK2 and 7.5 μM GST-L2 were used unless specified. When indicated, ATP, ADP, pyruvate, or combinations of

pyruvate and ATP or ADP were added at the indicated concentrations. Sedimentation was conducted at 20 °C and the profiles were recorded at 280 nm using double sector cells at a speed of 49,000 rpm and 5 min intervals. Sedimentation data were analyzed with $DCDT^{+}$ software (version 1.6).

Results

CD and fluorescence spectra of wild type PDHK2 and mutants

The mutants PDHK2 made were Q144A, R154C, I157F, R158A, L160A, R154C/L160A and W383F. The successful mutations were confirmed by DNA sequencing. The mutant proteins were expressed and purified as described previously for wild type PDHK2 (32). There were no significant differences in the yield of soluble mutant and the wild type kinase proteins.

Using a 1 mm cuvette, the CD spectra of wild type and mutant PDHK2 were measured in 50 mM potassium phosphate buffer, pH 7.5, containing 0.5 mM EDTA and 2.0 mM $MgCl_2$ (Fig. 2-2). The CD spectra of wild type PDHK2 had two peaks at 208 nm and 220 nm, an indication that α helices dominated the secondary structure. All mutants apart from L160A had CD spectra similar to wild type PDHK2, indicating that they had secondary structure similar to wild type PDHK2. The CD spectrum of L160A had both peaks but was significantly different from that of wild type PDHK2 and other mutants. This indicated that there were some changes in the secondary structure of L160A.

There are three tryptophan residues in PDHK2. Fig. 2-3 shows the emission spectra of wild type PDHK2 and several mutants. The fluorescence spectra were measured from 320 nm to 420 nm with excitation at 295 nm in phosphate buffer. At this excitation wavelength, most of fluorescence comes from tryptophan residues (81, 82). Wild type PDHK2 had a broad emission (EM) peak with a maximum at 352 nm. The fluorescence spectra of R154C and R154C/L160A

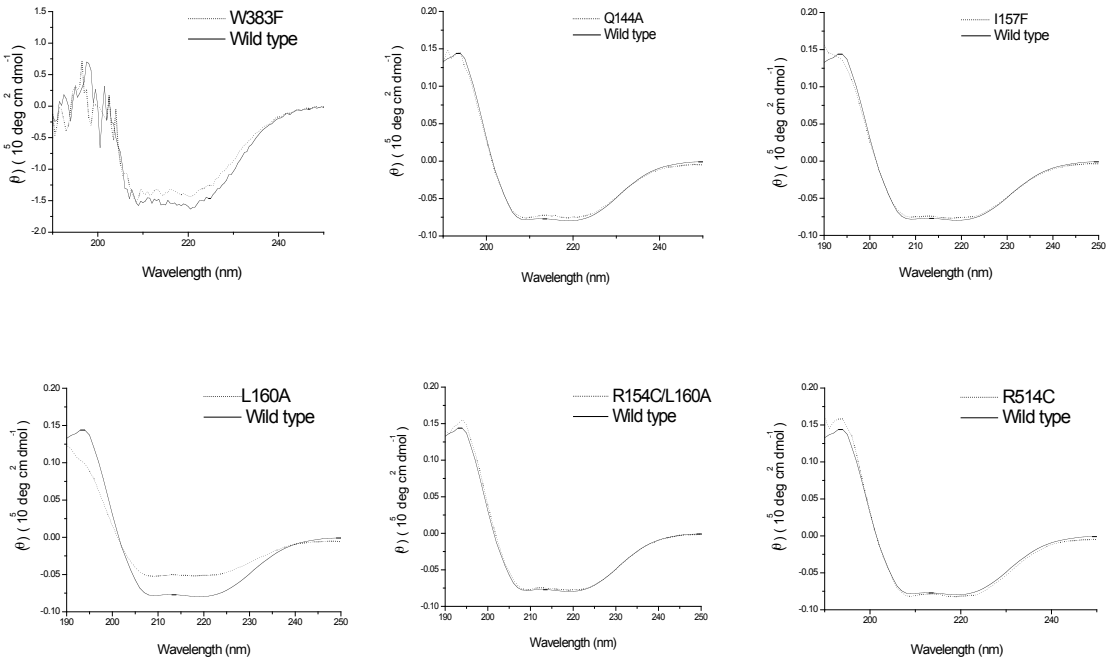

Figure 2-2. Circular dichroism patterns for wild type and mutated PDHK2. Using a 1 mm cuvette, the CD spectra of wild type and mutated PDHK2 were measured using a Jasco J720 spectrometer at room temperature (22 °C). Spectra were collected from 260 nm to 190 nm using 2.16 μM kinase dimer with the exception of 0.3 μM W383F. (Data were collected by Dr. Hiromasa, Y. The first panel was published in *J. Biol. Chem*, (2006) 281, 12568-12579 (43)). Published data were reproduced with permission as covered under the general Copyright Permission Policy of *J. Biol. Chem.*

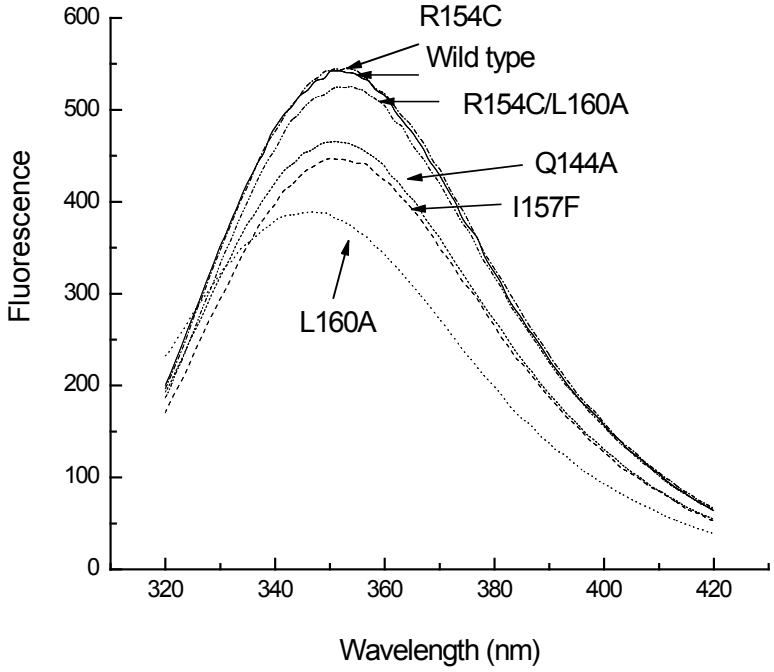

Figure 2-3. Fluorescence emission spectra of wild type and mutated PDHK2. Fluorescence spectra of 0.5 μM native and mutated PDHK2 were collected from 320 nm to 420 nm with excitation at 290 nm. (Data were collected by Dr. Hiromasa, Y.)

matched very well with wild type PDHK2. Q144A and I157F had the same EM peak maximum (352nm) as wild type PDHK2 but lower fluorescence intensities (~ 85% of wild type). L160A had a significantly different fluorescence emission spectrum. The EM peak of L160A was at 346 nm, a 6 nm blue shift comparing with the EM peak of wild type PDHK2. At the same time, the maximum fluorescence intensity was 30% lower than the maximum fluorescence intensity of the wild type kinase. The difference in the fluorescence emission spectra again suggests that the L160A mutant has a different conformation from wild type PDHK2 and other mutants. As a result, L160A was not active (below).

Kinase activities of mutants

L160A had no activity in several preparations, in agreement with the above CD and fluorescence results indicating this mutant had a different conformation from the wild type kinase. Other mutants of PDHK2 maintained the ability to phosphorylate E1. Table 2-2 shows the specific activities of these mutants in low salt buffer and high salt buffer (same as low salt buffer with additional 90 mM K^+ and 60 mM Cl^-) using E1 or E1•E2 as substrate. All assays (25 μl) were conducted in the presence of 100 μM ATP with 10 μg E1 (2.63 μM) in absence or presence of 10 μg E2 (0.11 μM 60mer)*.

Using E1 alone as substrate, I157F and R154C/L160A displayed activities comparable to wild type PDHK2 in a low salt buffer. The R154C mutant had the lowest activity that was only 11% of the activity of wild type PDHK2. Q144A had the highest activity that was 2.2-fold higher

---

* It should be noted that, without E2, this level of E1 is well below the K_m of wild type PDHK2 for E1 and that, with E2, adding additional E1 does not significantly increase the observed rates with wild type PDHK2 (40). Therefore, much of the observed activity increase with inclusion E2 is due to a change in availability of E1 as described in the general introduction. In the high salt buffers, 100 μM ATP is well above the K_m of PDHK2 for ATP in the absence of E2 and somewhat above the K_m for ATP with E2 (40). The K_m of wild type PDHK2 using the low salt buffers is not established. Fig. 2-8 below varied ATP at one E1 level in the absence of E2, but the apparent Km for ATP derived could be very different from the true K_m for ATP.

Table 2-2. Specific activities of wild type and mutant PDHK2. Kinase assays were conducted with 100 μM ATP at 30 °C in the presence or absence of E2 with the indicated buffer. Low salt buffer: 50 mM Hepes-Tris, pH7.6, 0.5 mM EDTA, 0.1% pluronic F-68, 2 mM $MgCl_2$, 2 mM DTT. High salt buffer: same as low salt buffer with additional 90 mM K^+ and 60 mM Cl^-. Around 10 mM or 12 mM K_xPO_4 was introduced by E1 or E1•E2. The kinase concentration was 8.8 nM in assays conducted in the presence of E2 and 44 nM in assays conducted in the absence of E2.

	Low salt		High salt	
	- E2	+ E2	- E2	+ E2
	$nmol \cdot min^{-1}.mg^{-1}$			
Wild type	106±8	715±6	9.5±0.5	172±4
R154C	12.1±0.5	421±3	3.1±1.3	167±3
R158A	29.7±0.9	393±2	5.8±0.2	157±9
R154C/L160A	77.6±0.3	481±9	25.7±0.3	225±17
I157F	81.2±0.5	647±5	4.8±1.0	73.5±3.4
W383F	53.4±0.1	579±27	4.1±0.1	113±3
Q144A	232±4	908±14	51.2±0.2	383±3

than the wild type kinase. The activities of R158A and W383F were somewhat lower than that of wild type PDHK2 under the same conditions. High salt, 90 mM K^+ and 60 mM Cl^- (near physiological levels), reduced the activity of kinase with E1 alone as substrate. The activity reductions varied from > 11-fold for wild type, I157A and W383F mutants to less than 5-fold for R154C, R158A, R154C/L160A and Q144A mutants. The different activity reduction due to elevated ions may be a reflection of the specific roles of mutated residues or be a result of changed stability in these PDHK2 constructs. As a result of different responses to an elevated level of ions, R154C/L160A and Q144A mutants had 2.7-fold and 5.4-fold higher specific activities than wild type PDHK2 with E1 as substrate in high salt buffers. Thus, the R154C/L160A dual mutant changed from less active to more active than wild type PDHK2 with the transition from a low salt buffer to a high salt buffer. At the same time, the Q144A mutant was 4-fold active than wild type PDHK2 in high salt buffer as it was less influenced by salt.

The activities of PDHK2 mutants were also assessed in the presence of E2 (Table 2-2). Using E1•E2 as substrate, all PDHK2 mutants had activities higher than using E1 alone as substrate in both buffers, indicating that these mutants maintained the capability of binding to the lipoyl groups in E2. The activity enhancement by E2 varied among mutants and was influenced by the ions levels in the buffer. E2 caused large activity increases for all kinases in a high salt buffer than in a low salt buffer. Under low salt conditions, the specific activity of native PDHK2 was increased around 7-fold by E2. While the activity of wild type PDHK2 was increase more than 18-fold by E2 in a high salt buffer. The R154C mutant, who had the lowest activity using E1 alone as substrate, underwent the largest activity increase by E2. E2 caused the lowest activity increase for Q144A, which had the highest activity using E1 alone as substrate.

In the presence of E2, elevated ions also decreased the specific activity of PDHK2 (wild type and mutants), but less of a decrease than in the absence of E2 (Table 2-2). These data suggested that lipoyl domain binding might stabilize PDHK2. Comparing with the wild type PDHK2, I157F and W383F, the activities of R154C, R158A, R154C/L160A and Q144A mutants again were reduced less by elevated salt even using E1•E2 as substrate. Therefore, these mutations (R154C, R158A, R154C/L160A, Q144A) might alter how ions affected PDHK2 activity.

As a result of unequal activity enhancement by E2 and different activity reduction by elevated salt, the activities of R154C and R158A changed from more than 70% lower than wild type PDHK2 in the low salt buffer using E1 as substrate to almost equal to the native kinase in the high salt buffer using E1•E2 as substrate (Table 2-2). Using E1•E2 as substrate in a high salt buffer, I157F had an activity similar to that under low salt conditions using E1 as substrate. Under these conditions, Q144A maintained the highest specific activity.

Based on above specific activity assays for the mutants, it was found that L160A was inactive as it had a conformation different from wild type PDHK2. All other mutants (R154C, R158A, R154C/L160A, I157F, W383F and Q144A) were active. These mutants maintained the capacity to bind to and be activated by E2. Elevated salt (K^+ plus Cl^-) reduced the activities of the wild type and mutants PDHK2. Binding of E2 to kinase appeared to stabilize the enzyme, reducing but not eliminating the influence of high salt. The activities of R154C, R158A, R154C/L60A and Q144A mutants were decreased less by high salt than wild type PDHK2. The reasons for such weaker ion effects would be discussed below.

Fluorescence of W383F

There are three tryptophan residues in human PDHK2: Trp79, Trp371 and Trp383 (see Fig. 1-5 and 1-6). Trp79 is located in helix α5 of the R domain of PDHK2. Trp371 and Trp383 are located in the cross arms. Trp371 is in the middle of the cross arm and is partially exposed to solvent. Trp383 is at the end of the cross arm, inserted between Arg362 and Arg149 of the other subunit at the interface of the R-Cat domain (76). Trp383 interacts with other residues from the other subunit (Leu152, Leu363 and Pro364). As noted in the introduction of part I, the cross arm was not observed in the crystal structure of rat PDHK2•ADP (74) and human PDHK2•ADP•DCA (76). Under those conditions, Trp371 or Trp383 are probably exposed to different environments, resulting in changes in their fluorescence. However, even small conformational changes can alter the electrostatic environment around Trp383, to thereby cause changes in fluorescence. Phe was used to replace Trp383, hoping the replacement would not significantly alter the PDHK2 structure, the cross arm would be maintained, and only the fluorescence of the kinase would be altered.

There was a large difference between the emission spectrum of W383F and wild type PDHK2 (Fig. 2-4). The fluorescence EM peak of W383F was at 342 nm, a 10 nm blue-shift from the 352 nm of wild type. The fluorescence intensity at 350 nm was decreased by 60%. These results indicated that Trp383 provided the major part of tryptophan fluorescence in PDHK2. Trp79 could be another contributor to total fluorescence and would be expected to have an EM peak at shorter wavelength as it is mostly buried with generally hydrophobic groups surrounding it. Trp371 is expected to contribute minimally to fluorescence because it was substantially exposed to solvent (81). When Trp383 was replaced by phenylalanine, it is likely that the majority of the residual tryptophan fluorescence is from W79.

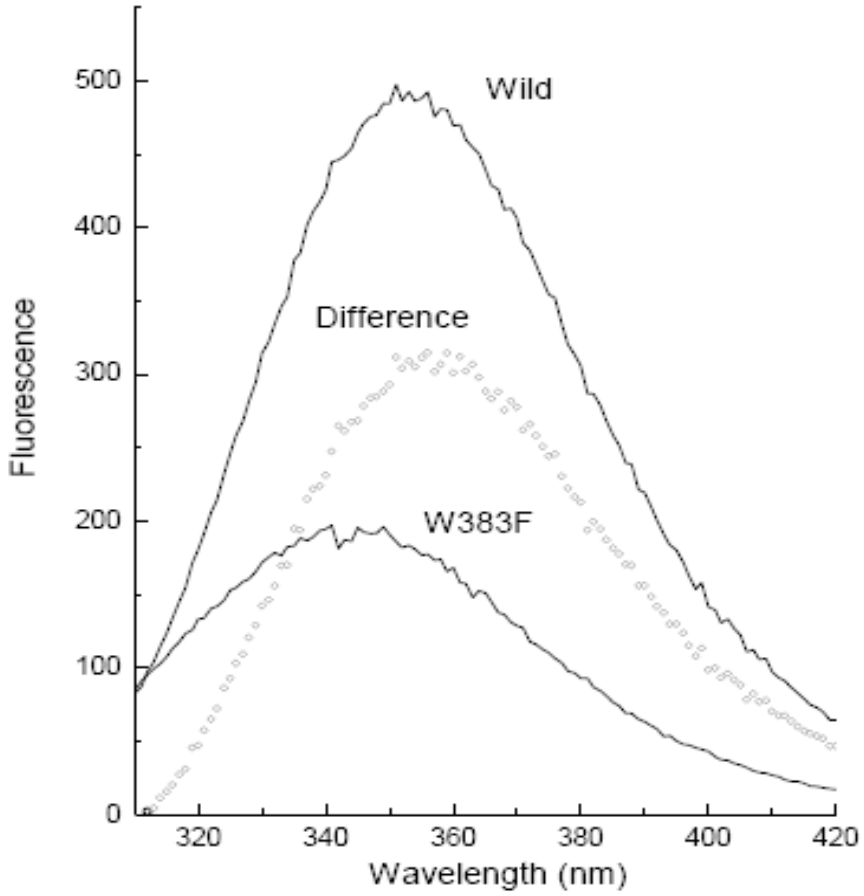

Figure 2-4. Fluorescence emission spectra of wild type PDHK2 and W383F. Fluorescence spectra of 0.7 μM native and mutated PDHK2 were collected from 320 nm to 420 nm when exited at 290 nm. The difference between the fluorescence spectra of wild type PDHK2 and W383F was shown in o-curve. (Data were collected by Dr. Hiromasa, Y. and published in *J. Biol. Chem*, (2006) 281, 12568-12579 (43)). Published data were reproduced with permission as covered under the general Copyright Permission Policy of *J. Biol. Chem.*

In the potassium phosphate buffer, the K_m for ATP of W383F was 35±7 μM, which was close to the K_m of wild type PDHK2. But W383F had a V_{max} 30% lower than wild type using E1•E2 as substrate (Fig. 2-5). Therefore, the W383F mutant maintained the ability not only to interact with substrates (E1 and ATP) but also to bind to lipoyl domain of E2. Combined with above information from the CD spectra and activity assays, these results demonstrated that the replacement of W383 with Phe did not significantly alter the structure of PDHK2.

Fluorescence quenching

Fig. 2-6A shows how ADP and ATP influenced the tryptophan fluorescence spectrum of PDHK2. In the potassium phosphate buffer, 150 μM ADP caused the fluorescence intensity at 350 nm to be decreased by 45%, while 150 μM ATP caused a decrease of 53%. ADP and ATP also caused a blue-shift of fluorescence EM peak. Mg^{2+} was required for ADP and ATP binding to PDHK2. PDHK2 has no activity in the absence of Mg^{2+}. There was no change in the fluorescence spectra of PDHK2 in the presence of either ADP or ATP (less than 1.0 mM) when there was no Mg^{2+} (data not shown). Therefore, the observed fluorescence quenching was due to specific binding of nucleotides as a Mg^{2+} complex to PDHK2.

Fig. 2-6B and 2-6C show the change of fluorescence intensity at 350 nm with the increasing of ADP or ATP concentration. Fluorescence quenching of PDHK2 by nucleotide was fit by a simple equilibrium binding at a single class of sites as described in previous studies (30, 40). The estimated maximum quenching by ATP was 53.5 ± 1.5% and ADP had maximal quenching of 48.8 ± 2.5%. ATP underwent half-maximal quenching at a concentration ($L_{0.5}$) of 2.8 ± 0.3 μM. The $L_{0.5}$ for ADP of PDHK2 was 15.3 ± 1.5 μM. The estimated $L_{0.5}$ for ATP was close to the K_d determined in other studies (30, 40).

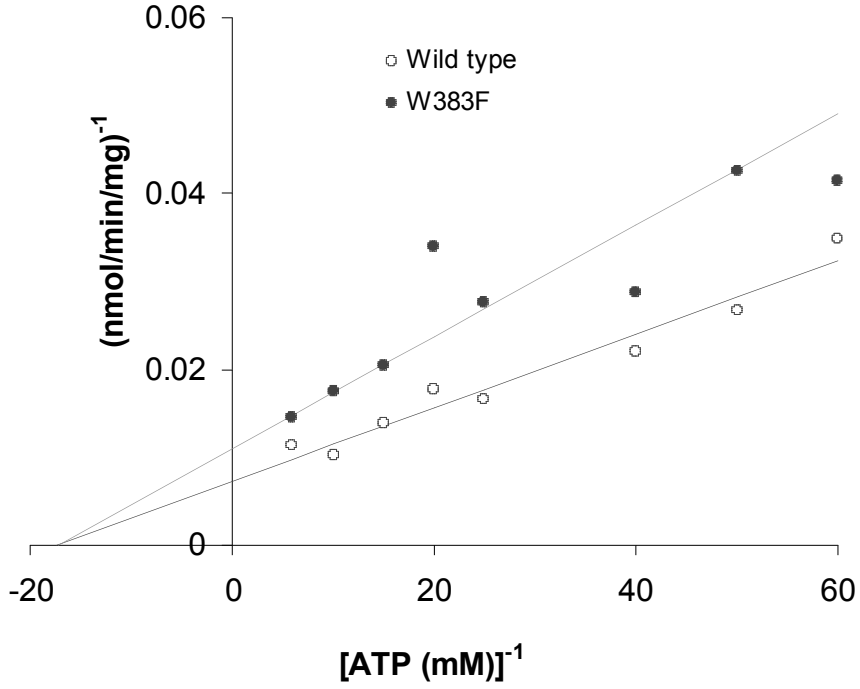

Figure 2-5. Double reciprocal plot showing the variation in the activities of W383F and wild type PDHK2 with the ATP concentration. Assays were conducted in a potassium phosphate buffer with additional 90 mM K^+ and 60 mM Cl^-. The concentrations of PDHK2 dimer, E1 and E2 were 41 nM, 2.6 μM and 0.11 μM (60mer) respectively.

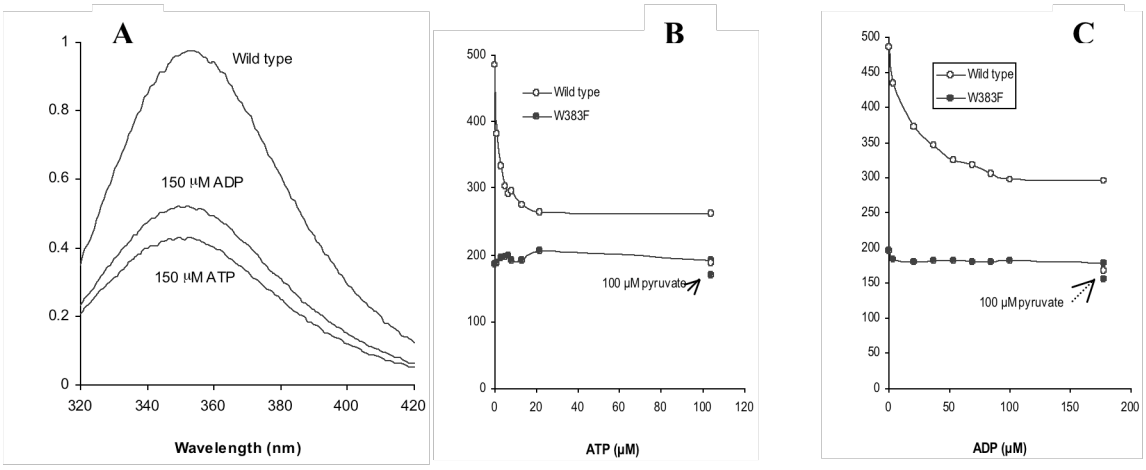

Figure 2-6. Quenching of the intrinsic fluorescence of wild type PDHK2 and W383F by ATP or ADP. All data were obtained in 50 mM potassium phosphate buffer (pH7.6) with excitation at 290 nm. A, Influence of ATP or ADP on fluorescence spectra of native PDHK2. B and C, Fluorescence quenching at 350 nm of wild type PDHK2 (open circle) and W383F (closed circle) by ATP (B) or ADP (C). 100 μM pyruvate was added to the mixture after the highest level of ATP or ADP (arrow). (Data were collected by Dr. Hiromasa, Y. and published in *J. Biol. Chem*, (2006) 281, 12568-12579 (43)). Published data were reproduced with permission as covered under the general Copyright Permission Policy of *J. Biol. Chem.*

As shown in Fig. 2-4, W383 provides most of the tryptophan fluorescence of PDHK2. To evaluate the role of W383 in fluorescence quenching by nucleotide, quenching of fluorescence of wild type and W383F PDHK2 were compared. Contrary to wild type PDHK2, ATP or ADP caused no fluorescence quenching of W833F (Fig. 2-6B and 2-6C). These results indicate that fluorescence quenching of wild type PDHK2 by ADP or ATP resulted mainly from the changes in W383 fluorescence. Nucleotide binding at the active site must introduce changes in the electronic environment around Trp383 on the cross-arm to lower the fluorescence intensity.

Pyruvate caused fluorescence quenching of wild type PDHK2 with a $L_{0.5}$ of 590 ± 60 μM (Fig. 2-7). These data indicate that pyruvate could bind to free PDHK2. Pyruvate also caused a fluorescence quenching in W383F (Fig. 2-7). In the presence of 105 μM ATP or 175 μM ADP, fluorescence quenching of wild type PDHK2 by nucleotide almost reached the maximum. Addition of 100 μM pyruvate caused further fluorescence quenching of wild type PDHK2 (Fig. 2-6B and 2-6C). Under the same condition, addition of pyruvate also caused fluorescence quenching of W383F. But the further quenching of W383F mutant was significantly less than that of the wild type kinase (Fig. 2-6B, 2-6C). Pyruvate inhibition studies (below) confirmed that W383F maintained the capability of binding to pyruvate. These results indicate that binding of pyruvate introduced changes not only in the electronic environment around W383 and but also around at least one other tryptophan residue.

From the studies of the W383F mutant, it could be concluded that the cross arm anchoring W383 provides the majority of intrinsic Trp fluorescence of PDHK2. Nucleotide binding to the active site caused mostly the fluorescence quenching of W383. While pyruvate binding to the DCA/pyruvate site resulted in not only the fluorescence quenching of W383 but

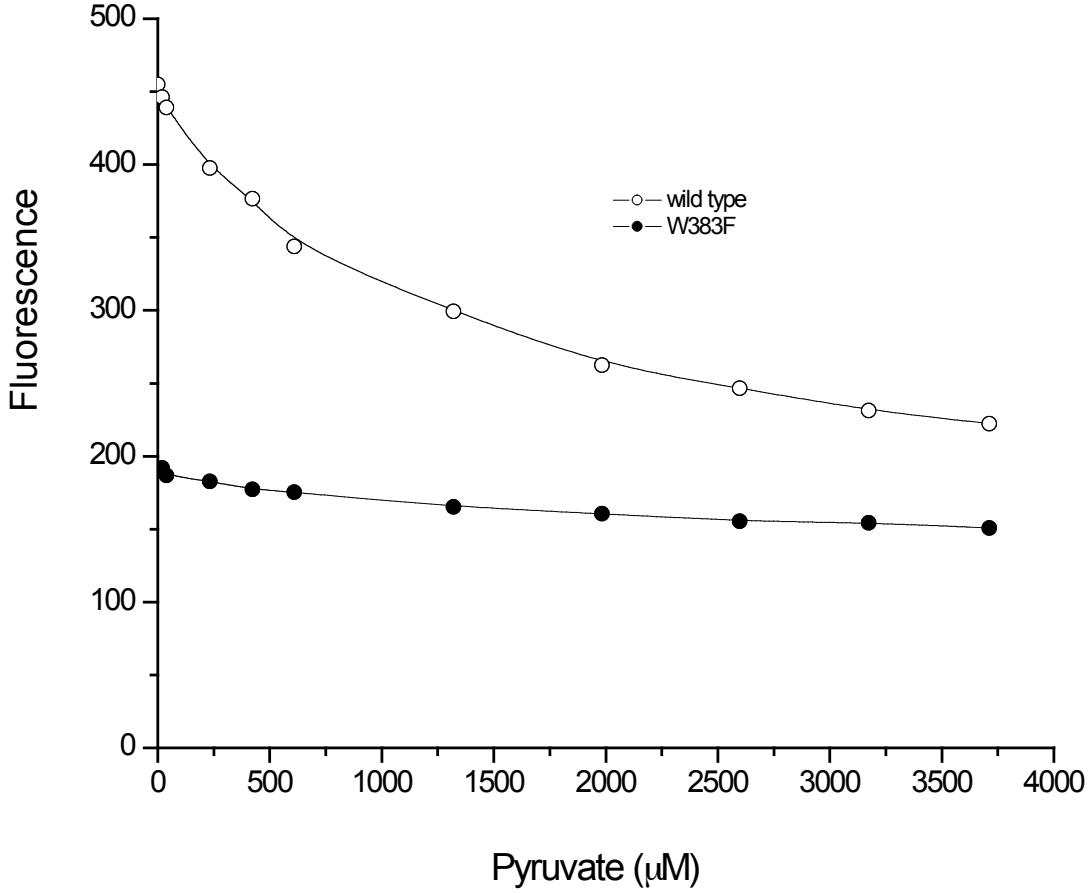

Figure 2-7. Fluorescence quenching of wild type PDHK2 and W383F by pyruvate. All data were obtained at 350 nm in 50 mM potassium phosphate buffer (pH 7.6) when excited at 290 nm using 0.7 μM PDHK2 dimer. (Data were collected by Dr. Hiromasa, Y.).

also other tryptophan residue (see discussion). The intrinsic Trp fluorescence quenching was used to evaluate the binding of ligand (43).

PDHK2 activity using E1 as substrate

There was much evidence that PDHK2 activity was influenced by ions. The combination of elevated levels of Cl^-, K^+ and Pi reduced the activity of PDHK2 in the presence of E2 (30, 32). PDHK2 was more active in the presence of low levels ions such as K^+, Cl^- and Pi than with elevated ion levels in the presence of E2 (30, 32, 40). From above activity assays, it was found that E2 stabilized and made PDHK2 less affected by K^+ and Cl^-. Most reports about the functional regulation of PDHK2 activity have used E1•E2 as substrate, as E2 enhanced the activity of PDHK2 and the activity of PDHK2 was relatively low under high salt conditions (32, 36, 85). To exclude the influence of E2, E1 alone was used as substrate in some studies in this thesis.

The kinetic basis for the change of the specific activities of human PDHK2 with salt levels was partially evaluated using 2.6 μM E1 alone as substrate with the ATP concentration varied from 10 μM to 400 μM (Fig. 2-8). The native PDHK2 had an apparent K_m for ATP of ~ 23 μM and an apparent V_{max} of ~ 139 nmol·min^{-1}·mg^{-1} with low salt buffer containing 10 mM K_xPO_4 from E1 source. With the addition of extra 90 mM K^+ and 20 mM Pi, the apparent K_m for ATP was decreased by 4-fold to ~ 6.4 μM, and the apparent V_{max} was decreased 2.7-fold to ~ 49 nmol·min^{-1}·mg^{-1}. The reduction of both the V_{max} and the K_m for ATP by elevated ions using E1 alone as substrate was very similar to previous studies using E1•E2 as substrate (40). These data suggest that elevated ions increase the affinity of binding adenine nucleotide at the active site and the tighter binding reduces the reaction speed even when E1 is the substrate. These results are consistent with an ordered mechanism in which ADP dissociation remains (as with E1•E2)

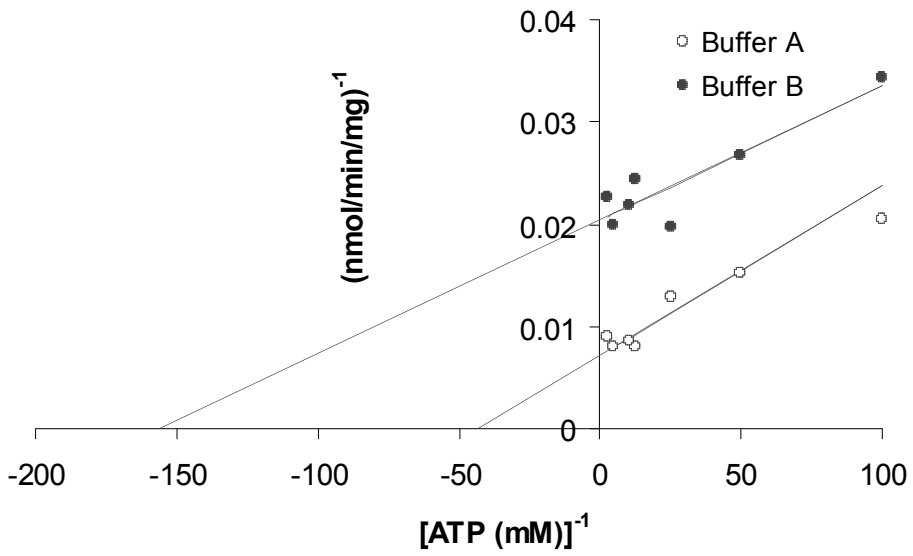

Figure 2-8. Double reciprocal plot of the variation in initial velocity of wild type PDHK2 with ATP in different buffers. Data shown by open circles were obtained in buffer A: 50 mM Hepes-Tris, pH 7.6, 0.5 mM EDTA, 0.1% pluronic F-68, 2 mM $MgCl_2$, 2 mM DTT. Data shown by closed circles were obtained in Buffer B (Same as Buffer A but also containing additional 90 mM K^+ and 20 mM Pi). Around 10 mM K_xPO_4 was also introduced with E1.

a slow step even with E1 being used as a substrate at a level well below the K_m for E1.

Mutant Q144A and K^+ influence

Q144 on helix α8 forms hydrogen bonds with backbone carbonyl groups of Y298 and F296 that are adjacent to S297, one of the residues that chelate to K^+ in the active site. The highest specific activities under different conditions were observed with the Q144A mutant. Q144A had ~ 2-fold less activity reduction than wild type PDHK2 in a high salt buffer (Table 2-2). These results suggested that Q144A responses to elevated levels of ions might be different from the native PDHK2.

To evaluate how K^+ influenced the Q144A mutant, the responses of Q144A to increasing K^+ were compared to those of wild type (Fig. 2-9, Fig. 2-10, Table 2-3). Q144A initially had a specific activity (~ 79 nmol·min^{-1}·mg^{-1}) lower than the wild type PDHK2 using E1 as substrate with 0.5 mM potassium phosphate. A nearly 2-fold increase in specific activity was observed with by 10 mM K^+. In contrast, there was little change in wild type PDHK2 at this range of K^+ (Fig. 2-9). Further increasing of K^+ concentration led to the gradually decreasing of the specific activities of both Q144A and wild type kinase. Q144A underwent less activity loss (21%) beyond the peak at 10 mM K^+ than wild type (58%) at 90 mM K^+. To fully understand these profiles for changes in activity of wild type and Q144A with K^+ level, more studies needed to be done to determine how the V_m and K_m values for ATP and E1 change with different K^+ levels.

When E1•E2 was used as substrate, 3.5 mM K_xPO_4 (~ 6.5 mM K^+) was initially introduced from E1 and E2. In the presence of E2, Q144A had a higher specific activity than wild type at all levels of K^+ tested (Fig. 2-10). The specific activity of Q144A first increased by ~ 20% with 10 mM K^+ and then decreased at higher K^+ levels. The specific activity of wild type PDHK2 decreased slowly but constantly with increasing K^+. In the presence of E2, only small

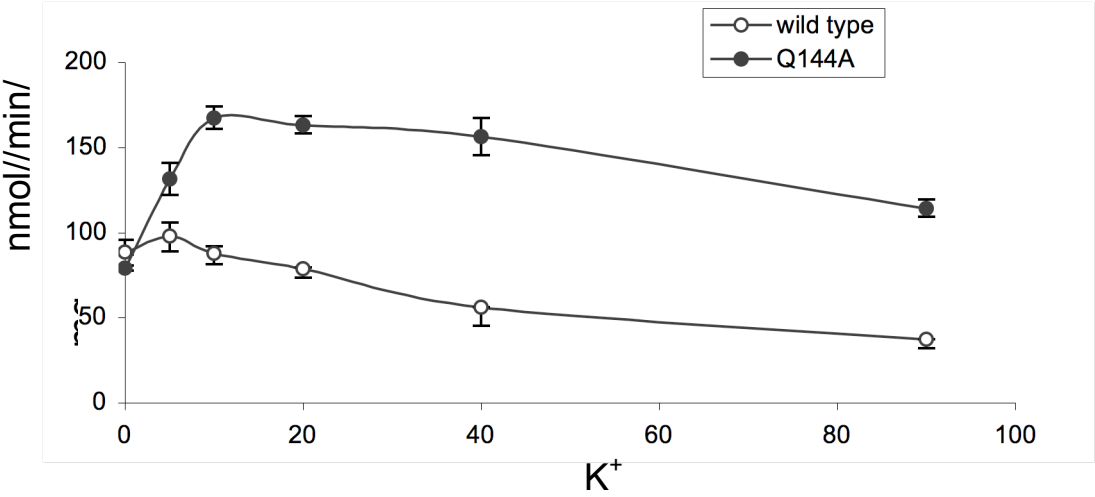

Figure 2-9. K^+ influence on the specific activities of wild type and Q144A PDHK2 using E1 as substrate. Open and closed circles show the changes in activities of wild type and Q144A PDHK2 respectively with K^+ concentration. All assays were conducted in low salt buffer with 0.5 mM K_xPO_4 introduced with E1.

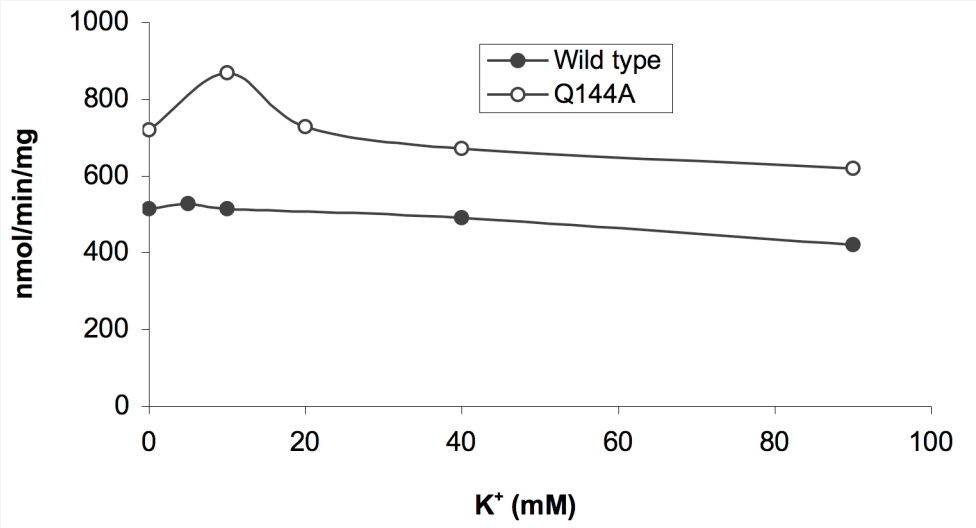

Figure 2-10. K^+ influence on the specific activities of wild type (open circle) and Q144A (closed circle) PDHK2 using E1•E2 as substrate. All assays were measured in low salt buffer with 3.5 mM K_xPO_4 introduced with E1•E2.

decreases in activity of wild type PDHK2 were observed as K^+ was raised to 90 mM, suggesting that the interaction with E2 stabilized PDHK2 activity. The specific activity of Q144A first increased and then decreased with increasing K^+ concentration. These explained why high salt reduced the activity of Q144A less than wild type. It was not clear why kinase activity decreased at high levels K^+. One possibility was the ion strength. This could be resolved using other ions such as Na^+ to replace K^+. Another possibility was that kinase was unstable under elevated K^+ conditions especially with E1 as substrate.

The apparent K_m and apparent V_{max} of wild type PDHK2 for ATP were ~ 58 μM and ~ 602 nmol·min^{-1}·mg^{-1} using E1•E2 as substrate in a buffer containing 90 mM K^+ (Fig. 2-11). Substitution of Q144 by Ala caused small increase on the apparent K_m for ATP (~ 68 μM) but the apparent V_{max} for ATP increased more than 2-fold at ~ 1012 nmol·min^{-1}·mg^{-1} under this buffer conditions.

In the above steady state activity studies, 100 μM ATP was present and ADP was produced during the reactions. Using K^+-dependent fluorescence quenching linked to nucleotide binding, the binding of K^+ to wild type and Q144A PDHK2 was studied (Fig. 2-12, Table 2-3). In the presence of 100 μM ATP, same levels of K^+ resulted in substantially more fluorescence quenching with wild type PDHK2 than Q144A (Fig. 2-12). Half-maximal quenching ($L_{0.5}$) for wild type kinase was estimated at ~ 1.3 mM K^+ with 43% maximal quenching estimated under this condition (Table 2-3). Q144A required 12-fold higher K^+ to reach the half-maximal quenching. These results suggested that replacement of Q144 by alanine weakened the binding of K^+ to kinase in the presence of ATP and altered the capacity of ATP binding to quench the fluorescence of W383. The latter suggests that ATP/K+ binding at the active site is less effective in introducing conformational changes in the R domain.

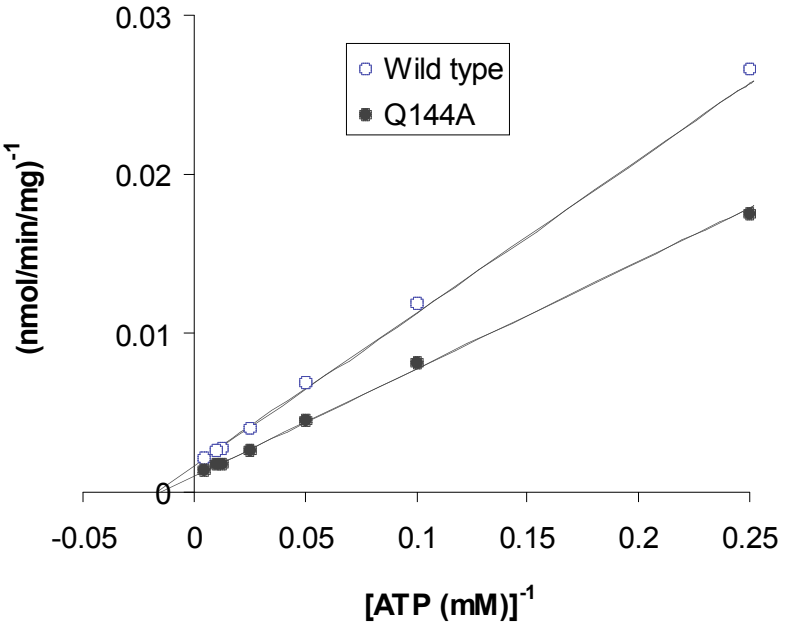

Figure 2-11. Double reciprocal plot of the variation in initial velocities of wild type (open circle) and Q144A (closed circle) PDHK2 using E1•E2 as substrate. All assays were conducted in the low salt buffer with around 10 mM K_xPO_4 introduced with E1•E2.

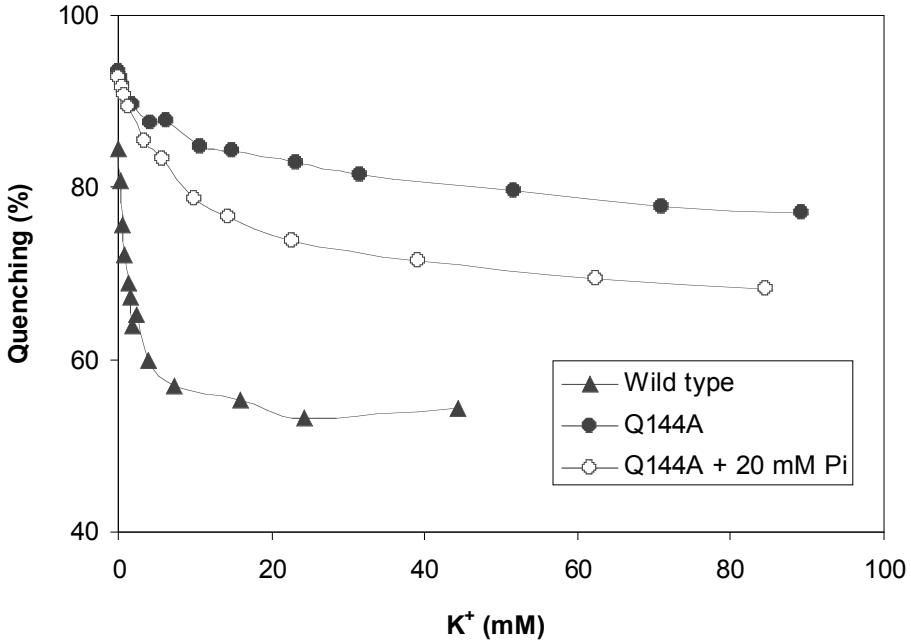

Figure 2-12. Influence of K^+ on fluorescence quenching of wild type and Q144A PDHK2 by ADP. All data were obtained at 350 nm in 50 mM Tris-Hepes buffer (pH 7.6) with excitation at 290 nm. (Data were collected by Dr. Hiromasa, Y.)

Table 2-3. Nucleotide effects on K^+ binding to wild type PDHK2 and Q144A. All parameters were derived from fluorescence quenching of 0.1 μM kinase by varying K^+. Parameters were derived from a Hill plot analysis that assumed binding was proportional to fluorescence quenching. (Data were collected by Dr. Hiromasa, Y.)

PDHK2 source	Fixed ligands	$L_{0.5}$ for K^+ (mM)	Hill Coefficient, n_H	Q_{max} (%)
Wild type	100 μ M ATP	1.3	1	43
Q144A	100 μ M ATP	17.2	0.74	20.4
Wild type	200 μ M ADP	12	1	34.5
Q144A	200 μ M ADP	14.3	1.2	15.7
Wild type	200 μ M ADP + 20 mM Pi	5.2	1.2	43
Q144A	200 μ M ADP + 20 mM Pi	9.6	1	27

The wild type PDHK2 binds K^+ 10-fold tighter in the presence of ATP than ADP, suggesting that the γ-phosphate of ATP might play some role in the tighter binding of K^+ (Table 2-3). On the contrary, there was no significant difference in the K^+ binding in the presence of 200 μM ADP with the estimated $L_{0.5}$ for wild type and Q144A PDHK2 were 12.0 mM and 14.3 mM separately. Addition of 20 mM Pi with ADP resulted in tighter binding of K^+ to both wild type and Q144A PDHK2 and led to somewhat greater maximal quenching (Fig. 2-12B, table 2-3). Under those conditions, K^+ bound almost 2-fold tighter to wild type than to Q144A PDHK2. It is possible that Pi ion may occupy the same position as the γ-phosphate of ATP to result in tighter binding of K^+ in the presence of ADP. Under all conditions, the maximal quenching for Q144A was less than that for wild type PDHK2. The difference might be due to the lower fluorescence of Q144A than wild type PDHK2 (Fig. 2-3).

As would be expected for coupled K+/ATP binding (89), substitution of Q144 by alanine also weakened the binding of ATP based on fluorescence quenching studies (Table 2-4). Native kinase had an estimated $L_{0.5}$ of 3.1 μM for ATP with ~ 45% maximal quenching in the saturated level of K^+ (100 mM). Q144A needed 3-fold more ATP to reach the half-maximal quenching with an almost 2-fold lower maximal quenching. The lower maximal fluorescence quenching probably results, in part, from less W383 fluorescence of Q144A that would decrease the potential for ATP quenching of the Trp fluorescence of Q144A. Under the same condition, wild type PDHK2 bound ADP 23-fold weaker than ATP with no significant change in the maximal fluorescence quenching. Addition of Pi caused tighter binding of ADP (2-fold). There was no significant difference in the estimated $L_{0.5}$ for ADP of Q144A and wild type PDHK2 in the presence or absence of Pi. These results suggested that signal transmission from the catalytic site to the cross arm anchoring W833 was changed with the mutation of Q144 to alanine.

Table 2-4. Nucleotide binding to wild type PDHK2 and Q144A. Binding of nucleotides to 0.1 μM kinase was determined by measuring fluorescence quenching in the presence of 100 mM K^+. Parameters were derived from a Hill plot analysis that assumed binding was proportional to fluorescence quenching. (Data were collected by Dr. Hiromasa, Y.)

PDHK2 source	Pi (20mM)	Nucleotide	$L_{0.5}$ for nucleotide (μM)	Hill Coefficient, n_H	Q_{max} (%)
Wild type	No	ATP	3.1	1.7	47
Q144A	No	ATP	9.9	1.1	26
Wild type	No	ADP	72.0	1.0	43
Q144A	No	ADP	77.1	0.9	24
Wild type	Yes	ADP	35.0	1.1	45
Q144A	Yes	ADP	39.3	1.0	32

In conclusion, mutation of Q144 resulted in different response of PDHK2 to K^+. The tighter binding of K^+ in the presence of ATP was weakened. While the weaker K^+ binding in the presence of ADP was not significantly reduced unless in the presence of Pi. Mutation of Q144 also weakened the binding of ATP but not ADP (even with Pi) at the saturated level K^+.

Mutations in the DCA/pyruvate binding pocket

To examine the critical residues of putative DCA binding pocket identified from the crystal structure (76), several residues (R154C, I157F, R158A and R154C/L160A) in the α helix 8 were mutated.

Fig. 2-13 shows the g(s*) profiles for selected mutants. Binding of GST-L2 to W383F, I157F and R154C gave faster sedimenting peaks due to complex formation (solid lines), with profiles similar to those previously reported for wild type PDHK2 (34). These results, in agreement with activity increase by E2, demonstrated that these mutants bound effectively to the L2 domain. For W383F and I157F, addition of 100 μM pyruvate plus 100 μM ADP decreased significantly the rate of sedimentation of fast moving peak (dot lines, Fig. 2-13). These results demonstrated that ADP plus pyruvate weakened the binding of GST-L2 to these mutants. On the other hand, the fast moving peak in R154C and GST-L2 mixture only underwent small changes upon addition of these ligands. These results suggest that ADP plus pyruvate caused little dissociation of GST-L2 from R154C, probably due to loss of pyruvate binding capacity in R154C as will be supported below.

In potassium phosphate buffers, ADP caused fluorescence quenching of wild type PDHK2 (open circles, Fig. 2-14). Addition of 100 μM pyruvate caused the $L_{0.5}$ of ADP to drop 7.6-fold to 2.0 μM. At the same time, the maximal quenching also increased from 48% to 70% (closed circles, Fig. 2-14). These results suggest that ADP binds tighter to PDHK2 when

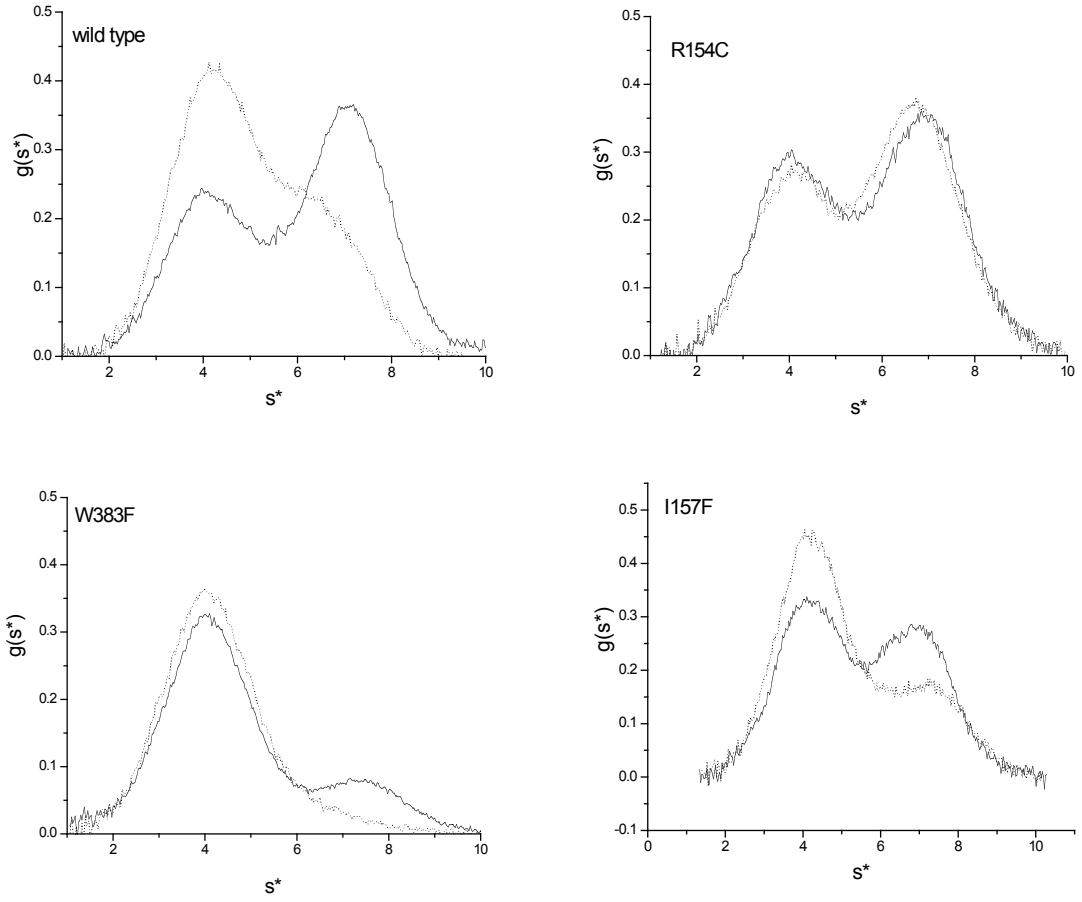

Figure 2-13. Sedimentation velocity analysis of binding of GST-L2 to selected mutants. In the absence (solid curve) and presence (dotted curve) of 100 μM ADP and 100 mM pyruvate, sedimentation velocity was conducted at 49,000 rpm at 20 °C using 3.7 μM kinase dimer and 7.5 μM GST-L2 with the exception W383F (1.2 μM kinase dimer and 4.1 μM GST-L2). Sedimentation was monitored at 280 nm. (Data were collected by Dr. Hiromasa, Y. and published (for wild type PDHK2 and W383F) in *J. Biol. Chem*, (2006) 281, 12568-12579 (43)). Published data were reproduced with permission as covered under the general Copyright Permission Policy of *J. Biol. Chem.*

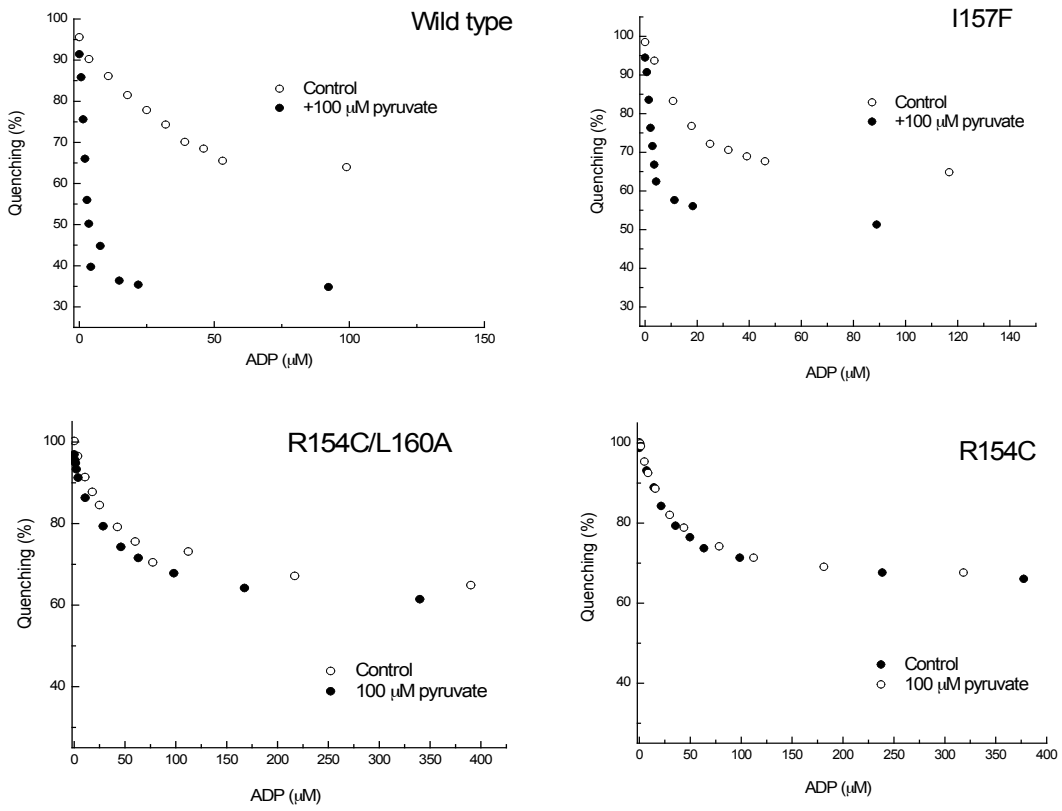

Figure 2-14. Fluorescence quenching of wild type PDHK2 or selected mutants by ADP in the absence (open circle) and presence (closed circle) of 100 μM pyruvate. All data were obtained with 0.7 μM kinase at 350 nm in potassium phosphate buffer with excitation at 290 nm. (Data were collected by Dr. Hiromasa, Y.)

pyruvate is also bound, in agreement with results from kinetic assays (40). The influence of pyruvate on ADP binding to mutants was also evaluated using fluorescence quenching (Fig. 2-14). Pyruvate also enhanced binding of ADP to I157F, while there was no significant difference in the fluorescence quenching profiles of R154C and R154C/L160A. These results suggest that pyruvate binding was greatly weakened or lost with R154C and R154C/L160A mutation of PDHK2.

Table 2-5 shows the DCA inhibition of the mutants surrounding the pyruvate/DCA binding site. The activities were measured using E1•E2 as substrate in a high salt buffer. 0.1 mM or 1.0 mM DCA reduced the specific activity of the wild type PDHK2 by ~ 59% and ~ 86% separately. These levels of DCA caused similar activity reductions with I157F (44% and 84%). Therefore, replacement of I157 with phenylalanine did not significantly influence the DCA inhibition. For mutants R158A, R154C and R154C/L160A, DCA gave smaller or no inhibition. Those data again suggest that R154 and R158 are important for DCA inhibition.

Ions and DCA inhibition

Buffers containing different combination of ions were used to evaluate how K^+ and Cl^- influenced the DCA inhibition of PDHK2 activity using E2 bound E1 as substrate (Fig. 2-15A). 3.5 mM K_xPO_4 was introduced with E1 and E2 addition in all assays. In the low salt buffer, 0.1 and 1.0 mM DCA caused ~ 22% and ~ 48% inhibition of wild type PDHK2 activities. Inclusion of 60 mM Cl^- reduced the kinase activity up to 48%. At the same time, the DCA inhibitions were reduced to ~ 9% and ~25% separately. With addition of 90 mM K^+, kinase activity was also decreased to 59% of the initial value; while DCA inhibition was greatly enhanced, giving 2.7- and 1.8- fold greater inhibition with those levels of DCA. The combination of both K^+ and Cl^- further reduced kinase activity to 34%. The DCA inhibition was only ~ 7% with 0.1 mM DCA

Table 2-5. DCA inhibition of wild type PDHK2 and mutants using E1•E2 as substrate. All assays were conducted in duplicate with 8.6 μM kinase in high salt buffer in the presence of E2 and 100 μM ATP at 30 °C.

DCA (mM)	Wild type	R154C	R154C/L160A	R158A	I157F
0	285±10	185±8	161±5	181±12	219±5
0.1	118±2	169±4	178±12	182±8	122±18
1.0	41±2	175±9	197±10	148±1	36±2

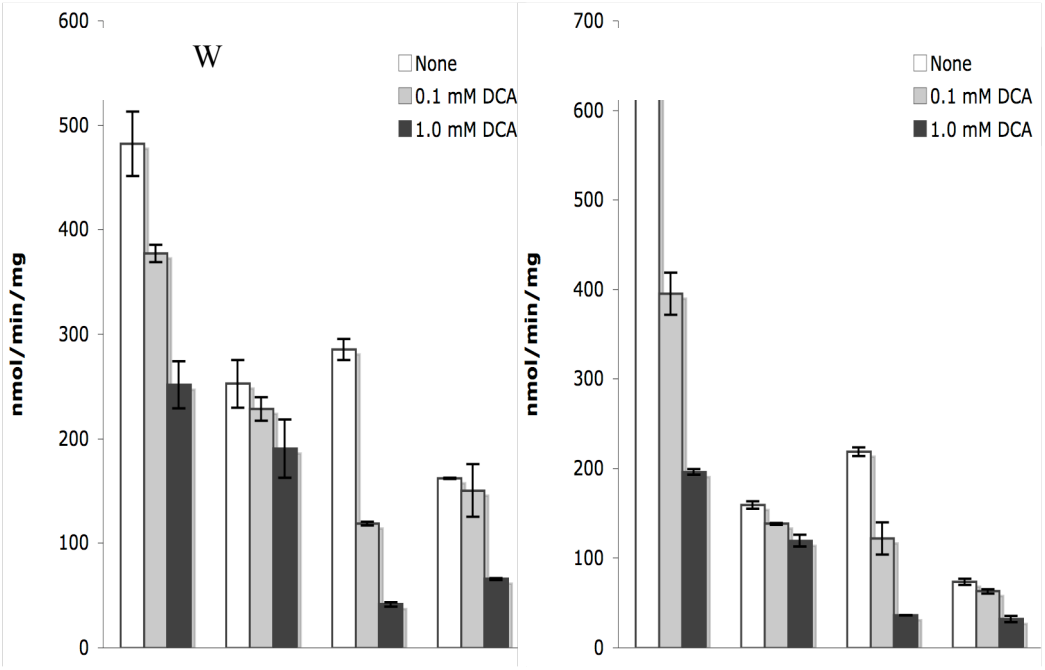

Ion conc.	K^+	none	none	90	90	K^+	none	none	90	90
(mM)	Cl^-	none	60	none	60	Cl^-	none	60	none	60

Figure 2-15. Influence of ions on DCA inhibition of wild type PDHK2 and I157F using E1•E2 as substrate. All the assays were measured with 9.5 nM native PDHK2 or 16 nM I157F. DCA was added 1 min before 100 μM ATP. The basic buffer used was the low salt buffer with around 3.5 mM K_xPO_4 introduced with E1 and E2.

and ~ 59% with 1.0 mM DCA. The DCA inhibition was greater than with Cl^- alone but less than with K^+ alone with 1.0 mM DCA. These results demonstrated that DCA inhibition was enhanced by K^+ and decreased by Cl^- using E1•E2 as substrate. This kinetic result for K^+ influence was in agreement with what got from fluorescence quenching studies, in which 100 μM ADP had no influence on pyruvate binding in the absence of K^+ while pyruvate bound to 14-fold tighter to PDHK2 in the presence of K^+ (89).

The influence of ions on DCA inhibition of mutant I157F was also evaluated using E1•E2 as substrate (Fig. 15B). I157F had a specific activity of ~ 647 $nmol \cdot min^{-1} \cdot mg^{-1}$ in a low salt buffer. Under theseconditions, 0.1 mM and 1.0 mM DCA inhibited the activity of I157F by 39% and 70% respectively, both higher than the inhibition of native kinase by the same levels of DCA. The specific activity of I157F decreased 75% with the addition of 60 mM Cl^-, which was 1.5-fold more reduced than native kinase. At the same time, the DCA inhibition was also decreased to 7% with 0.1 mM DCA or 12% with 1.0 mM DCA, both of which were lower than the inhibition of native kinase by same levels DCA. With the addition of 90 mM K^+ into the low salt buffer, the specific activity of I157F decreased by 66%, again 1.6-fold larger than the native kinase, with a small increase in inhibition (44% by 0.1 mM DCA and 84% by 1.0 mM DCA). The combination of both Cl^- and K^+ ions caused 80% loss of the specific activity of I157F with inhibition of 15% by 0.1 mM DCA and 57% by 1.0 mM. Based on these results, it appears that both K^+ and Cl^- had larger initial effects on I157F mutant than on wild type PDHK2. Again, the increased K^+ or Cl^- inhibition may be due none specific ion effects on the stability of I157F. K^+ enhanced the inhibition of I157F by DCA but by a smaller degree than wild type PDHK2. At the same time, Cl^- reduced the inhibition of I157F by DCA by a larger degree than wild type PDHK2.

Pyruvate/DCA inhibition using E1 alone as substrate

The direct influence of pyruvate on kinase activity was measured using E1 alone as substrate (Fig. 2-16). To minimize the influence of K^+ and Cl^-, no extra K^+ or Cl^- was added apart from the initial potassium phosphate (~ 10 mM) introduced with E1. The specific activity of wild type PDHK2 decreased with increasing pyruvate (Fig. 2-16). Because R154C had lower specific activity under these conditions, its inhibition by pyruvate was not conducted. Therefore, pyruvate directly inhibited PDHK2 activity apart from causing the dissociation of lipoyl groups as was known (32). With 100 μM ATP, ~ 110 μM pyruvate was required to inhibit 50% activity of wild type PDHK2. Mutants W383F and I157F had inhibition patterns by pyruvate similar to native kinase. The replacement of Q144 with alanine somehow decreased the inhibition by pyruvate, requiring ~ 250 μM pyruvate to reach 50% inhibition with ~ 85% being the maximal inhibition.

In general, these mutations did not abolish pyruvate inhibition. On the contrary, pyruvate caused little or no inhibition with R158A and R154C/L160A even up to 1.0 mM (Fig. 2-16). These results indicate that R154 and R158 play important roles in the pyruvate binding.

The DCA inhibition profiles are shown in Figure 2-17, using E1 as substrate under low salt conditions. Compared with pyruvate, same levels DCA caused less maximal inhibition to wild type PDHK2. Q144A, I157F and W383F mutants had DCA inhibition patterns similar to that of the wild type PDHK2. In agreement with the lack of pyruvate inhibition, R154C/L160A and R158A mutants were not inhibited by up to 2.0 mM DCA. These results from DCA inhibition again suggest R154 and R158 play important roles in the DCA/pyruvate binding.

Using AUC, fluorescence quenching, and activity inhibition studies using E1 alone or E1•E2 as substrate, it was found that mutations of R154 and R158 weakened or abolished the

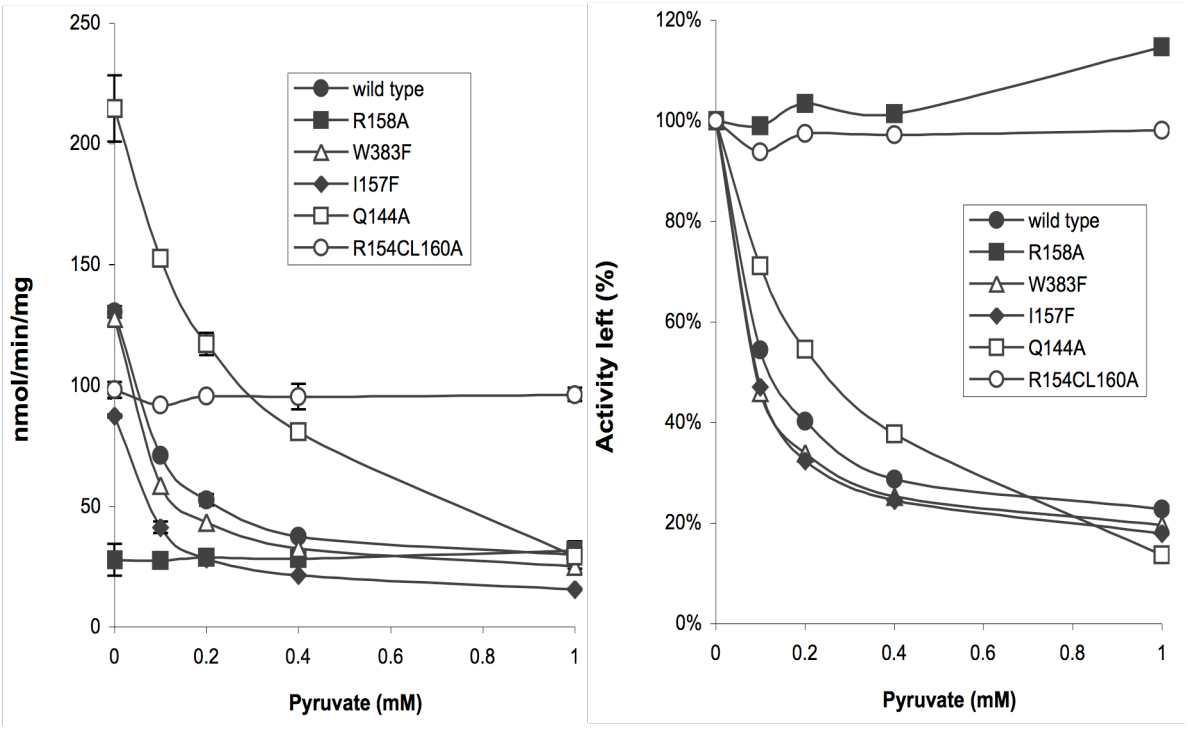

Figure 2-16. Pyruvate inhibition of wild type and mutants PDHK2 using E1 alone as substrate. Panel A shows the change of specific activity with pyruvate. Panel B shows the change of percentage of activity left. All assays were conducted with 43 nM kinase dimer in low salt buffer with 10 mM $KxPO_4$.

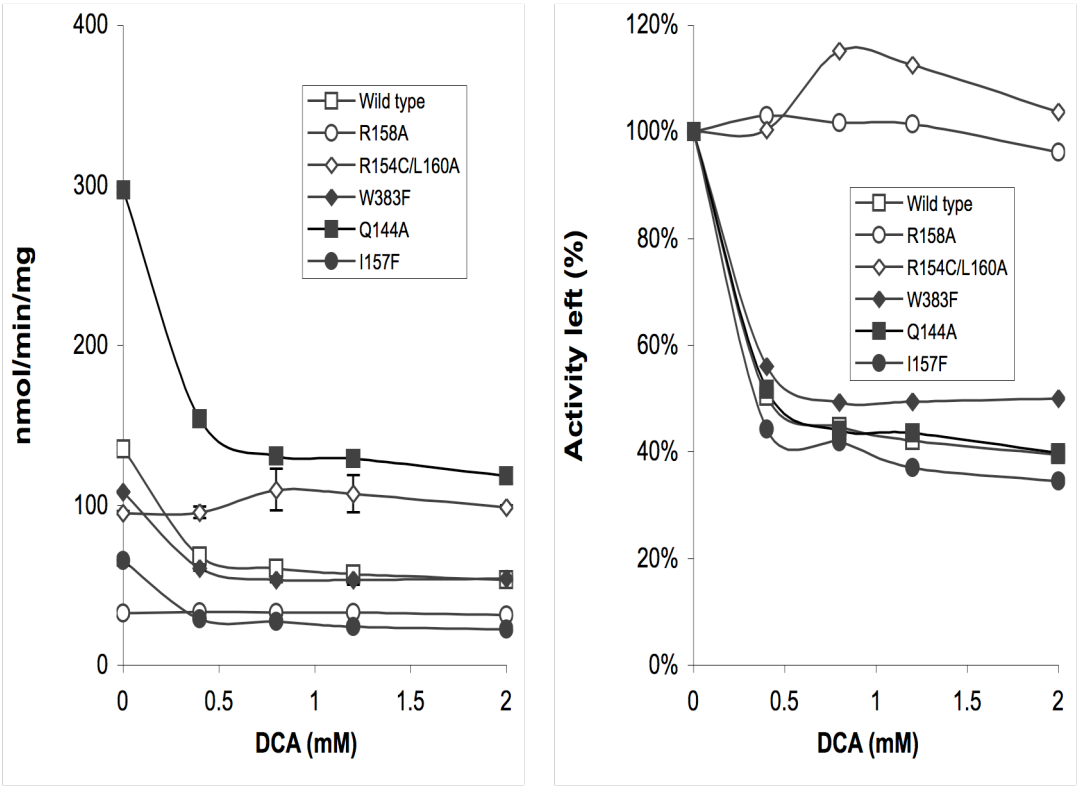

Figure 2-17. DCA inhibition of wild type and mutants PDHK2 using E1 alone as substrate. Panel A shows the change of specific activity of the kinase with increasing DCA. Panel B shows the change in the percentage of activity left. All assays were conducted with 43 nM kinase dimer in low salt buffer with 10 mM $KxPO_4$.

DCA/pyruvate binding capacity and resulted in little or no DCA/pyruvate inhibition. Therefore, R154 and R158 are important residues for DCA/pyruvate binding to human PDHK2, which is consistent with the crystal structure (76). DCA or pyruvate caused not only the dissociation of L2 from the kinase (if combined with ADP) but also directly inhibited the phosphorylation of substrate E1. The finding that replacement of I157 by Phe did not reduce inhibition of PDHK2 suggests this difference may not be the major reason for weaker pyruvate inhibition of PDHK3 (see discussion for the reasons).

The importance of R154 and R158 of human PDHK2 in the DCA/pyruvate inhibition was contradicted to previous studies on rat PDHK2, in which R154A and R158A had similar DCA inhibition as the wild type PDHK2 (85). As Cys has a bigger side chain than Ala, it was possible (although unlikely) that loss of DCA/pyruvate inhibition of human R154C was due to a physical interference to binding of DCA/pyruvate instead of due to lacking of specific Arg side chain. Further mutation of R154 to Ala would help to resolve such difference between human and rat PDHK2.

Cl^- inhibition on PDHK2 and mutants

Using E1 alone as substrate, the effects of Cl^- on PDHK2 activity were evaluated (Fig. 2-18). Increasing Cl^- levels decreased the activity of wild type PDHK2. I157F, Q144A and W383F generally responded like wild type kinase with increasing Cl^-. It required ~ 21 mM Cl^- to reach 50% inhibition for those mutants and native kinase. The specific activities of R158A and R154C/L160A were less sensitive to Cl^-. It required 2-fold more Cl^- (~ 56 mM) to reach 50% inhibition. These data suggest that mutation of R154 and R158 also weakened the influence of Cl^-.

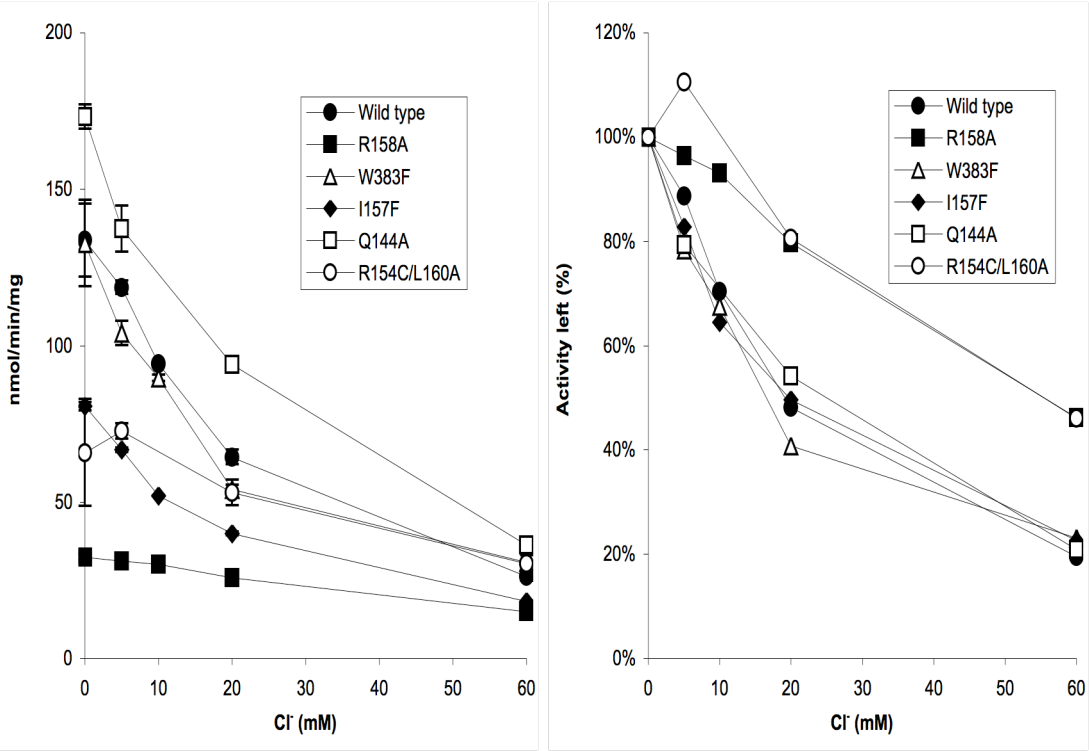

Figure 2-18. Cl^- inhibition of wild type and mutants PDHK2 using E1 alone as substrate. Panel A shows the change in specific activity with Cl^- concentration. Panel B shows the change of percentage of activity. All assays were conducted with 43 nM kinase in a low salt buffer with 10 mM $KxPO_4$.

Using E1•E2 as substrate, Cl^- effects on R158A and R154C/L160A were also evaluated (Fig. 2-19). Compared with using E1 alone as substrate, Cl^- reduced kinase specific activities of these constructs less in the presence of E2. Wild type PDHK2 activity was reduced only ~ 10% by 10 mM Cl^- in the presence of E2, a 1/3 fold less than that using E1 alone as substrate. 60 mM Cl^- resulted ~ 50% activity reduction of wild type PDHK2. The specific activities of R158A and R154C/L160A were decreased little by 10 mM Cl^-. Both R158A and R154C/L160A retained greater fractions of their initial specific activities than wild type at 60 mM Cl^-. These data again suggest that replacements of R154 and R158 result in reduced kinase sensitivity to Cl^- inhibition. It was not clear why Cl^- reduced the activity of R154C/L160A and R158A at high levels using E1 or E1•E2 as substrate. Further experiment was required to determine if non-specific ion effects cause it or there is a second Cl binding site.

Relationship between Cl^- and pyruvate inhibition

Cl^- hindered the inhibition of PDHK4 by DCA (Dong, *et. al*, unpublished data). The above studies showed PDHK2 had reduced DCA inhibition in the presence of Cl^-. The mutants that lacked pyruvate inhibition also had reduced sensitivity to Cl^- with or without E2, while those mutants that maintained pyruvate inhibition also had greater Cl^- sensitivity as wild type PDHK2. These finding suggested that there might be a specific connection between pyruvate inhibition and the Cl^- response. One possibility is that Cl^- may bind to PDHK2 at the same pocket as DCA/pyruvate. If that was true, they should compete against each other. To examine this concept, pyruvate inhibition was measured in the presence of different levels of Cl^- using E1 as substrate (Fig. 2-20, Table 2-6). Addition of Cl^- lowered the initial kinase activities. Increasing pyruvate decreased PDHK2 activity gradually with or without Cl^- (Fig. 2-20). The same levels of pyruvate gave less inhibition with increasing Cl- levels. The estimated IC50 was ~ 81 μM in the

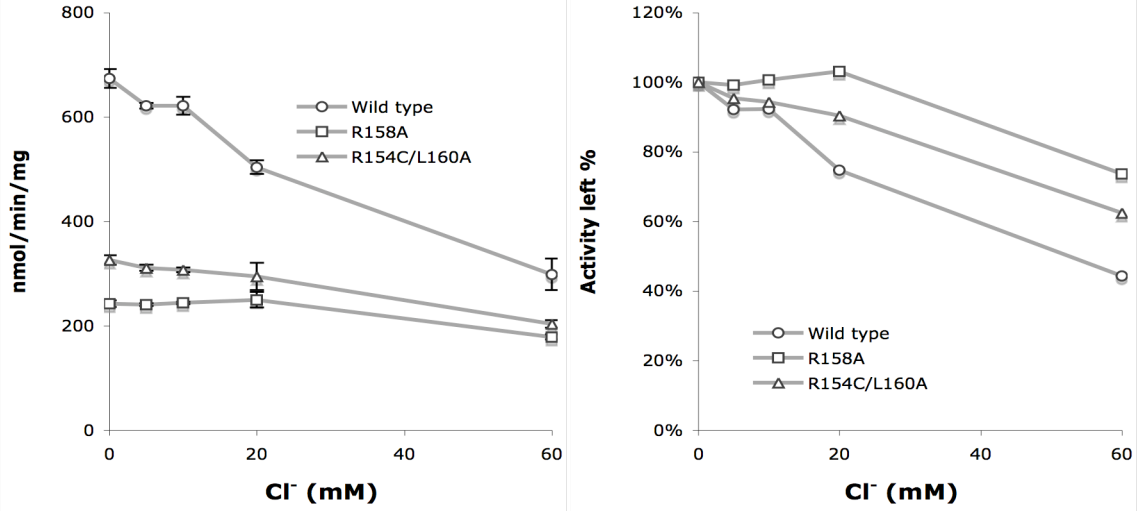

Figure 2-19. Cl^- inhibition on native and mutants PDHK2 using E1•E2 as substrate. Panel A shows the change of specific activity with Cl^- concentration. Panel B shows the change of percentage of activity. All assays were conducted with 10 nM kinase dimer in a low salt buffer with 13 mM $KxPO_4$.

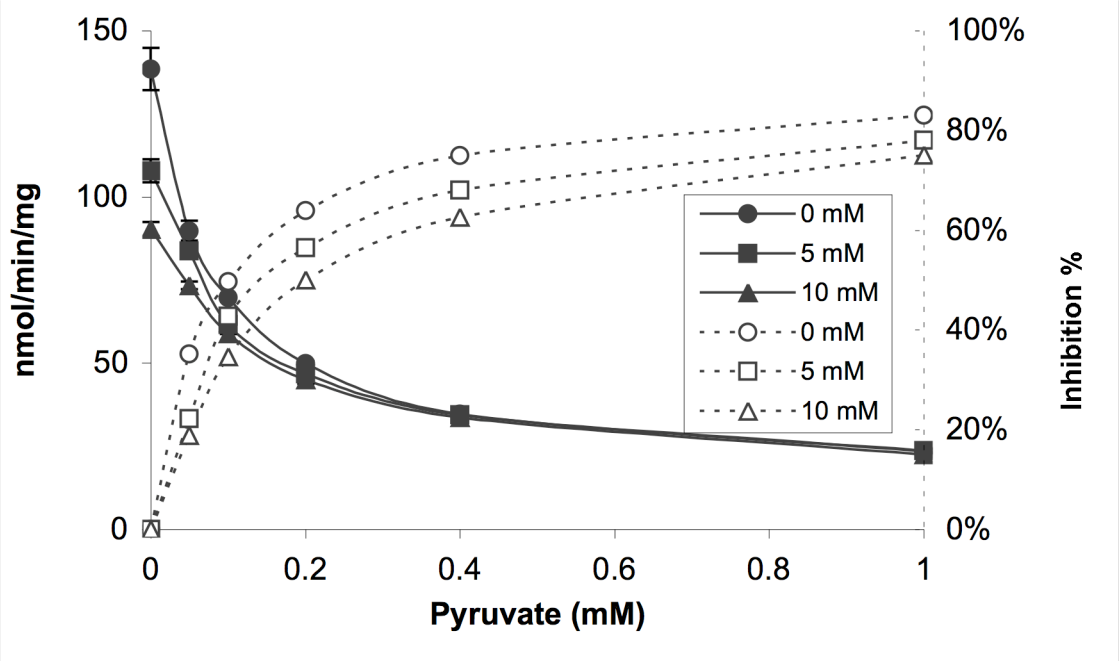

Figure 2-20. Cl^- influence on pyruvate inhibition of native PDHK2 using E1 as substrate. Solid lines show the changes of specific activity. Dashed line show the change of percentage of inhibition of the initial activities. All assays were conducted with 43 nM kinase dimer in low salt buffer with 10 mM $KxPO_4$.

Table 2-6. Effects of Cl^- and Nov3r on pyruvate inhibition using E1 alone as substrate. Inhibition of kinase was measured using 100 μM ATP. The parameters were derived from a Hill plot analysis. Assay conditions were described under the materials and methods. *, 2% DMSO was present in all assays.

Ion conditions	Changed factors	IC50 (μM)	Maximal inhibition (%)
10 mM K_xPO_4	none	80.6±1.5	90 ±1
10 mM K_xPO_4	5 mM Cl^-	101 ±10	82 ±1
10 mM K_xPO_4	10 mM Cl^-	137 ±9	82 ±2
90 mM K^+ 20 mM PO_4	None	27.9 ±1.4	93 ±1
90 mM K^+ 20 mM PO_4	1 μM Nov3r	115 ±11	82 ±2

absence of Cl^- (Table 2-6). Addition of 5 and 10 mM Cl^- increased the IC50 for pyruvate inhibition by 1.3- and 1.7-fold separately. As predicated by competition at the same site, PDHK2 approached the same activity as pyruvate was increased to 400 μM no matter the initial concentration of Cl^-. This is expected with competition at same site due to bound Cl^- being replaced by pyruvate. These results agree with the proposal that Cl^- and pyruvate inhibitions are not independent and suggest that they bind to the same site on PDHK2.

Form the studies of Cl^- effects, it was found that the R154 and R158 are important residues for Cl^- inhibition. Cl^- binds to the DCA/pyruvate site of human PDHK2 and competes with DCA/pyruvate to reduce their inhibition.

Stimulation of PDHK2

The influences of reductive acetylation were evaluated for several mutants (Fig. 2-21). The assay buffers included 90 mM K^+, 60 mM Cl^- and 20 mM extra Pi. This buffer is used because both the presence of elevated K^+ and the inhibitory anions are required for stimulation (30). In these assays, the ratio of NADH to NAD^+ was fixed 3:1 to prevent the conversion of E3 to the fully reduced (dithiol-$FADH_2$) form. The mutants with higher initial activities were stimulated less (Fig. 2-21). NADH/NAD^+ increased the activity of wild type PDHK2 by1.7-fold. The activity increased 3.9-fold with both NADH/NAD^+ and 50 μM acetyl-CoA. Both R154C and R158A underwent similar extents of stimulation as wild type, indicating that replacement of both residues interfering with pyruvate binding had no influence on stimulation by reductive acetylated lipoyl groups which bind at the adjacent lipoyl group binding site. W383F also had similar stimulatory response as wild type. Double mutant R154C/L160A had less NADH/NAD^+ and Acetyl-CoA stimulation (1.6- and 2.3-fold). Q144A, which had highest initial activity, had the lowest amount of stimulation (1.7-fold) by reductive acetylation (Fig. 2-21). These data

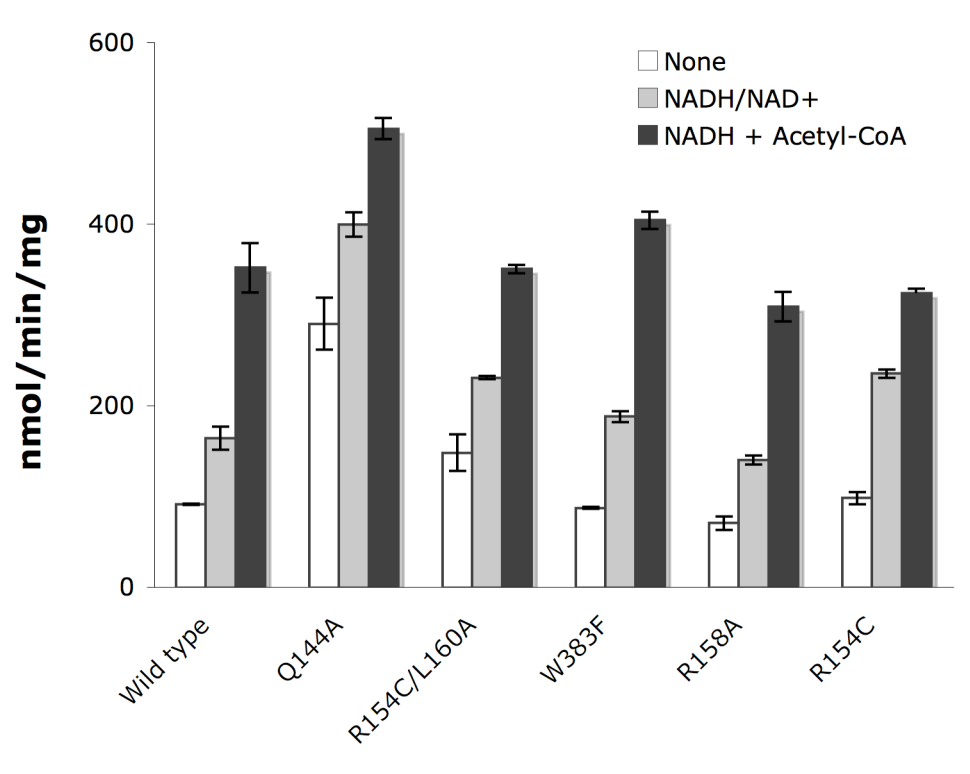

Figure 2-21. Stimulation of wild type and mutants PDHK2 by NADH and acetyl-CoA. $NADH/NAD^+$ ((0.6/0.2 mM) was added 60 s before 100 μM ATP and 50 μM acetyl-CoA was added 20 s before ATP. Other assay conditions were described in the materials and methods.

suggest that both L160 and Q144 may participate in the signal transmission from the lipoyl group binding site to the catalytic site.

Nov3r & PDHK2 activity using E1 as substrate

Nov3r is a PDHK2 inhibitor that inhibits E2-enhanced kinase activity (83, 84). Based on the crystal structure, Nov3r binds at the same site as the lipoyl group (76, 77). By competing with lipoyl prosthetic groups, Nov3r prevents PDHK2 binding to lipoyl domain of E2, resulting in loss of E2 activated kinase function (76). Using free E1 as substrate, the influence of Nov3r to kinase was evaluated (Fig. 2-22).

2% DMSO, which caused less than 8% reduction of kinase activity, was added to all assays. In a low salt buffer containing 10 mM K_xPO_4, binding of Nov3r increased PDHK2 activity with a maximal increase of ~ 20% by 100 nM Nov3r (Fig. 2-22). The estimated concentration to reach the half maximal stimulation was ~ 60 nM Nov3r. It was reported that Nov3r bound to PDHK2 with an affinity less than 10 nM under high salt buffers (88). The Kd for Nov3r binding was not determined under a low salt condition. However, it appeared that Nov3r bound to PDHK2 less tightly under low salt than high salt conditions. It was possible that the maximal activity increase by Nov3r might occur with single Nov3r bound per PDHK2 dimer. Further experiments would be needed to evaluate this possibility. Higher Nov3r levels caused a gradual decrease of kinase specific activity. These results were similar to previous studies with GST-L2 and ΔBE2 (lacking E1 binding domain) in which kinase activity was activated at low levels of effectors but was inhibited by higher levels (30, 32). These data agree with the conclusions that Nov3r binds to lipoyl group binding site of PDHK2.

Pyruvate weakens the binding of the lipoyl domain to PDHK2. The influence of pyruvate

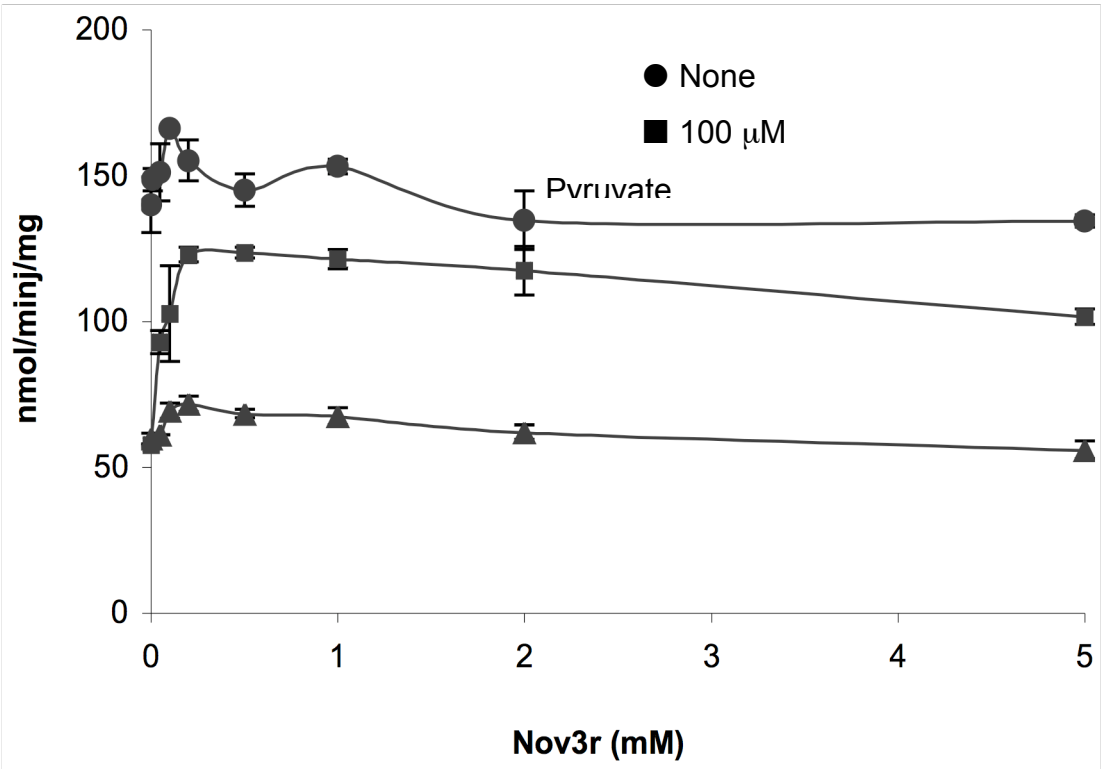

Figure 2-22. Nov3r influence on wild type PDHK2 using E1 alone as substrate. Data showing with circle, square and triangle were obtained with no inhibitor, 100 μM pyruvate and 20 mM Cl^- respectively. All assays were conducted in low salt buffer with 10 mM $KxPO_4$.

or Cl^- to Nov3r effects was investigated (Fig 2-22). 100 μM pyruvate reduced PDHK2 activity by ~ 60%. Nov3r gave a 115% maximal increase of activity at 200 nM Nov3r, but this activity was still 15% lower than the original PDHK2 activity in the absence of both pyruvate and Nov3r. Therefore, Nov3r reduced but did not abolish pyruvate inhibition. The concentration needed to reach half-maximal activity was estimated to be ~ 100 nM Nov3r, a ~1.5-fold higher than in the absence of pyruvate. Higher levels of Nov3r also slightly lowered kinase activity (Fig. 2-22). As Cl^- might occupy the same site as pyruvate based on its competing with pyruvate (above results), it was reasonable to suggest that Nov3r binding to PDHK2 might also have a similar effect in reducing Cl^- inhibition. In the presence of 20 mM Cl^-, PDHK activity dropped to 43%, similar to the effect of 100 μM pyruvate. However, Nov3r caused a much smaller increase (~20%) and then a gradual decrease in the kinase activity; a pattern more closely resembling that without Cl^- than that in the presence of pyruvate (Fig. 2-22). The estimated concentration to reach the half-maximal activity was ~ 75 nM Nov3r. Therefore, the influence of Nov3r on the inhibitory effects of pyruvate and Cl was different. The cause of Nov3r inhibition at higher levels was not clear.

I also studied how ions influenced the effects of Nov3r on pyruvate/DCA inhibition using E1 alone as substrate (Fig. 2-23). 1.0 μM Nov3r caused ~10% reduction in kinase activity in buffers tested. One possibility was that PDHK2 lost activity during a half hour gap because it was not stable when mixed with E1 alone. The specific activity of PDHK2 was reduced ~ 60% or 45%, respectively, by either 90 mM K^+ or 20 mM Pi in the presence or absence of 1.0 μM Nov3r. Therefore, Nov3r did not significantly influence the extent of inhibition by K^+ and Pi. In a low salt buffer (0.4 mM potassium phosphate from E1), 100 μM pyruvate or 200 μM DCA inhibited PDHK2 activity by ~ 23% and 24%. Addition of Nov3r did not significantly change the inhibition by either inhibitor (~19% by pyruvate and ~ 27% by DCA). Inclusion of 20 mM Pi

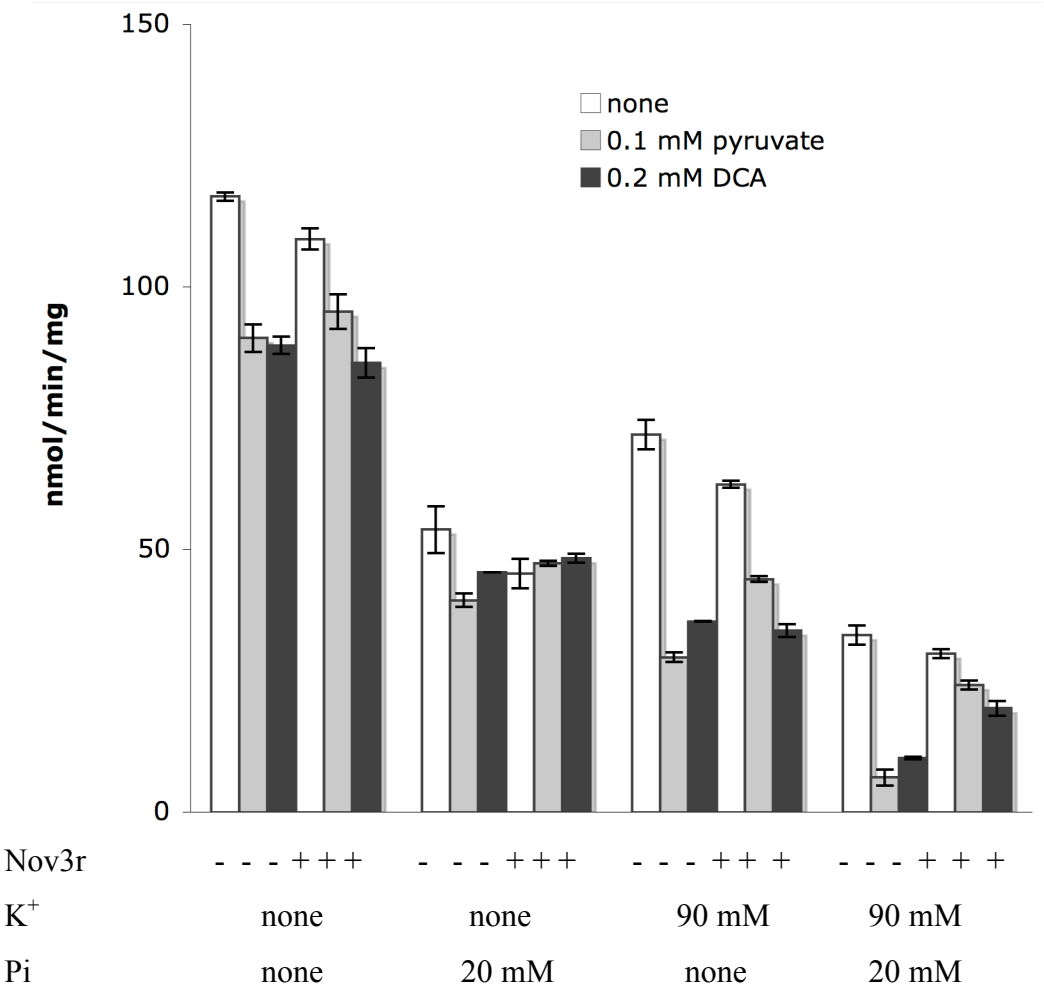

Figure 2-23. Ion effects on Nov3r influence to inhibition of wild type PDHK2 by pyruvate or DCA using E1 as substrate. 1.0 μM Nov3r, 200 μM DCA or 100 μM pyruvate were added 60 s before 100 μM ATP. The indicated levels of Pi and K^+ were added into assay buffers.

inhibited but had minimal effects on pyruvate (~25%) and DCA (~15%) inhibition. Nov3r caused small reduction in the low inhibition by pyruvate and DCA to 12 and 10%, respectively with this buffer. Addition of 90 mM K^+ caused 2-fold greater inhibition by both pyruvate and DCA than was observed with the low salt buffer. Nov3r had an increased capacity to reduce pyruvate inhibition but did not significantly reduce the DCA inhibition. In a buffer containing both K^+ and Pi, activity of PDHK2 was even lower (~ 30% of that in low salt buffer). At the same time, pyruvate and DCA were potent inhibitors giving ~ 81% and ~ 69% activity decreases respectively. Although addition of Nov3r, alone, modestly inhibited PDHK2 activity, Nov3r hindered pyruvate inhibition (3.7-fold rise in activity) and gave a smaller but substantial removal of DCA inhibition (1.9-fold rise in activity). These results indicated that just as pyruvate and DCA inhibition and binding are enhanced by K^+ and Pi, the capacity for Nov3r to block these effects is also fortified by these ions.

The effects of Nov3r on pyruvate inhibition were further assessed over a wide rage of pyruvate concentrations in a buffer containing 90 mM K^+ and 20 mM Pi (Fig. 2-24, table 2-6). At all levels of pyruvate, less kinase was observed in the presence than in the absence of 1.0 μM Nov3r (Fig. 2-24). Pyruvate maximally inhibited kinas activity up to ~93% with an estimated IC50 of ~ 28 μM without Nov3r (Table 2-6). Addition of 1.0 μM Nov3r weakened the pyruvate inhibition with an ~ 4-fold increase of the IC50 and 82% maximal inhibition. It needed to be noted that the IC50 without Nov3r was almost 3-fold higher than that in the buffer containing 10 mM K_xPO_4. It indicated that pyruvate inhibition was enhanced by elevated K^+ and Pi even using E1 alone as substrate.

Based on above studies of Nov3r effects, it can be concluded that binding of Nov3r to human PDHK2 increased kinase activity. Nov3r binding at the lipoyl group binding site reduced

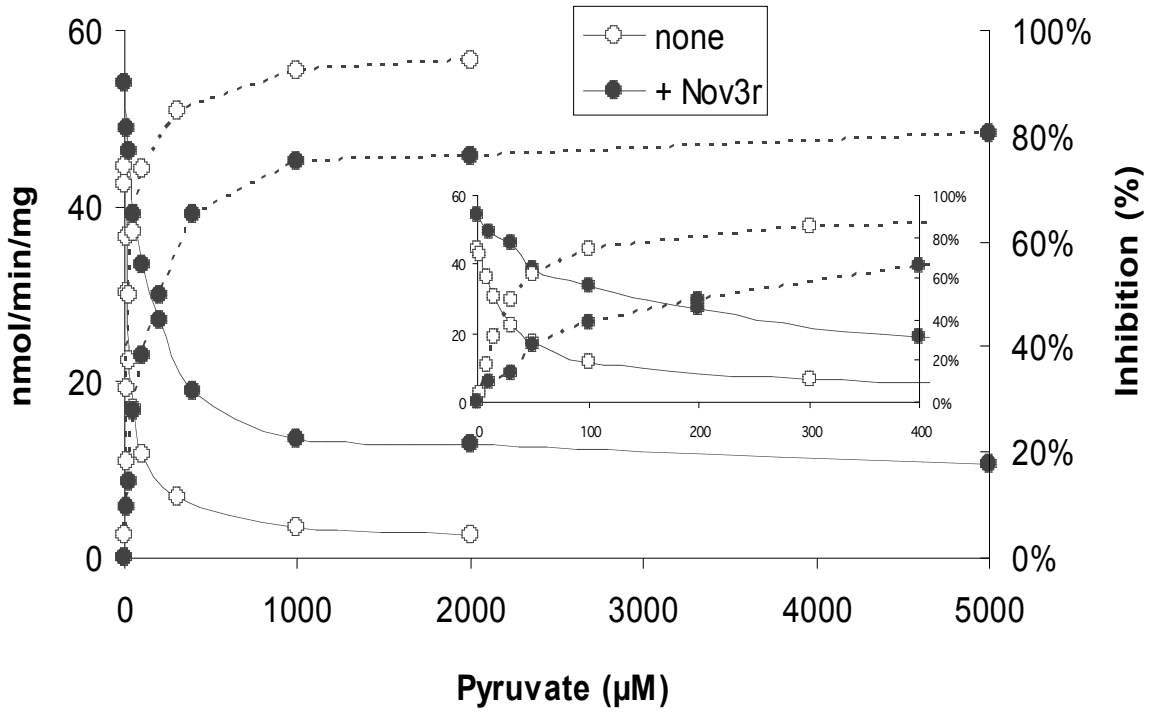

Figure 2-24. Influence of Nov3r on pyruvate inhibition of wild type PDHK2 using E1 as substrate. The changes of activity and percentage of inhibition are shown in solid and dashed curve respectively. The data with closed and open circle were obtained with or without Nov3r respectively. 1.0 μM Nov3r and pyruvate were added 60 s before 100 μM ATP. The assays were conducted with 2% DMSO in low salt buffer with 90 mM K^+ and 20 mM Pi added.

the DCA/pyruvate inhibition at the nearby DCA/pyruvate site. Even though Cl^- binds to the same site as DCA/pyruvate, Nov3r did not significantly affect its inhibition relatively because of the smaller size of Cl^-.

Discussion

Fluorescence quenching of the cross arm anchoring W383 with ligands binding— (Published in *J. Biol. Chem.* (2006) 281 12568-12579 (43)) Based on the crystal structure of human apo-PDHK2 dimer, a cross arm was formed by the C-terminal residues 361-384 of each subunit that extends from the Cat domain of one subunit to interact primarily via Trp383 with the dimerization face of the R-domain of the second subunit (Fig. 1-5, 76). Similar cross arms are observed in the crystal structures of human PDHK3•L2 and these cross arms plus the extended C-terminal tail contribute to the binding of lipoyl domain (77). The cross arm is not resolved in the crystal structure of human PDHK2•ADP•DCA (76). ADP or ATP alone interferes slightly with the binding of PDHK2 to E2 or L2 (43). AUC studies revealed that pyruvate plus ADP prevented binding of GST-L2 to PDHK2 and that PDHK2 dimers associated as tetramers under these conditions (34, 36, 43). To reduce PDHK2 association with L2, ligand binding may cause conformational changes in PDHK2 that alter the cross arm stability. That possibility is supported by ligand-induced changes in Trp383 fluorescence.

W383F-PDHK2 maintained the capacity to bind to E2 lipoyl domains and its activity was enhanced by E2. W383F had only one-third of the intrinsic fluorescence intensity of the native kinase at 350 nm. Even though PDHK2 contains three Trp, the loss of Trp fluorescence with W383F suggests that Trp383 provides most of the Trp fluorescence of wild type PDHK2. ADP or ATP caused fluorescence quenching of the native kinase did not influence the fluorescence of the W383F mutant, indicating that ADP or ATP binding at the active site significantly alters W383 interactions at the R-Cat domain interference that is occurring more than 20 Å from the active site. The fluorescence quenching of W383 confirmed that conformational changes happened to the cross arm-anchoring Trp environment with the binding of ADP or ATP because

the fluorescence of tryptophan is sensitive to the change of its electrostatic environment (81, 82). But it is still not clear how the cross arm changes with ligand binding. This may involve with ATP or ADP binding small conformational shifts around the Trp anchoring region with an increased probability of breaking free of the cross arm.

Pyruvate quenched the fluorescence of not only wild type PDHK2 but also W383F, but to a substantially reduced extent. Therefore, pyruvate binding at the DCA/pyruvate site resulted in conformational changes to the Trp383 environment. The residual quenching of W383F suggests that the surrounding environment of at least another Trp was also changed. Trp79 is located in helix α5 of the R domain next to Tyr80 and directly above His115, which sits above bound DCA/pyruvate (Fig. 1-6, 76). Both Trp79 and His115 shift with ADP and DCA bound (76). Interactions of Trp with a histidine side chain can cause Trp fluorescence quenching (81, 82). The fluorescence intensity of Trp371 may not change much with the binding of ligands as it is exposed to solvent on the cross arm.

ADP binds tighter to PDHK2 with bound pyruvate, as much lower concentration of ADP were required to reach same level of fluorescence quenching of PDHK2 in the presence of pyruvate. The reciprocal was also true that ADP greatly enhanced pyruvate binding. These results are consistent with kinetic studies that ADP dissociation was slowed by pyruvate (40). The increased fluorescence quenching by pyruvate plus ADP may occur with the disruption of the cross arm that leads to dissociation of L2 from kinase and formation of PDHK2 tetramer (34, 36, 43).

Basis for pyruvate/DCA inhibition—Crystallographic studies identified a DCA binding site on PDHK2. Based on structural considerations, it would appear that the carboxyl group of DCA forms a salt bridge with R154 and that R158 controls the access of DCA into the binding

pocket (76). It is reported that mutation of R154A and R158A of rat PDHK2 did not significantly affect the DCA inhibition although rat PDHK2 has exact same sequence at the R domain as human PDHK2 (85). The finding was carried out with my studies and as described below these findings are not with my studies seeking to determine the roles of these residues in DCA/pyruvate inhibition of human PDHK2. Previous studies reported that DCA/pyruvate strongly inhibited PDHK2 but weakly inhibited PDHK3 (32). Human PDHK2 and PDHK3 have generally conserved residues forming the proposed DCA/pyruvate binding site. A difference includes substitution of Ile157 by Phe in PDHK3. In the crystal structure of human PDHK2 (76), I157 has hydrophobic interactions with DCA. In apo-PDHK2, there is a large space between I157 and I111/His115 that is occupied by the side chain of Phe in human PDHK3 (77) with substitution of I157F by Phe and I111 by Val. It is possible that the single substitution causes weaker pyruvate/DCA inhibition in PDHK3 (32).

R154C and R158A mutants at the DCA/pyruvate site and the double mutant R154C/L160A maintained the capacity to bind to E2 lipoyl domains based on retention of E2-activation of kinase activity and similar GST-L2 binding observed by AUC studies. DCA or pyruvate gave little inhibition of these mutant kinases using E1 alone or E1•E2 as substrate. AUC data confirmed that pyruvate did not cause significant dissociation of GST-L2 from these mutants. Unlike with native PDHK2, pyruvate did not affect the binding of ADP to these mutants based on the fluorescence quenching studies. These results suggest that pyruvate or DCA did not inhibit the kinase activity due to lack of inhibitor binding with the mutation of R154 or R158. Therefore, R154 and R158 residues of human PDHK2 play important roles in DCA/pyruvate recognition.

The other mutation at this site, I157F, displayed inhibition patterns by pyruvate or DCA similar to wild type PDHK2. Pyruvate could also bind to I157F based on the pyruvate interference with this mutant binding to GST-L2 in AUC studies and pyruvate-enhanced fluorescence quenching profiles by ADP. Based on these results with PDHK2, the Phe residue in this position in native PDHK3 may not be the reason for weaker inhibition of PDHK3 by DCA/pyruvate. However, the weaking of inhibition of inhibition by the resident Phe in PDHK3 is not eliminated since crowding of the DCA binding space by this Phe is observed with native PDHK3 crystal structures but is not observed for Ile of native PDHK2 structures. PDHK2 may accommodate the Phe substitution with retention of an open inhibitor binding space. Other possible causes will be considered below.

The results of pyruvate/DCA binding site mutation in human PDHK2 were very different from recent reports with rat PDHK2 (85). In rat PDHK2, both R154A and R158A were inhibited by DCA, while DCA caused even stronger inhibition to rat I157A. It also needed to be noted that rat L160A was active. It was possible (although unlikely) that the difference between R154C in human and R154A in rat was due to the larger side chain of Cys blocking the binding of DCA or pyruvate. The basis for such different results with R158A and L160A substitutions are not well understood, as human and rat PDHK2 have identical sequences in the R domain.

Pyruvate plus ADP weaken the binding of lipoyl domains to PDHK2 (43). Thus, pyruvate/DCA inhibition of E2-enhanced kinase activity is probably, in part, due to increased dissociation of PDHK2 from the lipoyl domains of E2. This would decrease the access of PDHK2 to E1 substrate that also binds to E2 through E1-binding domains. It was reported that DCA inhibited PDHK2 in the absence of E2 although the inhibition was significantly weaker than with E2 (32). A critical condition in those studies was inclusion of high level Cl^- (see

below). Our studies on human PDHK4 also found that pyruvate/DCA directly inhibited kinase activity using E1 alone as substrate (unpublished data from our lab). Using E1 alone as substrate with a low Cl^- buffer, my studies found that pyruvate directly inhibited the phosphorylation of E1 with an estimated IC_{50} of ~ 91 μM, which indicates tight pyruvate binding. DCA also inhibited PDHK2 but the inhibition was weaker than pyruvate under these conditions. With E1•E2 as substrate, inhibition probably results from this direct effect and also from decreased access of kinase to E1 substrate due to inhibitor-enhanced dissociation of kinase from the lipoyl domains of E2. For PDHK2, DCA or pyruvate causes marked losses of kinase activity (using E1•E2 as substrate) because these inhibitors act on PDHK2 by both mechanisms. Due to tight binding to E2, the capacity of these inhibitors to reduce PDHK3 binding to E2 may be minimal. Lack of this effect may contribute to the less effective inhibition of this isoform either by reducing the maximal inhibition of PDHK3 or by reducing the affinity of pyruvate/DCA. Studies on PDHK3 inhibition by pyruvate/DCA using E1 in the absence of Cl^- are needed.

Mechanism for Cl^- inhibition—Most of the reported assays of kinase activity were performed using elevated levels Cl^- (at least 60 mM). Cl^- is one of the ions that reduce the activity of wild type PDHK2 and Cl^- inhibition is overcome as part of stimulation by reductive acetylation (30, 32, 40). My studies found that Cl^- weakened the DCA inhibition of E2-enhanced kinase activity. Using E1 alone as substrate, increasing levels of Cl^- reduced the specific activities of wild type PDHK2. It required ~ 21 mM Cl^- to drop the initial activity to 50% with an estimated maximal inhibition ~ 90%. Using E1 alone as substrate, both the R154C/L160A and R158A mutants, which had weakened DCA/pyruvate inhibition, also had greatly reduced inhibition by Cl^-. Two-fold higher Cl^- levels were required to reach 50% inhibition of these mutant kinases. Cl^- inhibited R154C/L160A and R158A less than native kinase in the presence

of E2 suggesting that both Arg residues also play important roles in Cl^- inhibition. With wild type PDHK2, the estimated IC50 for pyruvate increased 1.7- and 2.2-fold in the presence of 5 and 10 mM Cl^-. The full set of data could be fit by a model in which Cl^- binds to the same site and competes with pyruvate/DCA. Cl^- may form electrostatic interactions with R154 and R158 side chains in binding to PDHK2. Substitution of either amino acid would weaken the binding of Cl^- thereby causing less inhibition. The competition between Cl^- and DCA explained why reported DCA inhibition (32) was weaker in a MOPS-K^+ buffer, which containing 60 mM Cl^-, comparing with my results in a buffer with minimal Cl^-.

DCA caused more activity decrease when using E1•E2 as substrate than using E1 alone as substrate in a buffer with minimal Cl^-. On the contrary, Cl^- inhibited the activity of PDHK2 less using E1•E2 as substrate than using E1 alone as substrate under same conditions. It appeared that Cl^- was not as efficient as DCA in causing dissociation of L2 from PDHK2. This agrees with the AUC studies that found GST-L2 was dissociated from PDHK2 by pyruvate plus ADP (43) but not by Cl^- plus ADP (unpublished data from our lab). The binding of lipoyl group to kinase probably stabilized the kinase and weakened the Cl^- inhibition. Previous studies of DCA inhibition on PDHK3 were conducted in buffers containing 60 mM Cl^- (32). That may be another reason for weak DCA inhibition of E2-enhanced kinase activity of PDHK3. In fact, 1mM DCA gave 55% inhibition of PDHK3 activity in a buffer that contained a low level of Cl^- (unpublished data from our lab). It needs to be noted that substitution of I157F at the DCA/pyruvate site enhanced Cl^- inhibition. When comparing the crystal structures of PDHK2 (76) with PDHK3 (77), the larger side chain of Phe appears to occupy more space at where DCA bound than Ile. Possibly, decreased space at this site may strengthen Cl^- binding.

Linkage from the R domain to the Cat domain —K^+ decreases the K_m for ATP and K_i for ADP of PDHK and specifically PDHK2 (32, 80). In the presence of E2, elevated K^+ slows the dissociation of ADP from PDHK2 thereby also decreasing kinase activity (32, 40). Recent studies on PDHK2 (89) quantified large effects of K^+ in the tight ATP/ADP binding, ADP enhanced pyruvate binding, and Pi enhanced ADP/pyruvate binding. In the crystal structures of BCKD kinase and human PDHK3, a K^+ ion is found coordinated at the active site with ATP or ADP (73, 77). Based on the branched-chain kinase structure, a K^+ was modeled in a similar position in the active site of PDHK2 crystal structures (76).

In the apo-structure of PDHK2, the backbone carbonyl groups of Leu295, Ser297, Gly319 and hydroxyl group of Ser301 form the binding pocket for K^+. With ADP/DCA bound, the α-phosphate of ADP also chelates K^+. Based on the crystal structures, with bound ATP and Nov3r, hydrogen bonds formed by the backbone NH groups of Gly317 and Tyr320 with the oxygen atom that link the β and γ phosphate and the oxygen atom of γ-phosphate occur with an associated conformational changes around K^+ binding pocket that prevent the interactions between K^+ and C=O groups of Gly319 (Fig. 2-25) (76). As these crystal structures were obtained not only with different bound effectors (DCA or Nov3r) but also with ADP or ATP bound, respectively, it is still unknown whether binding of ATP versus ADP also contributed to changes at the active site. Based on the fluorescence quenching studies, it was observed that K^+ was bound 16-fold tighter in the presence of ATP than ADP, and 2-fold tighter K^+ binding was observed with ADP plus Pi. Therefore, binding of ATP or ADP alone probably favored different conformational states at the active site to result in different affinities in binding of K^+. Pi may occupy the same position as γ-phosphate of ATP and bring similar changes to the binding pocket of K^+ in the presence of ADP, resulting in tighter binding of K^+. Pi effects on pyruvate binding

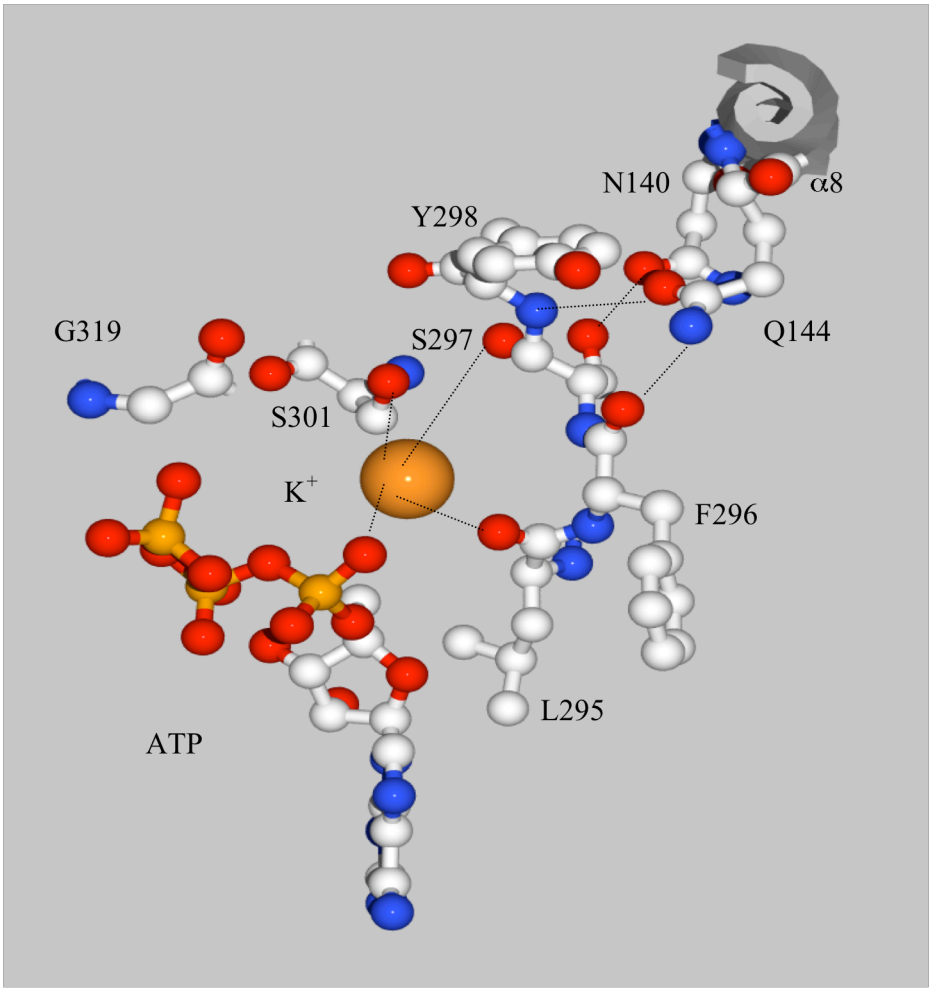

Figure 2-25. Linkage from the R domain to the catalytic site. Q144 and N140 residues on α8 helix of the R domain of PDHK2 link the R domain with loop 295-298 of the Cat domain through hydrogen bonds between N140-S297, Q144-Y298 and Q144-F296. K^+ ion is connected to the loop by interactions with S297 and L295. Finally, the K^+ interacts with the α-phosphate of ATP/ADP to complete the linkage from the R domain to the catalytic site. In the presence of ATP, K^+ also interacts with S301. In the presence of ADP or apo-PDHK2, G319 is also involved in the K^+ binding.

were observed even with bound ATP (89). It is possible that Pi has another binding site in PDHK2. The binding of K^+ with ADP or ATP at the active site was specific, as Na^+ did not influence the ADP/ATP binding (89). It was also reported that $NH4^+$ bound to PDHK2 even tighter than K^+ in the presence of ATP (89).

The side chain of Q144 in the α-helix 8 of R domain forms hydrogen bonds with backbone NH of Tyr298 and backbone C=O group of Phe296, residues adjacent to Ser297 that chelate K^+ via C=O group (Fig. 2-25) (76). The substitution of Q144 would abolish the hydrogen bonds, thus might lead to conformational changes in the ADP/ATP•K^+ binding site via repositioning of the 296-298 segment with altering S297 chelation of K^+. The specific activities of native kinase decreased with increasing K^+ concentration with or without E2. Using E1 alone as substrate, the specific activity of Q144A increased 2-fold when K^+ was increased from 0.9 mM to 10 mM, followed by a 21% reduction with K^+ increasing further to 90 mM. Similar trends were also observed for Q144A with less initial increase and less decrease in the presence of E2. Fluorescence quenching also confirmed the changes of K^+ binding with mutation of Q144A. Q144A mutation weakened the K^+ binding affinity by 15-fold in the presence of ATP but gave no change in the presence of ADP unless Pi was included. With 100 mM K^+, ATP binding was 3-fold weaker due to substitution of Q144 with Ala. Therefore, Q144 at the R domain is an important residue that affects the binding of K^+ and coupled ATP or ADP at the active site in the Cat domain.

Nov3r binding and pyruvate inhibition— Based on the crystal structures of PDHK3, L2 binding involved the binding of lipoyl prosthetic group by mostly hydrophobic interactions and by mostly electrostatic interactions between the C-terminal tail of PDHK3 and L2 domain (77). Mutations at the lipoyl group-binding site resulted in less stimulation of PDHK3 by L2 (79). As

described in introduction, Nov3r binds at lipoyl goup binding site in human PDHK2. Nov3r is probably an analog of acetyl-dihydrolipoyl group (86). This compound and the related AZD7545 inhibit E2-activated kinase activity through preventing binding of lipoyl domains to kinase (77, 83, 84, 88). It was reported that L2 or ΔBE2 increased kinase activity less than 30% (32, 40). Using E1 alone as a substrate, binding of Nov3r to kinase caused maximally a 20% activity increase with 100 nM Nov3r and the kinase activity decreased with higher levels Nov3r under a low salt buffer. Therefore, over a narrow concentration range, Nov3r mimics the lipoyl domain structures in activating kinase activity although the former activities were performed with a high salt buffer.

Based on crystal structures of PDHK2 (76), the Nov3r binding site is adjacent to the DCA binding site. Therefore, binding of ligand at one site may affects ligand binding at the other site. With PDHK2 inhibited by 100 μM pyruvate, Nov3r enhanced kinase activity, suggesting that Nov3r binding was hindering pyruvate binding and inhibition at the nearby site. It needs to be noted that kinase activity increased maximally 2-fold, which was still 15% less than the initial activity without pyruvate under these low salt conditions. This indicates that Nov3r substantially reduced but did not eliminate the inhibitory effects of pyruvate. Varying the level of pyruvate with or without Nov3r established that probably the affinity for pyruvate was reduced but the maximal inhibition was also decreased somewhat.

In studies where salt conditions were varied and inhibition by pyruvate or DCA compared with the effects of Nov3r, strong DCA or pyruvate inhibition required both elevated K^+ and also elevated Pi. This result was in agreement with results from fluorescence quenching studies, in which Nov3r interfered the tighter binding of ADP•pyruvate•PDHK2 via a Pi dependent mechanism (88). In the presence of both K^+ and Pi, Nov3r reduced the weaker DCA

inhibition less effectively than it reduced the stronger pyruvate inhibition. Although my results indicate that Cl^- binds to the same site as pyruvate/DCA and inhibits kinase activity, Nov3r did not efficiently reduce Cl^- inhibition. Therefore, Nov3r influence in reducing inhibition at the pyruvate/DCA site might depend on the size of the inhibitor. Binding of Nov3r to the lipoyl group-binding site may allosterically cause specific conformational changes at pyruvate/DCA binding site. The changes may be small as inhibition by the larger pyruvate is weakened but not the inhibition by the much smaller Cl^-. Additionally, increasing of the size of inhibitors at the pyruvate/DCA site may tighten the coupled binding of ADP/ATP•K at the catalytic site to lead to conformational changes at the cross arm to reduce binding of lipoyl domain. These data are consistent with the findings that pyruvate plus ADP prevent binding of GST-L2 to kinase (43) but their association was not significantly influenced by Cl^- plus ADP as compared to ADP alone (Hiromasa, Y., unpublished data).

Communication from ligand binding site on the R domain to the active site—Reducing of the lipoyl groups of E2 by E3 using NADH/NAD^+ increases E2-enhanced PDHK2 activity. Acetylation of reduced lipoyl groups by E3 using acetyl-CoA results in even bigger increases in kinase activity. These effects could only be observed with elevated levels of ions. The stimulation by reductive acetylation was small with L2 and bigger with tightly bound GST-L2 (21, 30, 32). Nov3r/lipoyl group binding pocket is formed by L23, Q27, F28, F31, T40, S41, F44, L45, L160, Q163, H164, I167 and F168. The CF3 group of Nov3r sits close to the side chain of L160 at a location (Fig. 2-26) where it is estimated by structural analog analysis that the CH3 of acetyl group of 8-acetyl-DHL-Lys would be positioned (86). It was anticipated that substitution of L160 with alanine might increase the distance from the CH3 group to the side chain of L160 and thereby weaken the interactions of acetylated dihydrolioyl-Lys with the end of

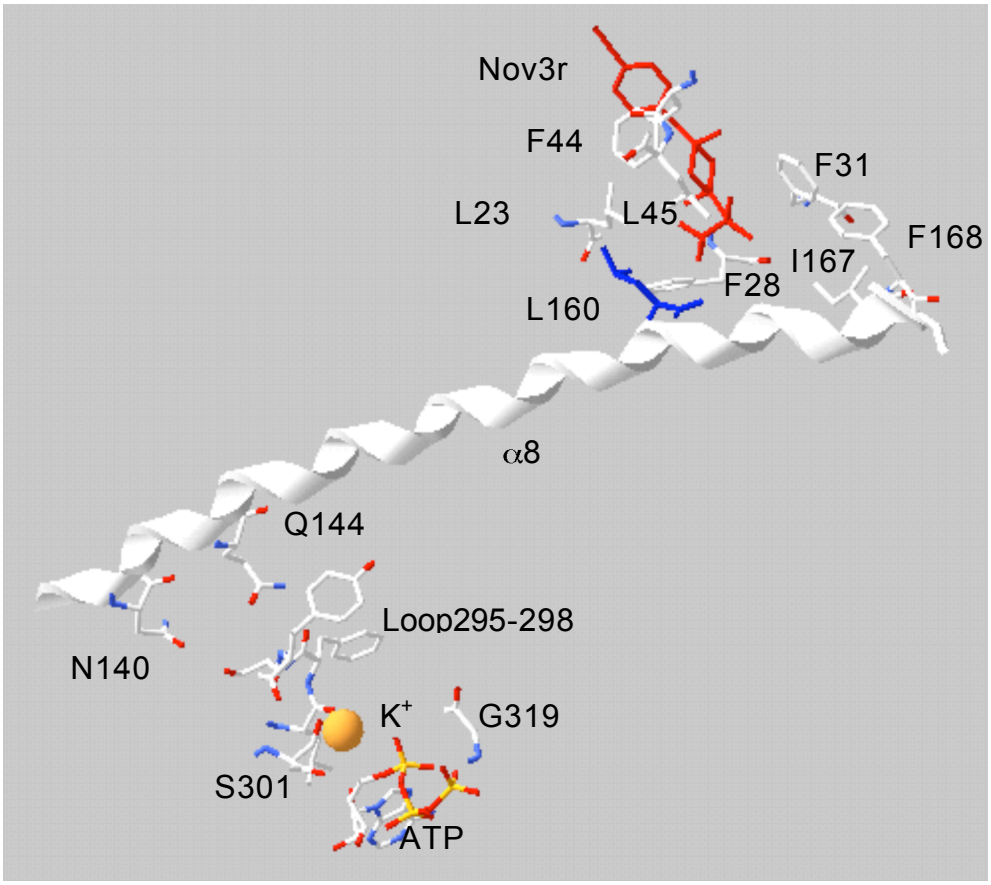

Figure 2-26. Signal transmission from the lipoyl group (Nov3r) binding site to the catalytic site. Nov3r appears to be an analog of acetyl-dihydrolipoyl-lys. Nov3r binds to a hydrophobic site in the R domain. This is also the binding site for the lipoyl groups of lipoyl domain. The information from the reductive acetylation may be transferred to helix α8 by interactions between the CH3 group of acetyl and side chain of L160. The signal is then transfer to Q144 or N140 along helix α8. Through the hydrogen bonds, the signal is further transferred to the loop 295-298 of the Cat domain. Finally, the signal reaches the catalytic site with the interactions by loop 295-298 with K^+ and K^+ with α-phosphate of ADP or ATP.

the binding pocket, resulting in less stimulation. The double mutant R154C/L160A underwent significantly lower stimulation by reductive acetylation. As R154C was stimulated to an extent similar as native kinase, the smaller activity increase of R154C/L160A likely resulted from mutation of L160A. This suggests that the communication from lipoyl group binding site to active site was changed by mutation of L160 although some impact of R514C mutation cannot be eliminated. L160A of rat PDHK2 was active with no significantly altered binding capacity to L2 domain (87). But these authors did not evaluate whether stimulation by reductive acetylation was altered with rat L160A-PDHK2 using E1•E2 as substrate.

Helix α8 spans the whole R domain of PDHK2 (76). Its C-terminus is involved in the binding of lipoyl group (L160, Q163, H164, I167 and F168). The adjacent DCA/pyruvate binding site has several residues from α8 (S153, R154, I157 and R158). At the N-terminal end of helix α8, N140 forms a hydrogen bond with S297 from the Cat domain and Q144 provides two hydrogen bonds with F296 and Y298 from the Cat domain. As emphasized above, S297 appears to interact with K^+ in active site. These hydrogen bonds may provide a linkage between helix α8 of R domain and the catalytic site through bound K^+ at the active site. Therefore, it is possible that helix α8 plays a particularly important role in communication between these sites at the R domain and the active site.

Mutation of Q144A weakened the binding of K^+. This cross arm anchoring Trp inserts between R149, L152 in helix α8 and R362 (76). It was reported that reductive acetylation enhanced PDHK2 activity by increasing the rate of ADP dissociation (30). Reductive acetylation stimulated activity of Q144 only half of that with native PDHK2. The major change was a higher control activity that is consistent with weaker K^+ binding allowing faster ADP dissociation (rate limiting step) in the absence of stimulation. The final dissociate rates were similar. Therefore,

Q144 might be involved in the signal transmission from the lipoyl site to the active site. A possible communication pathway from lipoyl group binding site to active site is: acetylated lipoyl group···Leu160···helix α8···Gln144···loop 296-301···K^+•ADP/ATP (Fig 2-26). Specifically in native PDHK2, this may result in weakened K^+ binding that, in turn, could allow faster dissociation of ADP. The residential stimulation of Q144A mutant by reductive acetylation indicates that communication probably involves other residues in different pathways. One residue involved is probably N140 that also linked helix α8 with the Cat domain through hydrogen bond with F296.

Steady-state kinetic assays and binding studies measured by fluorescence quenching or a cold trap approach indicated that pyruvate/DCA binding was tighter to PDHK2•ATP but much tighter to PDHK2•ADP (40, 43). Fluorescence studies confirmed that binding of ADP or ATP enhanced the binding of inhibitors while pyruvate also tightened the binding of ADP but not ATP in potassium phosphate buffers (43). DCA inhibits PDHK2 by slowing down the dissociation of ADP (40). It was reported that K^+ enhanced the DCA inhibition on kinase (40) and that K+ and Pi enhanced the binding of pyruvate with ADP (88). My studies confirmed that K^+ enhanced the DCA/pyruvate inhibition of PDHK2 using not only E1•E2 but also E1 alone as substrate. Pyruvate/DCA weakly inhibited the kinase activity in a buffer containing minimal levels of ions. One possible reason is that ADP or ATP signal transmission from the DCA/pyruvate site to the active site may involve the bound K^+. Mutation of Q144A resulted in somewhat weaker pyruvate inhibition using E1 alone as substrate. Therefore, Q144 may play some roles in the communication from DCA/pyruvate site to the active site. To better understand this communication, more studies would be required.

Conclusions—Through studying mutants of several residues in the R domain of PDHK2, there were several new findings about the molecular mechanisms by which PDHK2 kinase is regulated. 1) Binding of ATP or ATP at the catalytic site in the Cat domain caused mostly the fluorescence quenching of W383 that was lost with W383F mutant. W383 anchors the cross arm and provides the majority of intrinsic Trp fluorescence of PDHK2. The sensitive fluorescence change of the structurally defined Trp residue was used to evaluate changes in ligand binding. Pyruvate, binding to DCA/pyruvate site, caused the fluorescence quenching of not only W383 but also other Trp (W79). Therefore, ligand binding resulted in changes of the electrostatic environment surrounding W383. But it is still unclear what caused the fluorescence quenching: a smaller shift around this region or a total opening up of the cross arm. 2) Mutation of Q144 resulted in a different response of PDHK2 to K^+ ion level. Q144 residue in the α8 helix of the R domain may serve as an important linkage between the R domain and the Cat domain. This linkage involves the K^+ ion that binds with ATP or ADP to the ATP/ADP binding site. 3) Residues R154 and R158 at the DCA/pyruvate site play important roles in the DCA/pyruvate inhibition (for both the dissociation of lipoyl domains and inhibition of phosphorylation of substrate E1). 4) Cl^- ion binds specifically to the DCA/pyruvate site and competes with DCA or pyruvate to reduce their inhibition. 5) Substitution of I157 by Phe did not reduce PDHK2 inhibition by pyruvate, DCA or Cl^-. Therefore, the Phe residue in PDHK3 may not be the major reason for the reported weaker inhibition of PDHK3 by DCA. One reason these inhibitions may be less effective with PDHK3 is that the tighter binding of lipoyl domains to PDHK3 does not allow the inhibitors to reduce activity by hindering binding to E2. 6) Residues L160 (through interaction at the lipoyl group binding site) and Q144 (linkage between the R domain and the Cat domain) appear to be important for lowering control activity with elevated ions which is

overcome in stimulation by reductive acetylation. This suggests these residues contribute to conformations that aid lowering of control activity and /or removal of diminished activity during stimulation. And 6) Binding of Nov3r at the lipoyl group binding site reduced the inhibition at the nearby DCA/pyruvate site with diminishing effects as the size of the inhibitors decreases.

Overall, this thesis established that fluorescence quenching of W383 could be used to evaluate the ligand binding and uncovered specific residues in helix $\alpha 8$ of the R domain that contribute to pyruvate/DCA inhibition, K^+-linked signal transduction within PDHK2 structure and stimulation by reductive acetylation. This thesis provided new insight that Cl^- reduces PDHK2 activity by binding at the pyruvate/DCA binding site. This thesis also supported that binding of Nov3r at the lipoyl group binding site hindered the inhibition at the nearby DCA/pyruvate site in a manner that requires specific ions such as K^+ and Pi and diminishes with the size of the inhibitors. These novel insights advance the understanding the molecular mechanisms regarding how ligand binding to the R domain modulates the catalytic use of ATP in the Cat domain.

References

1. Patel, M.S., and Roche, T.E. (1990) Monecular biology and biochemistry of pyruvate dehydrogenase complex. *FASEB J.* 4, 3224-3233.
2. Randle, P.J. and Priestman, D.A. (1996) Shorter term and long term regulation of pyruvate dehydrogenase kinase. In: Alpha-Keto Acid Dehydrogenase kinases. 151-161, Patel, M.S., Roche, T.E. and Harris, R.A. (eds.), Birkhäuser verlag, Basel.
3. Sugden, M.C., Bulmer, K. and Holness, M.J. (2001) Fuel-sensing mechanisms integrating lipid and carbohydrate utilization. *Biochem. Soc. Trans*. 29, 272-278.
4. Frank, R.E., Titman, C.M., Pratap, J.V., Luisi, B.F. and Perham, R.N. (2004) A molecular switch and proton wire synchronize the active sites in thiamine enzymes. *Science*. 306, 872-876.
5. Ciszak, E.M., Korotchkina, L.G., Dominiak, P.M., Sidhu, S. and Patel, M.S. (2003) Structural basis for flip-flop action of thiaqmine pyrophosphate-dependent enzymes revealed by human pyruvate dehydrogenase. *J. Biol. Chem*. 278, 21240-21246.
6. Seifert, F., Golbik, R., Brauer, J., Lilie, H., Schroder-Tittmann, K., Hinze, E., Korotchkina, L.G., Patel, M.S. and Tittmann. (2006) Direct kinectic evidence for half-of-the-sites reactivity in the E1 component of the human pyruvate dehydrogenase multienzyme complex trough alternating sites cofactor activation. *Biochemistry*. 45, 12775-12785
7. Nemeria, N., Chakraborty, S., Baykal, A., Korotchkina, L.G., Patel, M.S. and Jordan, F. (2007) The 1',4'-iminopyrimidine tautomer of thiamine diphosphate is poised for catalysis in asymmetric active center on enzymes. *PNAS.* 104, 78-82.

8. Roche, T.E, Hiromasa, Y., Turkan, A., Gong, X., Peng, T., Yan, X. and kasten, S.A. (2003) Central organization of mammalian pyruvate dehydrogenase (PD) complex and lipoyl domain-mediated function and control of PD kinases and phosphatase 1. In: Thiamine: catalytic mechanisms and Role in Normal and Disease States. 363-386, Jordan, F. and Patel, M.S. (eds.), Marcel Dekker, New York.

9. Harris, R.A., Bowker-Kinley, M.M., Wu, P., Jeng, J. and Popoc, K.M. (1997) Dihydrolipoamide dehydrogenase-binding protein of the human pyruvate dehydrogenase complex. DNA-derived amino acid sequence, expression, and reconstitution of pyruvate dehydrogenase complex. *J. Biol. Chem*. 272, 19746-19751.

10. Maeng, C.Y., Yazdi M.A., Niu, X.D., Lee, H.Y. and Reed, L.J. (1994) Expression, purification, and characterization of the dihydrolipoamide dehydrogenase-binding protein of the pyruvate dehydrogenase complex from Saccharomyces cerevisiae. *Biochemistry*. 33, 13801-13807.

11. Hiromasa, Y., Fujisawa, T., Aso, Y. and Roche, T.E. (2004) Organization of the cores of the mammalian pyruvate dehydrogenase complex formed by E2 and E2 plus the E3-binding protein and their capacities to bind the E1 and E3 component. *J. Biol. Chem*. 279, 6921-6933.

12. Spriet, L.L and Watt, M.J. (2003) Regulatory mechanisms in the interaction between carbohydrate and lipid oxidation during exercise. *Acta Physiol. Scand.* 178, 443-452.

13. Linn, T.C., Pettit, F.H. and Reed L.J. (1969) Alpha-keto acid dehydrogenase complex. X. Regulation of the activity of the pyruvate dehydrogenase complex from beef kidney mitochondria by phosphorylation and dephosphorylation. *Proc. Natl. Acad. Sci. USA*. 62, 234-241.

14. Patel, M.S. and Kprotchkina L.G. (2001) Regulation of mammalian pyruvate dehydrogenase complex by phosphorylation: complexity of multiple phosphorylation sites and kinases. *Exp. Mol. Med.* 33, 191-197.

15. Patel, M.S. and Kprotchkina L.G. (2006) Regulation of pyruvate dehydrogenase complex. *Bioch. Soc. Tran*. 34, 217-222.

16. Sugden M.C. and Holness M.J. (2003) Recent advance in mechanism regulating glucose oxidation at the level of the pyruvate dehydrogenase complex by PDKs. *Am. J. Physiol. Endocrinol. Metab*. 284, 855-862.

17. Gudi, R., Bowker-kinley, M.M., Kedishvili, N.Y., Zhao, Y. and Popov K.M. (1995) Diversity of the pyruvate dehydrogenase kinase gene family in humans. *J. Biol. Chem.* 270, 28989-28994.

18. Rowles, J., Scherer, S.W., Xi, T., Majer, M., Nickle, D.C., Rommens, J.M., Popov, K.M., Harris, R.A., Reibow, N.L., Xia, J., Tsui, L.C., Bogardus, C. and Prochazka, M. (1996) Cloning and characterization of PDK4 on 7q21.3 encoding a fourth pyruvate dehydrogenase kinase isozyme in human. *J. Boil. Chem.* 271, 22376-22383.

19. Roche, T.E., Baker, J.C., Yan, X., Hiromasa, Y., Gong, X., Peng, T., Dong, J., Turkan, A and Kasten, S.A. (2001) Distinct regulatory properties of pyruvate dehydrogenase kinase and phosphatase isoforms. *Nucleic Acid res. Mol. Biol*. 70, 33-75.

20. Huang, B., Gudi, R., Wu., Harris, R.A., Hamilton, J. and Popov, K.M. (1998) Isozymes of pyruvate dehydrogenase phosphatase. DNA-derived amino acid sequences, expression, and regulation. *J. Biol. Chem*. 273, 17680-17688.

21. Bowker-Kinley, M.M., Davis, W.I., Wu, P., Harris, R.A. and Popov K.M. (1998) Evidence of existence of tissue-specific regulation of the mammalian pyruvate dehydrogenase complex. *Biochem. J.* 329, 191-196.

22. Pettit, F.H., Roche, T.E. and Reed, L.J. (1972) Function of calcium ions in pyruvate dehydrogenase phosphatase activity. *Biochem. Biophys. Res. Commun.* 49, 563-571.

23. Turkan, A., Hiromassa, Y. and Roche, T.E. (2004) Formation of a complex of the catalytic subunit of pyruvate dehydrogenase phosphatase isoform 1 (PDP1c) and the L2 domain forms a Ca^{2+} binding site and captures PDP1c as a monomer. *Biochemistry*. 43, 15073-15085.

24. Dahl, H.H., Hunt, S.M., Hutchison, W.M. and Brown, G.K. (1987) The human pyruvate dehydrogenase complex. Isolation of cDNA clones for the E1 alpha subunit, sequence analysis, and characterization of the mRNA. *J. Biol. Chem*. 262, 7398-7403.

25. Yeaman, S.J., Hutcheson, E.T., Roche, T.E., Pettit, F.H., Brown, J.R., Reed, L.J., Watson, D.C. and Dixon, G.H. (1978) Sites of phosphorylation on pyruvate dehydrogenase from bovine kidney and heart. *Biochemistry*. 17, 2364-2370.

26. Korotchkina, L.J. and Patel, M.S. (2001) Site specificity of four pyruvate dehydrogenase kinase isoenzymes toward the tree phosphorylation sites of human pyruvate dehydrogenase. *J. Biol. Chem*. 276, 37223-37229.

27. Kolobova, E., Tuganova, A., Boultatnikov, I. and Popov K.M. (2001) Regulation of pyruvate dehydrogenase activity through phosphorylation at multiple sites. *Biochem. J.* 358, 69-77.

28. Sale, G.J. and Randle, P.J. (1982) Occupancy of phosphorylation sites in pyruvate dehydrogenase phosphate complex in rat heart in vivo. Relation to proportion of inactive complex and rate of re-activation by phosphatase. *Bioichem. J.* 206, 221-229.

29. Roche, T.E., Hiromasa, Y., Turkan, A., Gong, X., Peng, T., Yan, X., Kasten, S.A., Bao, H. and Dong, J. (2003) Essential roles of lipoyl domains in the activated function and control of pyruvate dehydrogenase kinases and phosphatase isoform 1. *Eur.J.Biochem*. 270, 1050-1056.

30. Bao, H., Kasten, S.A., Yan, X., Hiromasa, Y. and Roche, T.E. (2004) Pyruvate dehydrogenase kinase isoform 2 activity stimulated by speeding up the rate of dissociation of ADP. *Biochemistry*. 43, 13442-13451.

31. Gong, X., Peng, T., Yakhnin A., Zolkiewski, M., Quinn, J., Yeaman, S.J. and Roche, T.E. (2000) Specificity determinants for the pyruvate dehydrogenase component reaction mapped with mutated and prosthetic group modified lipoyl domains. *J. Biol. Chem.* 275, 13645-13653.

32. Baker, J.C., Yan, X., Peng, T., Kasten, S. and Roche, T.E. (2000) Markeed difference between two isoforms of human pyruvate dehydrogenase kinase. *J. Biol. Chem.* 275, 15773-15781.

33. Tuganova, A., Boulantnikov, I. and Popov, K.M. (2002) Interaction between the individual isozymes of pyruvate dehydrogenase kinase and the inner lipoyl-bearing domain of transacetylase component of pyruvate dehydrogenase complex. *Biochem. J.* 366, 129-136.

34. Hiromasa, Y. and Roche, T.E. (2003) Faciliated interaction between the pyruvate dehydrogenase kinase isoform 2 and the dihydrolipoyl acetyltransferase. *J. Biol. Chem.* 278, 33681-33693.

35. Liu, S., Baker, J.C. and Roche, T.E. (1995) Binding of the pyruvate dehydrogenase kinase to recombinant constructs containing the inner lipoyl domain of the dihydrolipoyl acetyltransferase component. *J. Biol. Chem*. 270, 793-800.

36. Tuganova, A. and Popov, K.M. (2005) Role of protein-protein interactions in the regulation of pyruvate dehydrogenase kinase. *Biochem. J*. 387, 147-153.

37. Klyuyeva, A., Tuganova, A. and Popov, K.M. (2005) The carboxy-terminal tail of pyruvate dehydrogenase kinases 2 is required for the kinasae activity. *Biochemistry.* 44, 13573-13582.

38. Rahmatullah, M., Radke, G.A., Andrews, P.C. and Roche, T.E. (1990) Changes in the core of the mammalian-pyruvate dehydrogenase complex upon selective removal of the lipoyl domain from the transacetylase component but not from the protein X component. *J. Biol. Chem*. 265, 14512-14517.

39. Radke, G.A., Ono K., Ravindran, S. and Roche, T.E. (1993) Critical role of a lipoyl cofactor of the dihydrolipoyl acetyltransferase in the binding and enhanced function of the pyruvate dehydrogenase kinase. *Biochem. Biophys. Res. Commun*. 190, 982-991.

40. Bao, H., Kasten, S.A., Yan, X. and Roche, T.E. (2004) Pyruvate dehydrogenase kinase isoform 2 activity limited and further inhibited by slowing down the rate of dissociation of ADP. *Biochemistry*. 43, 13432-13441.

41. Whitehouse, S., Cooper, R.H. and Randle, P.J. (1974) Mechanism of activation of pyruvate dehydrogenase by dichloroacetate and other halogenated carboxylic acids. *Biochem. J*. 141, 761-774.

42. Cate, R.L. and Roche, T.E. (1978) A unifying mechanism for stimulation of mammalian pyruvate dehydrogenase kinase activity by NADH, dihydrolipoamide, acetyl Coenzyme A, or pyruvate. *J. Biol. Chem*. 253, 496-503.

43. Hiromasa, Y., Hu, L. and Roche, T.E. (2006) Ligand-induced effects on pyruvate dehydrogenase kinase isoform 2. *J. Biol. Chem*. 281, 12568-12579.

44. Sugden, m.C., Fryer, L.G., Orfali, K.A., Priestman, D.A., Donald E. and Holness, M.J. (1998) Studies of the long-term regulation of hepatic pyruvate dehydrogenase kinase. *Biochem. J.* 329, 89-94.

45. Wu, P., Blair, P.V., Sato, J., Jaskiewicz, J., Popov, K.M. and Harris, R. A. (2000) Starvation increases the amount of pyruvate dehydrogenase kinase in several mammalian tissues. *Arch. Biochem. Biophys*. 381, 1 – 7.

46. Wu, P., Sato, J., Zhao, Y., Jaskiewicz, J., Popov, K.M. and Harris, R.A. (1998) Starvation and diabetes increase the amount of pyruvate dehydrogenase kinase izoenzyme 4 in rat heart. *Biochem. J*. 329, 197-201.

47. Sugden, M.C., Holness, M.J., Donald, E. and Lall, H. (1999) Substrate interactions in the short- and long-term regulation of renal glucose oxidation. *Metabolism.* 48, 707 – 715.

48. Wu, P., Inskeep, K., Bowker-Kinley, M.M., Popov, K.M. and Harris, R.A. (1999) Mechanism responsible for inactivation of skeletal muscle pyruvate dehydrogenase complex in starvation and diabetes. *Diabetes.* 48, 1593 – 1599.

49. Sugden, M.C., Kraus, A., Harris, R.A. and Holness, M.J. (2000) Fibre-type specific modification of the activity and regulation of skeletal muscle pyruvate dehydrogenase kinase (PDK) by prolonged starvation and refeeding is associated with targeted regulation of PDK isoenzyme 4 expression. *Biochem. J*. 346, 651-657.

50. Peters, S.J., Harris, R.A., Heigenhauser, G.J.F. and Spriet L.L. (2001) Muscle fiber type comparison of PDH kinase activity and isoform expression in fed and fasted rats. *Reg., Integ. And Comp. Phys*. 280, R661-668.

51. Peters, S.J., Harris, R.A., Wu, P., pehleman, T.L., Heigenhauser, G.J.F. and Spriet L.L. (2001) Human skeletal muscle PDH kinase activity and isoform expression during 3-day high fat/low-carbohydrate diet. *Endocrinology and Metabolism*. 281, E1151-E1158.

52. Sugdenm M.C., Lall, H.S., Harris, R.A. and Holness, M.J. (2000) Selective modification of the pyruvate dehydrogenase kinase isoform profile in skeletal muscule in hyperthyroidism: implications for the regulatory impact of glucose on fatty acid oxidation. *J. Endocrinology*. 167, 339-345.

53. Holness, M.J., Kraus, A., Harris, R.A. and Sugden, M.C. (2000) Targeted upregulation of pyruvate dehydrogenase kinase (PDK)-4 in slow-twitch skeletal muscle underlies stable modification of the regulatory characteristics of PDK induced by fat feeding. *Diabetes*. 49, 775 – 781.

54. Wu, P., Sato, J., Zhao, Y., Kedishvili, N.Y., Shimomura, Y. and Crabb, D.W. (1998) Starvation and diabetes increase the amount of pyruvate dehydrogenase kinase isoform 4 in rat heart. *Biochem. J*. 329, 197 – 201.

55. Wu, P., Blair, P.V., Sato, J., Jaskiewicz, J. , Popov, K.M. and Harris, R.A. (2000) Starvation increases the amount of pyruvate dehydrogenase kinase in several mammalian tissues. *Arch. Biochem. Biophys*. 381, 1 – 7.

56. Andrews, M. T., Squire, T.L. , Bowen, C.M. and Rollins, M.B. (1998) Low-temperature carbon utilization is regulated by novel gene activity in the heart of a hibernating mammal. *Proc. Natl. Acad. Sci. USA*. 95, 8392 – 8397

57. Motojima, K. (2002) A metabolic switching hypothesis for the first step in the hypolipidemic effects of fibrates. *Boil. Pham. Bull.* 25, 1509-1511.

58. Huang, B., Wu, P., Popov, K.M. and Harris, R.A. (2003) Starvation and diabetes reduce the amount of pyruvate dehydrogenase phosphatase in rat heart and kidney. *Diabetes*. 52, 1371 – 1376.

59. Kwon, H.S., Huang, B, Ho Jeoung, N., Wu, P., Steussy, C.N. and Harris R.A. (2006) Retinoic acids and trichostatin A (TSA), a histone deacetylase inhibitor, induce human pyruvate dehydrogenase kinase 4 (PDK4) gene expression. *Biochim. Biophys. Acta*. 1759, 41 – 51.

60. Kwon, H.S. and Harris, R.A. (2004) Mechanisms responsible for the regulation of pyruvate dehydrogenase kinase 4 gene expression. *Adv. Enzyme Regul*. 44 109 – 121.

61. Wu, P., Peters, J.M. and Harris, R.A. (2001) Adaptive increase in pyruvate dehydrogenase kinase 4 during starvation is mediated by peroxisome proliferator-activated receptor a. *Biochem. Biophys. Res. Commun*. 287, 391 – 396.

62. Huang, B., Wu, P., Bowker-Kinley, M.M. and Harris, R.A. (2002) Regulation of pyruvate dehydrogenase kinase expression by peroxisome proliferator-activated receptor-α ligands, glucocorticoids, and insulin. *Diabetes*. 51, 276 – 283.

63. Muoio, D.M., MacLean, P.S., Lang, D.B., Li, S., Houmard, J.A., Way, J.M., Winegar, D.A. Corton, J.C., Dohm, G.L. and Kraus, W.E. (2002) Fatty acid homeostasis and induction of lipid regulatory genes in skeletal muscles of peroxisome proliferator-activated receptor (PPAR) α knock-out mice. *J. Biol. Chem*. 277, 26089 – 26097.

64. Abbot, E. L., McCormack, J.G. , Reynet, C., Hassall, D.G., Buchan, K.W. and Yeaman, S.J. (2005) Diverging regulation of pyruvate dehydrogenase kinase isoform gene expression in cultured human muscle cells. *FEBS J*. 272, 3004 – 3014.

65. Degenhardt, T., Saramäki, A., malinen, M., rieck, M., Väisänen, S., Huotari, A., Herzig, K., Muller, R. and Carlberg, C. (2007) Three members of the human pyruvate dehydrogenase kinase gene family are direct targets of the peroxisome proliferators-activated receptor β/δ. *J. Mol. Biol.* 372, 341-355.

66. Puigserver, P., Wu, Z., Park, C. W., Graves, R., Wright, M., and Spiegelman, B. M. (1998) A cold-inducible coactivator of nuclear receptors linked to adaptive thermogenesis. *Cell.* 92, 829–839.

67. Kwon, H. S. , Huang, B. , Unterman, T. G. and Harris, H. A. (2004) Protein kinase B-alpha inhibits human pyruvate dehydrogenase kinase-4 gene induction by dexamethasone through inactivation of FOXO transcription factors. *Diabetes.* 53, 899 – 910.

68. Guidi, R., Bowker-Kinley, M.M., Kedishvili, N.Y., Zhao, Y. and Popov, K.M. (1995) Diversity of the pyruvate dehydrogenase kinase gene family in humans. J.Biol. Chem. 270, 28989-28994.

69. Hanks, S.K. and Hunter, T. (1995) Protein kinases 6. The eukaryotic kinase superfamily: kinase (catalytic) domain structure and classification. *FASEB J.* 9, 576-596.

70. Popov, K.M., kedishvili, N.Y., Zhao, Y., Shimomura, Y., Crabb, D.W. and Harris, R.A. (1993) Primary structure of pyruvate dehydrogenase kinase establishes a new family of eukaryotic protein kinase. *J. Biol. Chem*. 268, 26602-26606.

71. Harris, R.A., Popov, K.M., Zhao, Y., Kedishvili, N.Y., Shimomura, Y. and Crabb, D.W. (1995) A new family of protein kinases-the mitochondrial protein kinases. *Adv. Enzyme Regul.* 35, 147-162.

72. Wynn, R.M., Chuang, J.L., Cote, C.D. and Chuang, D.T. (2000) Tetrameric assembly and conservation in the ATP-binding domain of rat branched-chain alpha-ketoacid dehydrogenase kinase. *J. Biol. Chem.* 275, 30512 – 30519.

73. Machius, M., Chaung, J.L., Wynn, R.M., Tomchick, D.R. and Chuang, D.T. (2001) Structure of rat BCKD kinase: nucleotide-induced domain communication in a mitochondrial protein kinase. *Proc. Nat. Acad. Sci. USA*. 98, 11218 – 11223.

74. Steussy, C.N, Popov, K.M., Bowker-Kinley, M.M., Sloan, R.B., Harris, R.A. and Hamilton, J.A. (2001) Structure of pyruvate dehydrogenase kinase. Novel folding pattern for a serine protein kinase. *J. Biol. Chem*. 276, 37443 – 37450.

75. Bowker-Kinley, M. and Popov, K.M. (1999) Evidence that pyruvate dehydrogenase kinase belongs to the ATPase/kinase superfamily. *Biochem. J.* 344, 47 – 53.

76. Knoechel, T.R., Tucker, A.D., Robinson, C.M., Phillips, C. Taylor, W., Bungay, P.J., Kasten, S.A., Roche, T.E. and Brown, D.G. (2006) Regulatory roles of the N-terminal domain based on crystal structures of human pyruvate dehydrogenase kinase 2 containing physiological and synthetic ligands. *Biochemistry*. 45, 402 – 415.

77. Kato, M., Chuang, J.L., Tso, S-C., Wynn, R.M. and Chuang, D.T. (2005) Crystal structure of pyruvate dehydrogenase kinase 3 bound to lipoyl domain 2 of human pyruvate dehydrogenase complex. *EMBO J.* 24, 1763 – 1774.

78. Devedjiev, Y., Steussy, C.N. and Vassylyev, D.G. (2007) Crystal structure of an asymmetric complex of pyruvate dehydrogenase kinase 3 with lipoyl domain and its biological implications. J. Mol. Biol. 370, 407-416.

79. Tso, S.C., Kato, M., Chuang, J.L. and Chuang, D.T. (2006) Structural determinants for cross-talk between pyruvate dehydrogenase kinase 3 and lipoyl domain 2 of the human pyruvate dehydrogenase complex. J. Biol. Chem. 281, 27197-27204.

80. Roche, T.E. and Reed, L.J. (1974) Monovalent cation requirement for ADP inhibition of pyruvate dehydrogenase kinase. *Biochem. Biophys. Res. Commun.* 59, 1341-1348.

81. Vivian, J.T. and Callis, P.R. (2001) Mechanism of tryptophan shifts in proteins. *Biophys. J*. 80, 2093-2109.

82. Liu, T., Callis, P.R., Hesp, B.H., Groot, M., Buma, W.J. and Broos, J. (2005) Ionization potentials of fluorescence decay in proteins. *J. Am. Chem. Soc*. 127, 4104-4113.

83. Aicher, T.D., Anderson, R.C., Bebernitz, G.R., Coppola, G.L.J., Jewell, C.F., Knorr, D.C., Liu, C., Sperbeck, D.M., Brand, L.J., Strohschein, R.J., Gao, J., Vinluan, C.C., Shetty, S.S., Draland, C., Kaplan, E.L., DelGrande, D., Islam, A., Liu, X., Lozito, R.J., Maniara, W.M., Walter, R.E., and Mann, W.R. (1999) (R)-3,3,3-Trifluoro-2-hydroxy-2-methypropionamides are orally active inhibitors of pyruvate dehydrogenase kinase. *J. Med. Chem.* 42, 2741-2746

84. Morrell, J.A., Orme, J., Butlin, R.J., Roche, T.E., Mayers, R.M. and Kilgour, E. (2003) AZD7545 is a selective inhibitor of pyruvate dehydrogenase kinase 2. *Biochem. Soc. Trans*. 31, 1168-1170.

85. Klyuyeva, A., Tuganova, A. and Popov. K.M. (2007) Amino acid residues responsible for the recognization of dichloroacetate by pyruvate dehydrogenase kinase 2. *FEBS Letters*. 581, 2988-2992.

86. Roche, T.E. and Hiromasa, Y. (2007) Pyruvate dehydrogenase kinase regulatory mechanisms and inhibition in treating diabetes, heart ischema, and cancer. *Cell. Mol. Life. Sci*. 64, 830-849.

87. Tuganova, A., Klyuyeva, A. and Popov, K.M. (2007) Recognition of the inner lipoyl bearing domain of dihydrolipoyl trasacetylase and of the blood glucose-lowering compound AZD7545 by pyruvate dehydrogenase kinase 2. *Biochemistry*. 46, 8592-602.

88. Hiromasa, Y., Yan, X. and Roche, T.E. (2008) Specific influence on self-association of pyruvate dehydrogenase kinase isoform 2 (PDHK2). Binding of PDHK2 to the L2 lipoyl domain, and effects of the lipoyl group-binding site inhibitor, Nov3r. *Biochemistry*. 47, 2312-2324

89. Hiromasa, Y. and Roche, T.E. (2008) Critical role of specific ions for ligand-induced changes regulating pyruvate dehydrogenase kinase isoform2. *Biochemistry*. 47, 2298-2311